

**SOIL MECHANICS AND BITUMINOUS MATERIALS
RESEARCH LABORATORY**



**ASPHALT MIXTURE BEHAVIOR IN
REPEATED FLEXURE**

by

C. L. MONISMITH

J. A. EPPS

and

D. A. KASIANCHUK

**TE
68-8**

ATION

**DEPARTMENT OF CIVIL ENGINEERING
INSTITUTE OF TRANSPORTATION AND TRAFFIC ENGINEERING**



University of California • Berkeley

Soil Mechanics and Bituminous Materials
Research Laboratory

ASPHALT MIXTURE BEHAVIOR IN REPEATED FLEXURE

A report on an investigation
by

C. L. Monismith
Professor of Civil Engineering and
Research Engineer

J. A. Epps
Assistant Professor of Civil Engineering
Texas A & M University, College Station, Texas
formerly Research Assistant

and

D. A. Kasianchuk
Associate Professor of Engineering
Carleton University, Canada
formerly Research Assistant

to

The Materials and Research Department
Division of Highways
State of California
under

State of California Standard Agreement M and R 633153
Research Technical Agreement 13945-13002

Prepared in cooperation with
The United States Department of Transportation
Federal Highway Administration
Bureau of Public Roads

Report No. TE 68-8, Office of Research Services
University of California, Berkeley, California
December 1968

INTRODUCTION

This report is part of a continuing study of the fatigue response of asphalt paving mixtures which includes not only investigation of the factors affecting the behavior of asphalt mixtures in repeated flexure, but also consideration of the fatigue factor in the design of asphalt concrete pavements. During the 1967-68 period, the investigation was concerned with (1) a reexamination of the data and analyses for an in-service pavement near Morro Bay, California (V-SLO-56-C,D) which had been reported in TE 67-4 (1); (2) development of a pavement design subsystem to include the fatigue factor; and (3) influence of a number of mixture variables on fatigue response for a range in paving mixtures corresponding to those which would be used in California. References (2) and (3) contain more detailed discussions of the material summarized in this report.

FATIGUE SUBSYSTEM

Proper design of asphalt concrete pavements requires consideration of a number of complex and interrelated factors. Attempts have been made in the past few years to formulate pavement design systems which attempt to bring these factors together as the first step in the development of improved methods of pavement design, methods which can accommodate changing requirements both with respect to load and to materials (4,5). The complexity of such an approach is illustrated in Fig. 1 (4).

A method which has the potential to assist in achieving improved design procedures is to develop a series of subsystems, the goal of each of which is to minimize a particular form of distress. If such a series of subsystems can be developed, they can then be combined utilizing the weighting functions (Fig. 1) which can assume particular values for a specific pavement structure and environment. In effect, the weighting functions may be related to limiting design criteria for a particular condition.

One form that the subsystem for considering the fatigue mode of distress can take is shown in Fig. 2 (2). This particular subsystem can be seen to parallel the conventional

structural engineering approach, in which a structure is selected (designed)*, its behavior under anticipated service conditions analyzed, and its adequacy with respect to a specific distress criterion determined.

At this point it should be noted that this fatigue subsystem constitutes only a small part of the entire system (Fig. 1). Other causes of distress can be analyzed using a similar line of reasoning, examples of which are shown in Fig. 3 for distortion and in Fig. 4 for cracking (other than fatigue). In comparing the diagrams of Figs. 3 and 4 with that of Fig. 2, it will be noted that a number of the elements are similar (e.g. environment) and, in effect, can be considered subsystems themselves.

For specific situations, when such a series of subsystems have been developed, it is possible that the weighting functions of Fig. 1 (i. e. W_{fr} , W_{cs} , W_d) can be assigned values representative of their respective contributions to reduction pavement serviceability.

Alternatively, as is done in structural design, the pavement structure may be selected to minimize a particular mode of distress and checked to insure that others do not occur or are themselves minimal. If the potential for other forms of distress exist (to an intolerable degree) then the design can be modified to preclude or reduce their effects. Initially this may well be the approach adopted until more information can be developed regarding the weighting factors.

In this report only the fatigue subsystem is considered. Moreover, it should also be noted that only the upper portion of the system shown in Fig. 1 is being treated at this time. No attempt is made to consider the influence of the decision criteria shown in the lower portion although some effort has been made in this direction by other investigators (e. g. (Ref. (5)).

*The State of California pavement design procedure (6) or those developed by the Corps of Engineers (7) and the Asphalt Institute (8) might serve as the starting point for such an analysis.

The design subsystem shown in Fig. 2 can be divided into three general sections:

1. Preliminary data acquisition.
2. Materials characterization.
3. Analysis and evaluation.

Each of these in turn embody a series of steps as noted in the subsequent paragraphs.

Preliminary Data Acquisition

Traffic Characteristics. An estimate of the traffic and wheel load distribution to be served by the proposed facility taking into account the nature of the area as well as its expected growth is required. From such estimates the following traffic information should be obtained:

1. The number of vehicles in each load and axle classification.
2. Wheel and axle configurations (dual or single tires and single or tandem axles).
3. The distribution of vehicles throughout the day and during the year.
4. Tire inflation pressures of the various classes of vehicles.
5. Vehicular velocities.

In addition, data on the lane distribution of truck traffic for multilane facilities and distribution of traffic across the wheel paths are also desirable.

Environmental Conditions. Since the response of asphalt concrete to load is dependent on temperature, distributions of temperature within the asphalt bound layer must be obtained. Such distributions can be determined using a form of the heat conduction equation where the temperature input is assumed independent of the x and y coordinates, i. e.

$$\frac{\partial^2 \phi}{\partial z^2} = \frac{c\rho}{k} \frac{\partial \phi}{\partial t} \dots\dots\dots (1)$$

where:

- ϕ = temperature field
- c = specific heat of the material
- k = thermal conductivity
- ρ = density of the material

Available data (9) indicate that c is of the order of 0.2 BTU per lb per $^{\circ}\text{F}$ and k is of the order of 0.7 BTU per ft^2 per hr per $^{\circ}\text{F}$ per ft. It is possible to include not only daily temperature variations (assumed to vary sinusoidally about the daily mean) but also the effects of solar insolation, sky (or cloud) cover, and wind velocity (10). The generalized equation is for a semi-infinite mass in contact with air at a temperature $T_M + T_V \sin 0.2625$; the 24 hr periodic temperature of the mass is (10):

$$T = T_M + T_V \cdot \frac{e^{-xC}}{\sqrt{(H+C)^2 + C^2}} \sin \left(0.262t - xC - \arctan \frac{C}{H+C} \right) \dots \dots \dots (2)$$

where:

- T = temperature of mass, $^{\circ}\text{F}$
- T_M = mean effective air temperature, $^{\circ}\text{F}$
- T_V = maximum variation in temperature from mean, $^{\circ}\text{F}$
- t = time from beginning of cycle, hours
- x = depth below surface, ft
- H = h/k
- h = surface coefficient, BTU per sq ft per hr, $^{\circ}\text{F}$
- k = conductivity, BTU per sq ft per hr, $^{\circ}\text{F}$ per ft
- C = $\sqrt{0.131 \text{ per } c}$
- c = diffusivity, sq ft per hr = k/sw
- s = specific heat, BTU per lb, $^{\circ}\text{F}$
- w = density, lbs per cu ft.

To include the other effects noted above:

1. The effects of forced convection due to wind and average reradiation from the surface are accounted for by stating the surface coefficient as:

$$h = 1.3 + 0.62 v^{0.75}$$

where:

- v = wind velocity, miles per hour

2. The affect of solar radiation can be included by defining the effective air temperature to include solar radiation as:

$$T_E = T_a + \frac{bI}{h}$$

where:

T_E = effective air temperature, $^{\circ}\text{F}$

T_a = air temperature, $^{\circ}\text{F}$

b = absorptivity of surface to solar radiation

I = solar radiation, BTU per sq ft hr

Solar radiation on a horizontal surface is reported in Langleys per day. *

There is an average net loss by long-wave reradiation of about 1/3, so that the average contribution to $T_E(R)$ is:

$$R = 0.67b \frac{3.69L}{24 h}$$

where: L = solar radiation, Langleys per day

The deviation of R from the average may be roughly approximated by a sine wave with a half amplitude of $3R$. The maximum temperature obtained is then

$$T_M = T_A + R$$

where:

T_A = average air temperature, $^{\circ}\text{F}$

$T_V = 0.5 T_R + 3R$

T_R = daily range in air temperature, $^{\circ}\text{F}$

In addition to the effects of temperature, other environmental influences must also be taken into account. Among the most important of the environmental effects is that of water, particularly its influence on the response of paving materials to stress. At the present time the influence of water can be considered to the extent that properties of untreated materials should be measured at water contents corresponding to those obtained from in situ measurements at the time of sampling.

Recently a method has been proposed for fine-grained soils whereby the influence

*One Langley per day = one calory per sq cm day or 3.69 BTU per sq ft day.

of environment (particularly as it influences water content) might be accounted for utilizing considerations of soil moisture suction (11, 12).

Data obtained by Dehlen (13) for specimens obtained from the San Diego Test Road are presented in Figs. 5 and 6. On both of the figures it will be noted there is a distinct relationship between suction and resilient modulus.

Also shown in Fig. 6 are data obtained by Sauer (12) for a glacial till from Saskatchewan (data obtained from Fig. 7). It is interesting to conjecture, at this time, that if one could estimate the ultimate suction profile to be expected under the pavement (e.g. Fig. 5 contains suction profiles, though not necessarily ultimate ones) then one might be in a position to estimate the variation of modulus with depth for analysis purposes (Fig. 5 also illustrates the resilient modulus variation with depth).

It should also be noted that the concept of suction also permits an assessment of distortion of the pavement structure due to volume change in the subgrade. Richards (14) has presented a technique whereby heave or settlement can be estimated provided the suction profile at the time of construction, the equilibrium suction profile, and the moisture content (void ratio) vs matrix suction* relation for the subgrade are known. In effect Richard's procedure can be considered another portion of the distortion subsystem (Fig. 3).

Materials Identification and Selection. Included in this phase are the following considerations:

1. Survey of subgrade soils traversed by the proposed route and the performance of identification and classification tests.
2. Selection of the most economic materials to be used in the construction of the highway.
3. Design of the asphalt concrete mixture to be used.

*Total suction is equal to the sum of matrix (or soil water) suction and osmotic suction. In the absence of dissolved salts, the osmotic suction is zero; for uniform salt concentrations the osmotic suction can be neglected. Under these circumstances, therefore, the total suction can be considered equal to the matrix suction.

As has been emphasized in earlier reports (e. g. 15), the design of the mixture is related to the type of pavement in which the mixture is utilized. Hence, it must be emphatically noted that mixture and structural pavement design must be treated together.

Materials Characterization

Determination of "Elastic" Properties* of Paving Materials. The characterization technique presently utilized as a part of the fatigue subsystem may be classed as a process whereby significant properties are measured to permit prediction of response under special (and/or limited) loading conditions, rather than the process whereby fundamental properties are measured to predict response under any system of applied loads. This latter characterization technique has not been accomplished as yet for conventional paving materials. The difficulty of such a process will be illustrated briefly, later in this section, by showing the type of data merely required to begin to develop a non-linear elastic characterization of subgrade soils (13).

While a number of methods have been developed to describe the "elastic" response of paving materials, the results of a test procedure developed by Seed and Fead (20) for subgrade soils and untreated base and subbase materials is utilized for the characterization process. From the test a resilient modulus is determined. At this point, it should be emphasized that other techniques for measuring such response could also be utilized (e. g. procedures, such as those described by Kallas (21) and by Coffman (22)).

For the clay subgrade soils which have been tested thus far, the resilient modulus is stress-dependent, particularly in the range of stresses to which the subgrade soils of well-designed pavements are subjected (i. e. less than 3 to 5 psi).

*Considerable evidence has been presented in recent years that elastic theory produces, at least to an engineering approximation, a reasonable indication of pavement response to moving wheel loads (15, 16, 17, 18, and 19).

Similarly, the modulus of untreated granular materials has been shown to be dependent on stress and can be expressed either in terms of the confining pressure or the sum of the principal stresses according to the following relationships:

$$M_R = K \cdot \sigma_3^{n'} \text{ or } K'(\theta)^{h'} \dots \dots \dots (3)$$

where:

$$\theta = \sigma_1 + \sigma_2 + \sigma_3$$

Because of such stress dependency, changes in the characteristics and thickness of the asphalt concrete will result in variations in the elastic response of these materials and thereby influence the pavement selection process. Moreover, the presence of water will modify the elastic response of granular materials, e.g. Fig. 8 (23). This appears to be particularly true when the aggregate is completely saturated and has the potential for pore water pressure development, which may increase resilient deformations under load (1). This factor undoubtedly must be considered in analysis of pavements in California containing untreated bases because of the seasonal variations in rainfall leading, in turn, to seasonal variations in water content (1).

For asphalt-bound materials utilizing asphalt cements, stiffness as defined by the relation:

$$S(t, T) = \frac{\sigma}{\epsilon} \dots \dots \dots (4)$$

where:

$S(t, T)$ = mixture stiffness at a particular time of loading
and temperature

σ, ϵ = axial stress and strain respectively

can be used at this stage in time and either measured directly or estimated from the properties of the asphalt contained in the mix (penetration and ring and ball softening point) together with the volume concentration of the aggregate and the percent air voids in the compacted mixture (24, 25, 26, and 27).

For asphalt treated materials using liquid asphalts or asphalt emulsions, additional testing may be required if the materials will be subjected to traffic prior to curing. Characterization utilizing the procedures developed for untreated aggregates may be necessary since these materials in the partially cured state are dependent on stress conditions (28).

To consider non-linear materials response characteristics additional testing will be required. Dehlen (13) has developed a procedure for such characterization and has examined the response of the subgrade soil and asphalt concrete from the San Diego Test Road within this framework.

In this process the stress state is important and in order to minimize testing it is necessary to cover only the range which occurs in a pavement under the anticipated traffic.

Fig. 9a illustrates types of stress paths which might be selected for laboratory testing and Fig. 9b illustrates typical data obtained from a pattern of stressing corresponding to (c) of Fig. 9a.

Results from a complete pattern of stressing are shown in Fig. 10 for an asphalt concrete mixture. This figure illustrates the variation of axial strain corresponding to various stress states in triaxial compression. A similar figure would be required to define the variation of radial strain with stress state.

Fatigue Response of Asphalt Concrete Mixtures. In the design subsystem of Fig. 2, some measure of the fatigue response of asphalt mixtures is required. For thick sections of asphalt concrete this response should be measured by means of the controlled-stress mode of loading (29). For comparatively thin asphalt bound layers (~2 in.) the controlled-strain mode of loading is more appropriate. Available evidence suggests that the fatigue behavior of asphalt concrete can be represented by an equation of the form:

$$N_f = K \left(\frac{1}{\epsilon_{\text{mix}}} \right)^n \dots \dots \dots (5)$$

where:

N_f = stress applications to failure

ϵ_{mix} = tensile strain repeated applied to the mix

K, n = constants depending on mixture characteristics

The coefficient n in the above equation appears to be dependent on mixture stiffness. For the range of stiffnesses encountered in practice, n appears to vary in the range 2 to 6. Data illustrating this point will be presented subsequently. Since stiffness of the asphalt bound layer will vary in the road due to temperature variations, one fatigue curve with a particular slope probably will not suffice to estimate damage development. From a design standpoint this should present no difficulty since only a small increase in input to the subsystem of Fig. 2 is required.

Since pavements are subjected to a range of loadings in practice, a cumulative damage hypothesis is required since fatigue data (defined by equation (5)) are usually determined from the results of simple loading tests. One of the simplest of such hypothesis is the linear summation of cycle ratios. This cumulative damage hypothesis states that fatigue failure occurs when

$$\sum_{i=1}^i \frac{n_i}{N_i} = 1 \dots \dots \dots (6)$$

where:

n_i = number of applications at strain level i

N_i = number of applications to cause failure in simple loading at strain level i

Equation (6) indicates that fatigue life prediction under compound loading becomes a determination of the time at which this sum reaches unity.

Some measure in the scatter of fatigue test data can also be considered at this time.

Pell and Taylor (30) and Kasianchuk (2) have indicated that the distribution function

for fatigue lives at a particular stress level can be represented as logarithmic normal:

$$f(y) = \frac{1}{\sigma^i \sqrt{2\pi}} \left\{ \exp \left[- (y - m^i)^2 / z(\sigma^i)^2 \right] \right\} \dots \dots \dots (7)$$

where:

$f(y)$ = the normal density of Y^{i*}

Y^i = log of the service or fracture life, N^i

m^i = mean of Y^i

σ^i = variance of Y^i

Results of a reanalysis of data developed by Deacon using this approach are shown in Fig. 11. Comparison between the experimentally determined relationship and that estimated on the basis of a logarithmic normal distribution function indicate the reasonableness of this approach.

Data developed by Pell and Taylor (30) and shown in Figs. 12 and 13 also substantiate such an assumption.

Use of this distribution function permits prediction of not only mean fracture or service life but also the life corresponding to any desired confidence level.

Analysis and Evaluation

To estimate the stresses and deformations resulting from moving wheel loads so that the potential for development of fatigue distress can be obtained, a realistic representation of the pavement structure is required.

At this time, the most readily usable method which would appear to represent the behavior of an asphalt pavement under moving wheel loads (at least in the judgment of the authors) is the solution for stresses and displacements in a multilayer elastic system subjected to circular loads (and uniform contact pressures) at its surface (31, 32).

*The superscript, i, refers to a particular strain level.

It should be noted, however, that even though layered system theory has been utilized to estimate stresses and strains for the fatigue subsystem, one must recognize the possibility of improved solution techniques becoming available in the near future. Moreover, as these techniques become available they should, without hesitation, be incorporated in the analysis procedure. It is anticipated, for example, that numerical techniques such as that presented by Dehlen (13) (i. e. the finite element procedure) will find greater utility in the very near future.

For the subsystem shown in Fig. 2, analysis and evaluation consists of the following:

1. Definition of the seasonal variation in the stiffness of the asphalt concrete together with variations in water content (and/or suction) of the underlying untreated materials.
2. Determination of the expected response of the asphalt concrete layer in the trial design section to the action of the range of wheel loads and climatic environment.
3. Prediction of the fatigue life of the trial design under the action of the expected traffic volumes.
4. Evaluation of the trial design with respect to the adequacy of the section in providing the requisite life for fatigue.

If the trial section which has been selected is inadequate or conservative, another trial section is selected and the procedure repeated.

These steps have been programmed for use with a digital computer and the programs are included as an appendix to the report.

From an examination of Fig. 2 it will also be noted that the subsystem provides a guide for the analysis of existing pavements as well as a procedure for design. In the next section the Morro Bay pavement will be analyzed following essentially the format of Fig. 2.

PREDICTION OF SERVICE LIFE — MORRO BAY PAVEMENT

In Report No. TE 67-4 (1) an analysis was presented for the Morro Bay pavement. Since the original analysis was completed, some of the techniques utilized have been modified or improved (2). Accordingly, it was deemed appropriate to reanalyze the Morro Bay project within this modified framework. Results of this reanalysis are presented in this section. For completeness, basic data which had been included in TE 67-4 and which are necessary to the analysis have also been incorporated where appropriate.

Field Testing and Sampling

Traveling Deflectometer deflection data were obtained by the California Division of Highways on March 10, 1964 on sections of State Sign Route 1 near Morro Bay, California (Designation V-SLO-56-C,D). Measurements were made using a 15,000 lb axle load and 90 psi inflation pressure in the test truck tires and the results are summarized in Table 1.

Samples of the materials in the pavement section were taken on December 14 to 16, 1965 and in-place densities and water contents were determined at this time. Table 2 indicates the deflections that were measured at the locations from which these samples were taken.

Table 3 shows the mean values of the in situ physical properties of the materials in the pavement. Also included in this table are the thicknesses of the various layers, as supplied by the Division of Highways.

Laboratory Test Results

Subgrade Soil. Results of repeated load tests on undisturbed samples of the subgrade soil are contained in Fig. 14. The curve shown in this figure represents the mean line drawn through the data points. This material exhibits a modulus which is dependent on the applied stress, with the stress dependence being most marked in the low stress range.

Untreated Aggregate Subbase. Resilient modulus determinations of the subbase material were made using laboratory prepared specimens. Mean density, water content, and degree of saturation are shown in the accompanying tabulations for the specimens tested.

	<u>Mean</u>	<u>Standard Deviation</u>	<u>Coefficient of Variation-percent</u>
Dry density, lb per cu ft	117.0	4.6	3.9
Water content, percent	9.7	0.55	5.7
Degree of saturation, percent	60.0	9.5	15.6

From a comparison of this data with that presented in Table 3 for the in situ measurements, it will be noted that the dry densities are about the same, but that the degree of saturation of the laboratory prepared specimens is less than that for the field samples.

The resilient modulus — sum of principal stresses relationship,

$$M_R = 2900 (\theta)^{0.47} \dots \dots \dots (8)$$

shown in Fig. 15 has a correlation coefficient of 0.884.

Untreated Aggregate Base. Repeated load tests were performed on laboratory prepared specimens of the aggregate base course material. Density, water content, and degree of saturation data for these specimens were as follows:

	<u>Mean</u>	<u>Standard Deviation</u>	<u>Coefficient of Variation-percent</u>
Dry density, lb per cu. ft	113.2	1.45	1.2
Moisture content, percent	8.55	0.59	6.8
Degree of saturation, percent	52.8	3.6	6.8

It will be noted that the average dry density for the laboratory prepared specimens is somewhat less than the average reported for the in-place density measurements (Table 3); in addition the average water content for these specimens was somewhat less than that measured in-place.

Fig. 16 shows the relationship obtained between the resilient modulus and the sum of the principal stresses. The equation:

$$M_R = 3830 (\theta)^{0.53} \dots\dots\dots (9)$$

has a correlation coefficient of 0.907.

Asphalt Concrete Surface. Stiffness data for asphalt concrete specimens obtained from pavement samples are presented in Table 4. These values were determined from deflection measurements made at the start of the fatigue testing (after 200 stress repetitions) and determined from the relationship:

$$S(t, T) = K \cdot \frac{P}{I \cdot \Delta} \dots\dots\dots (10)$$

where:

$S(t, T)$ = flexural stiffness at a particular time of loading and temperature

K = constant depending on loading geometry

P = applied load

I = moment of inertial of beam cross section

Δ = measured center deflection of beam (at 200 stress repetitions)

Both controlled-stress and controlled-strain fatigue tests were performed on specimens obtained from pavement samples and on laboratory prepared specimens composed of essentially the same materials as used in the original construction. To define the potential for distress, however, the controlled-strain test results were selected as discussed in earlier reports (1, 15).

From controlled-strain tests on laboratory prepared specimens of the paving mixture, service lives corresponding to a 50 percent reduction in stiffness were selected as being representative of the behavior of the pavement section. The equation for the curve of strain vs. applications corresponding to this reduction in stiffness is:

$$N_s = 2.78 \cdot 10^{-7} \left(\frac{1}{\epsilon}\right)^{3.38} \dots\dots\dots (11)$$

with a correlation coefficient of 0.87 and a standard error of the estimate of 0.248.

Traffic Data

To obtain traffic information for the Morro Bay Project, it was necessary to combine data from a series of sources.

The following data were abstracted from the annual traffic census of the State of California Division of Highways for a station located near the end of the freeway at Cayucos:

<u>Year</u>	<u>Annual ADT</u>
1963	4700
1964	5900
1965	6100

The ADT used in the following calculations is 5600 which is the mean for the years 1963-65. Additional traffic data were provided by the Materials and Research Department as shown below:

1963 Vehicle Census

Average Daily Traffic — Morro Bay

All Vehicles	3400
Trucks and Buses	282
Percent Trucks and Buses	8.3
Buses	0
2-Axle	120
3-Axle	32
4-Axle* or More	282

*77 percent are 5-axle

For the purposes of the calculations, the number of trucks in each class has been increased proportionally so as to conform to the average ADT of 5600 actually measured.

In order to obtain the appropriate number of applications of each axle load, the following assumptions have been made:

1. 50 percent of the ADT moves in each direction.
2. 100 percent of the commercial vehicles travel in the right lane of the divided highway. This assumption would appear reasonable since Taragin (33) has shown that about 90 percent of commercial traffic travels in the right lane at low traffic volumes.
3. Each vehicle stresses the same point in the traffic lane, i. e., every vehicle tracks the same wheel path. This assumption is somewhat conservative (2).

The axle load distribution was obtained from the statewide W-4 loadometer surveys (All Main U & R) for the years 1961-66. On the basis of this data and the assumptions made above, the monthly axle load applications shown in Table 5 were determined and used in the fatigue calculations.

The daily variation was assumed to conform to a typical pattern exhibited in California Interstate general purpose routes and shown in Fig. 18.

Prediction of Service Life

Using the format shown in Fig. 2 together with the data presented in this section it is possible to make an estimate of the service life for the Morro Bay pavement considering the fatigue mode of distress.

As indicated in Report No. TE 67-4 (1), the reasonableness of the procedure has already been checked against deflections as measured by the Traveling Deflectometer.

Material Properties. In addition to the material properties, summaries of which have been presented earlier, i. e.

1. Subgrade soil. Fig. 14
2. Untreated aggregate subbase Fig. 15
3. Untreated aggregate base. Fig. 16
4. Asphalt concrete (stiffness) Table 4*

*The time of loading employed in the tests, the results of which are shown in Table 4, was 0.1 sec. To obtain stiffnesses corresponding to moving traffic, (0.015 sec. - representative of truck speeds of about 30 mph), the procedure developed by Heukelom and Klomp (26) was utilized. However, the estimations were influenced by the measured data shown in Table 4.

Poisson's ratio for each of the components was assumed to be:

1. Asphalt concrete, at 68°F	0.40
at 40°F	0.35
2. Aggregate (base and subbase)	0.40
3. Subgrade soil	0.50

The service life vs. initial strain relationship as defined by equation (11) was used to represent the fatigue behavior of the asphalt concrete.

Determination of Tensile Strains in the Asphalt Concrete. The tensile strains on the underside of the asphalt concrete layer were determined for several axle loads and for several stiffness values using the five layer computer solution for the elastic layered system. The strains were found to be a maximum in a direction parallel to the direction of travel in the highway under the center of one of the wheels of the dual wheel load.

Fig. 19 indicates the tensile strains as functions of both axle load and stiffness as obtained in these calculations. Tensile strains were interpolated from these curves to obtain values corresponding to the axle load groups for the available traffic data.

Traffic Weighted Mean Stiffness. Using the technique developed by Kasianchuk (2) the traffic weighted mean stiffness was then calculated by weighting the mean stiffness for each hour by the proportion of the average daily traffic experienced during the hour considered. The hourly traffic distribution through the day was a typical curve for a California General Purpose Interstate Route. This hourly variation has already been shown in Fig. 18.

The weather data used and the stiffnesses obtained are shown in Tables 6 and 7.

Stiffness profiles for several months are shown in Fig. 20. These profiles provided the basis for the assumption that this pavement could be adequately represented by a single layer.

The average air temperatures were obtained from readings taken at the Morro Bay Fire Station, with slight corrections to conform to 1931-1960 normals. The daily

temperature range, the average wind velocity, and solar insolation were obtained from the records at Santa Maria. The mean sky cover was taken from the records of the San Francisco International Airport.

Fatigue Life Prediction. Using the linear summation of cycle ratios (Miner's hypothesis) the fatigue life can be estimated. A computer program to do this is included in Appendix B as a part of the design subsystem. The step-by-step procedure used in this program and applied to the Morro Bay pavement is:

1. The tensile strain against stiffness curves for each axle load group (Fig. 19) were stored.
2. The tensile strain under each wheel load magnitude was obtained from the appropriate relationship by a numerical interpolation procedure at the stiffness value representing the month under consideration.
3. The fatigue life that would be expected under simple loading at that strain level was determined from the fatigue curve developed for the material. At the same time, the fatigue life corresponding to a 90 percent confidence level was obtained making use of the assumption of a log normal distribution of fatigue life at any strain level.
4. The cycle ratio for each of the strain levels (axle load groups) was formed using the number of applications per month of each axle load group (n_i) shown in Table 5 and the fatigue life at each strain level determined above (N_i).
5. The sum of the cycle ratios per month was taken and the process repeated for consecutive months until first, the sum at the 90 percent confidence level reached unity, and then, the sum at the mean level reached unity.
6. The fatigue life predictions at the two levels of confidence were taken as the times at which these values were obtained.

Using the data presented herein, the shortest probable fatigue life, at a 90 percent level, was calculated to be 0.8 years. The mean fatigue life of the Morro Bay pavement was predicted to be 1.8 years.

Discussion

Assuming that this pavement was opened to traffic on the completion date of the paving contract in October, 1963, some distress should have been evident at the time of the first sampling in December, 1965. This was not the case. A second sampling of the pavement in August, 1967 did, however, show some effects of the onset of fatigue. Fig. 21 shows the crack pattern observed on the underside of the asphalt concrete slab specimens recovered at one of the sample locations at this time.

The condition of these samples conforms to that which would be anticipated after some fatigue damage has occurred. The cracks, as suggested by the location of the maximum strain values, have initiated at the bottom of the asphalt concrete and have progressed upward in the layer, but have not yet reached the surface of the pavement. This condition is approximately the same as that which was observed in the laboratory fatigue tests in the controlled-strain mode of loading, when they had attained their service lives, as defined by a 50 percent reduction in stiffness. In both the laboratory and field situations, then, the effects of this level of fatigue damage is visible only near the location of the maximum repeated strain. It should also be noted that the visible manifestation of this level of damage in the actual pavement will be effectively masked by the texture of the thin, open-graded surface course overlying the asphalt concrete in the Morro Bay pavement.

Some confidence in the use of the fatigue subsystem is provided by the condition of these samples. Although the predicted life is shorter than that which has actually been experienced in the pavement studied, the type of distress shown does conform to that which is anticipated. The conservative nature of the prediction is to be expected on the basis of the discussion of the method, but several features of this particular analysis

deserve comment as special contributors to the discrepancy shown between the analytical and the actual results.

One probable cause of the difference between the actual and predicted conditions of the pavement lies in the use of a wheel load distribution based on the results of statewide loadometer surveys for the fatigue life simulation. While the use of such data is suggested for the design situation in which no other information is available, a survey of the traffic actually using the facility is preferred when analyzing an in-service pavement such as Morro Bay. Considering the nature of this highway and the area which it serves, it is probable that the statewide data overestimate the proportion of heavy wheel loads to which the actual pavement is subjected, resulting, in turn, in an overestimate of the calculated rate of damage accumulation. (Note: a similar comment could also be made with respect to the design analysis, emphasizing the necessity of accurate traffic predictions.)

A second reason for the difference between predicted and actual behavior is the use of an average condition for the degree of saturation of both the base and subbase materials. Although it is probable that conditions more severe than those assumed for this estimate have occurred during the life of the pavement, it is equally probable that less severe conditions could be assumed for longer time periods within the year. Insufficient field data, however, were available to account for this probability. This point also emphasizes the importance of properly defining the conditions of the paving materials in order to make a reasonable assessment of the response of the pavement to load. Since the computer is being utilized it would involve only a small amount of additional input to consider the influence of moisture on the resilient response of granular materials and, in effect, would merely require the stipulation of a family of curves (e.g. Fig. 8) rather than a single curve (e.g. Fig. 16).

Finally, the difference between estimated and observed performance may also be attributed to the use of one laboratory determined fatigue curve. For example, it is

possible that the laboratory fatigue test imposes a more severe load condition on the asphalt concrete than is experienced in the actual pavement resulting in a laboratory fatigue curve which is conservative. (Bazin and Saunier (34) have suggested that the use of laboratory data may result in estimates of fatigue lines which are $1/4$ to $1/2$ of those in actual pavements.) In this regard, the use of the one laboratory determined curve does not permit consideration of crack propagation which undoubtedly will vary with temperature. Generally, the laboratory determined curve for the conventional type of fatigue equipment will have comparatively few load repetitions associated with crack propagation since from the time in which the crack is initiated until the time at which failure occurs is comparatively short. This may not be the case in the actual pavement. A schematic diagram is presented in Fig. 22 to illustrate this point. In effect, in thin pavements, the fatigue life is probably underestimated during the summer months when there is considerable number of load repetitions associated with a slow rate of crack propagation (i. e. curve furthest to right in Fig. 22).

In spite of these points, however, the application of the procedures embodied in the fatigue subsystem shown in Fig. 2 has provided a reasonable analysis of the observed conditions in the Morro Bay pavement considering a number of factors known to lead to a reduction in pavement serviceability with time. Accordingly, one can, with some confidence, propose the use of this analytical procedure to assist in the design of asphalt pavements.

INFLUENCE OF MIXTURE VARIABLES ON THE FLEXURAL FATIGUE PROPERTIES OF ASPHALT CONCRETE

Table 8 contains a summary of a number of variables influencing fatigue response. Of those variables listed only the effects of mixture stiffness, void content, and asphalt content will be discussed in this report. Moreover, the testing was conducted at only one temperature, 68°F, and only a controlled-stress procedure was utilized.

Materials

A list of mixture variables which have been studied is shown in Table 9.

Asphalts used for the laboratory study were supplied by Chevron Asphalt Company and as-received properties of the asphalts are shown in Table 10. Properties of the asphalts recovered from the various mixtures were also determined; these results are shown in Table 11.

Four different aggregate gradings were utilized as seen in Table 9. Three of the gradings correspond to State of California specifications for 1/2-in. maximum size aggregate and represent the extreme fine grading, the extreme coarse grading, and the middle of the medium grading. A grading corresponding to that specified in the British Standard 594 specification was also utilized. These four gradations are shown in Fig. 23 while other characteristics of the aggregates are summarized in Table 12.

Specimens for the laboratory fatigue testing were prepared by kneading compaction. Details of the preparation procedure have been reported elsewhere (3). Table 13 contains a summary of the asphalt contents used in the mixtures and also contains a summary of asphalt contents which would be selected for these mixtures based on State of California requirements for a Type B aggregate (35).

Table 14 presents a summary of the air void content data for each of the test series and Table 15 contains a summary of controlled-stress fatigue tests performed at 68°F.

Influence of Air Void Content

The influence of void content on fatigue response has been emphasized by Saal and

Pell (36) and in earlier reports related to this project (e. g. (15)).

Fig. 24 illustrates the influence of air void content on fatigue life at 68°F at a stress level of 150 psi for mixes with the granite aggregate and gradings conforming to the B.S. 594, California fine, and California coarse requirements. As with earlier test data, these results emphasize the importance of proper compaction in order to obtain good performance characteristics.

Results of linear regression analyses (fatigue life as the dependent variable) are superimposed on the data in Fig. 24. The regression lines, which have been plotted together in Fig. 24, indicate that a smaller change in void content is required to change the fatigue life by a specific amount for the California graded mixes (4 to 6 percent increase in air voids to reduce the fatigue life by one order of magnitude) than is required for the British Standard mix (10 percent increase to reduce fatigue life by one order of magnitude).

These data suggest that the structure of the voids (i. e. , size, shape, degree of inter-connection) as well as their absolute volume is of importance. For example, for mixes with the same absolute volume of voids, the size of the void may be important in that the presence of a very large void will produce a greater reduction in the load carrying solid cross section than several smaller voids which are likely to be scattered throughout the specimen. In addition, from a consideration of stress concentrations due to voids (37), the more elongated the void, the greater the stress concentration at the edge of the void.

The difference in fatigue life noted between the British and California graded mixes may thus in part be due to the size and shape of the voids in the two types of mixes since visual examination indicated that the British mix contained smaller size voids than the State of California fine and coarse mixes.

Influence of Mixture Stiffness

Stiffness as used herein is the relationship between stress and strain measured during the conduct of the flexural fatigue test and is dependent both on time of loading and

temperature. In addition, stiffness is dependent upon air void content, aggregate grading, aggregate type, asphalt type and amount, and the stress level at which it is measured.

As has been indicated earlier, stiffness affects the fatigue response of mixtures in the controlled-stress mode of loading; accordingly it is desirable to assess the effects of stiffness on fatigue life.

Data presented by Deacon (38) and Bazin and Saunier (34) indicate that stiffness is reduced with an increase in air void content. Fig. 26 illustrates such trends for the mixes whose fatigue life vs. void content data were presented in Fig. 24. Regression lines through the data show an increase in stiffness with reduction in air void content. Considering the change in void content required to change the fatigue life by one order of magnitude results in changes in stiffness as follows for the three mixes:

<u>Mix</u>	<u>Change in Void Content to Change Fatigue Life By One Order of Magnitude</u>	<u>Change in Stiffness</u>
British Standard	10%	375,000 psi
California Fine	~ 4%	130,000
California Coarse	6%	130,000

Thus part of the increase in fatigue life in the controlled-stress mode of loading due to decrease in air void content is due to the increase in stiffness resulting from this reduction.

To investigate the influence of stiffness on fatigue life, data from five mixes containing granite aggregate and with the same asphalt content (6 percent) were analyzed. Air void contents ranged from 4 to 6 percent (Table 14) with an average value of about 5.5 percent. The data for all mixes were grouped together at each of the stress levels utilized in the test program and linear regression lines were obtained for stiffness vs. fatigue life (fatigue life as the dependent variable). Fig. 27 illustrates the resulting relationships each of which had the following statistics:

<u>Stress Level, psi</u>	<u>Correlation Coefficient</u>	<u>Standard Error of Estimate</u>
150	.952	.167
100	.916	.227
75	.746	.290

By interpolation from Fig. 27, stress vs. fatigue life relationships were obtained for a range in stiffness of 150,000 psi to 700,000 psi and are shown in Fig. 28. In this figure it will be noted that as the stiffness increases, the fatigue life at a particular stress level increases, and that slope of the line also changes (in this case from 2.2 to 3.8* for the range of stiffness examined).

Strain vs. fatigue life relationships can also be obtained from the data presented in Fig. 27 utilizing the transformation:

$$\epsilon_{\text{mix}} = \sigma_{\text{mix}} / S_{\text{mix}} \dots \dots \dots (12)$$

where:

ϵ_{mix} = mixture strain — in. per in.

σ_{mix} = applied stress — psi

S_{mix} = mixture stiffness — psi

Results of such an analysis are presented in Fig. 29 for stiffnesses ranging from 200,000 to 500,000 psi. For this range in stiffness the data appear to be represented by a single relationship.

If a wider range in stiffness is considered, a single line will probably no longer represent the relation between strain and load applications. Such a point has been already illustrated in Fig. 22 and discussed in the previous section.

The mixes whose data have been presented in Figs. 27 and 29 also permit such an analysis to be at least partially developed; such results are presented in Fig. 30. While the shape of the curves shown in Fig. 30 are not precisely the same as those shown

*The slope is represented by the coefficient n of equation (5).

schematically in Fig. 22, the slope of the strain vs. cycles to failure relationship does change with change in stiffness as hypothesized in the figure. It is interesting to note on this plot (Fig. 30) that the differences in fatigue lives due to stiffness differences are not as large as indicated on the stress vs. fatigue life plot of Fig. 28.

Fig. 27 can also be used to ascertain the variation in fatigue life due to changes in mixture stiffness independent of large variations in air void content.

As shown previously the fatigue life of the California fine graded mix is increased an order of magnitude at a stress level of 150 psi by decreasing the air voids by approximately 4 percent, (Fig. 24). Assuming that the air void content is reduced from 8 percent to 4 percent, one would expect an increase in stiffness from 180,000 psi to 310,000 psi for the tests performed at 150 psi, (Fig. 26). This change in stiffness increases the fatigue life from 840 to 5,300 applications which is less than one order of magnitude. Correspondingly, the fatigue life of the State of California coarse graded mix will increase less than an order of magnitude for variation in air void content from 8.5 to 3.0 percent. Thus the change in fatigue life due to variations in air void content cannot wholly be explained by the change in stiffness produced by the same air void variation. Increased air void content tends to reduce the load carrying cross section of the specimen and to create additional locations for the formation of stress concentrations as noted earlier, thus contributing to a reduction in stiffness and fatigue life. These data reinforce those presented in TE 66-6 emphasizing the importance of proper field compaction!

Influence of Asphalt Content

To investigate the effect of asphalt content on fatigue behavior, a basalt aggregate from two different manufacturers but the same geological formation was graded to meet the California 1/2-in. maximum medium specification and mixed with a 60-70 penetration asphalt cement. Asphalt contents varied from 5.3 to 8.7 percent by dry weight of aggregate. Tests were performed at a stress level of 150 psi. Average values

of stiffness, strain, air voids, and fatigue life for the various asphalt contents are shown in Table 16.

Results of these tests suggest that a maximum fatigue life at a stress level of 150 psi will occur at an asphalt content of 6.7 percent (Fig. 31*). Fig. 32 indicates that maximum fatigue life occurs at the asphalt content resulting in the highest stiffness. Thus, as previously suggested by Pell (39) and Jimenez (40), a peak asphalt content exists for optimum fatigue life; and as shown in Fig. 32, this peak asphalt content also produces the mixture with the highest stiffness. It is interesting to note that the location in terms of asphalt content cannot be predicted from use of the nomograph developed by Heukelom and Klomp (26), since the nomograph will give values of decreasing stiffness with increasing asphalt content (Fig. 33).

As shown above, the optimum asphalt content based on fatigue behavior would be selected at 6.7 percent; however, as seen in Table 13, this is about 0.8 percent above the asphalt content that would be selected on the basis of stability requirements.

As noted in Table 15, fatigue tests at two different asphalt contents have been performed on the medium graded granite aggregate. Tests at an asphalt content of 5.2 percent (representative of an asphalt content based on stability requirements) result in an average fatigue life of 19,925 repetitions at a stress level of 75 psi; while the results in the mix with 6.0 percent asphalt show an average fatigue life of 73,310 at the same stress level. These two sets of results emphasize that the optimum asphalt content based on stability requirements for this rough textured aggregate is lower than that required for best fatigue results.

Increased use of thick sections of asphalt concrete in pavements will allow for the selection of the asphalt content to be based on two criteria. The upper portion of the

*It should be noted that only the mean values of the data presented in Table 15 have been plotted in Fig. 31.

asphalt section may be based on stability requirements whereas the remaining portion of the section may be designed for asphalt contents which result in optimum fatigue behavior (2). Thus it will become important to perform fatigue tests which identify the peak asphalt content necessary for optimum fatigue response for a certain mix. It will then be necessary to describe a mixture strain vs. fatigue life relationship for a mix of the chosen asphalt content so that damage due to fatigue may be precluded.

The above test series used to study the effect of asphalt content on fatigue life also illustrates the steps required to select an asphalt content to optimize fatigue response. These test results together with relationships developed by Pell (39) may be used to develop the necessary mixture strain vs. fatigue life relationship which is a necessary part of this design procedure.

Pell has suggested that the influence of a variation in asphalt content may be taken into account by using the following expressions:

$$N_f = K_3 (1/\epsilon_{bit})^{n_1} \dots \dots \dots (13)$$

where:

K_3, n_1 = constants

ϵ_{bit} = tensile strain in the bitumen, in. per in.

The strain in the bitumen may be obtained by using the following

asphalt section may be based on stability requirements whereas the remaining portion of the section may be designed for asphalt contents which result in optimum fatigue behavior (2). Thus it will become important to perform fatigue tests which identify the peak asphalt content necessary for optimum fatigue response for a certain mix. It will then be necessary to describe a mixture strain vs. fatigue life relationship for a mix of the chosen asphalt content so that damage due to fatigue may be precluded.

The above test series used to study the effect of asphalt content on fatigue life also illustrates the steps required to select an asphalt content to optimize fatigue response. These test results together with relationships developed by Pell (39) may be used to develop the necessary mixture strain vs. fatigue life relationship which is a necessary part of this design procedure.

Pell has suggested that the influence of a variation in asphalt content may be taken into account by using the following expressions:

$$N_f = K_3(1/\epsilon_{bit})^{n_1} \dots \dots \dots (13)$$

where:

K_3, n_1 = constants

ϵ_{bit} = tensile strain in the bitumen, in. per in.

The strain in the bitumen may be obtained by using the following equation:

$$\epsilon_{bit} = \frac{\epsilon_{mix}}{\alpha B_v} \dots \dots \dots (14)$$

where:

α = factor depending on amount of filler or voids present in the mix, or both

$B_v = 1 - C_v$; volume concentration of bitumen

C_v = volume concentration of aggregate

Thus assuming $\alpha = 1$ and using appropriate values of B_v for the various asphalt contents, the bitumen strain may be calculated from the measured mixture strain.

Computed values of bitumen strain have been plotted vs. fatigue life and the results are shown on Fig. 34 together with the mean regression line (determined with the fatigue life as the dependent variable). The resulting regression equation

$$N = 1.6 \times 10^{-4} (1/\epsilon_{\text{bit}})^{3.08} \dots\dots\dots (15)$$

is of the same form as equation (13) and may be converted into a mixture strain vs. fatigue life equation

$$N_f = K_1 (1/\epsilon_{\text{mix}})^{n_1} \dots\dots\dots (16)$$

by the following technique for any selected asphalt content.

Substituting equation (14) into equation (13) results in the following relationship:

$$N_f = K_3 \left(\frac{\alpha B_v}{\epsilon_{\text{mix}}} \right)^{n_1} \dots\dots\dots (17)$$

Rearranging equation (17) gives

$$N_f = K_3 (\alpha B_v)^{n_1} \left(\frac{1}{\epsilon_{\text{mix}}} \right)^{n_1} \dots\dots\dots (18)$$

and thus

$$N_f = K_1 \left(\frac{1}{\epsilon_{\text{mix}}} \right)^{n_1} \dots\dots\dots (16)$$

with

$$K_1 = K_3 (\alpha B_v)^{n_1} \dots\dots\dots (19)$$

As an example, an asphalt content of 6.2 percent has been selected for the mix containing the basalt aggregate; this asphalt content results in a value of B_v equal to 0.147. Using the above techniques with α again equal to one, the following equation results

$$N_f = 6.32 \times 10^{-7} (1/\epsilon_{\text{mix}})^{3.08} \dots\dots\dots (20)$$

Development of the above relationship has been dependent upon the assumption that bitumen strain may be calculated from equation (14) with α equal to one, together with the assumption that fatigue behavior may be represented as a straight line on a log-log

plot both in terms of mixture strain and bitumen strain vs. fatigue life. It seems reasonable to assume that both the fatigue life vs. bitumen and fatigue life vs. mixture strain relationships are linear on a log-log plot; therefore, to check the validity of the assumptions necessary to calculate bitumen strain from mixture strain, an additional series made with the same aggregate, aggregate grading, and asphalt type with a 6.2 percent asphalt content was tested. As seen in Fig. 35 the resulting relationship from tests performed on samples with 6.2 percent asphalt

$$N_f = 1.34 \times 10^{-7} (1/\epsilon_{mix})^{3.22} \dots\dots\dots (21)$$

agrees well with equation (20) above which in turn was based on tests performed with asphalt contents ranging from 5.3 to 8.7 percent.

Thus the above procedure appears to allow the designer to perform tests over a range of asphalt contents so that an optimum asphalt content may be selected to minimize fatigue distress. As shown, the longest fatigue life occurs at an asphalt content where maximum stiffness occurs.* Furthermore, these same tests may in turn be used to predict the mixture strain vs. fatigue life relationship for any selected asphalt content. It should also be noted that the maximum stiffness while producing optimum fatigue behavior also reduces somewhat the strain in the pavement due to wheel load (2).

Comparison of California and B. S. 594 Mix

A mix conforming to the British specifications was prepared and tested. The mixture gradation and asphalt content conformed insofar as possible to that used by Pell (39) for a test series for which extensive data were available. In this investigation a crushed granite aggregate and a 33 pen. asphalt were used for the mixes whereas Pell's data were obtained for a mixture containing a crushed gravel and limestone filler with a 43 pen. asphalt.

*It must be emphasized that this response is obtained in the controlled-stress mode of loading.

A comparison of the data is shown in Fig. 36. Individual data points appear to be scattered among each other; however, regression lines (with fatigue life as the dependent variable) result in two distinct lines with slopes of 6.05 and 3.38 for the crushed gravel (Pell) and crushed granite (Univ. of Calif.) mixes respectively.

In general, results of tests performed by Pell have shown slopes of the order of 5 or 6, while tests conducted for this study have resulted in slopes of approximately 3.0. Several possible reasons for this discrepancy exist and will be discussed at this time.

Pell's tests were performed utilizing a rotating cantilever loading system while tests at the University of California made use of a four-point bending machine. Thus Pell's specimens were subjected to reversal of extreme fiber stress and strain while specimens tested with the flexural apparatus did not undergo this reversal.

Pell determined the slopes of the fatigue diagrams from the average of two linear regressions, one regression considering fatigue life as the dependent variable while the second regression considering fatigue life as the independent variable. Regression lines for this study have been determined only by assuming fatigue life to be the dependent variable. Linear regression lines with fatigue life equal to the independent variable resulted in flatter slopes than lines with fatigue life equal to the dependent variable for the results of all mixes included in this report. Accordingly, Pell's averaging technique would result in a slightly flatter slope.

Pell's strain vs. fatigue life results were obtained by using the nomograph stiffness (26) which, as he has noted, may be in error by factor of two. Thus, the slope of the stress vs. fatigue life and strain vs. fatigue life plot will be identical for the results of a particular mix at a single temperature. Data developed by Epps (3) show in general that regression lines obtained from stress vs. fatigue life data result in flatter slopes; hence, if the nomograph stiffnesses were used for these mixes to obtain the strain vs. fatigue life relationships, the slopes for these lines would also be flatter.

The nomograph stiffness makes no provision for stiffness to be stress dependent; however, measured stiffness used in the test series reported herein incorporates the dependence of mixture stiffness on stress. Pell (39) has suggested that if stiffness is considered to be a function of the applied stress intensity, the resulting strain vs. fatigue life line will be slightly steeper for controlled-stress tests than if the assumption was made that stiffness has no dependency upon applied stress magnitude. Furthermore, Deacon (38) has shown that the stress vs. fatigue life plot and the strain vs. fatigue life plot cannot be simultaneously linear if the stiffness is dependent upon the applied stress magnitude. However, it has been assumed that both stress vs. fatigue life and strain vs. fatigue life plots are linear on the log-log representation.

The role of stiffness and slope is not clear. Pell suggests that a mix tested at different temperatures will result in a single line on the strain vs. fatigue life plot; however, he suggests that a steeper slope may result for mixes made with soft asphalts with low stiffness values and thus longer crack propagation times. Tests performed at different temperatures result in specimens of varying stiffnesses being tested. As suggested previously, tests at higher temperatures because of lower mixture stiffness may result in fatigue lines with steeper slopes. Since the majority of Pell's tests were performed at 10°C (50°F) and since the tests performed in this investigation were at a higher temperature it does not seem unreasonable that a steeper slope of the fatigue diagram would be obtained for the granite aggregate mix.

It is interesting to note that the results of Bazin and Saunier (34), which were apparently regressed with fatigue life as the dependent variable, also exhibit slopes near 3.0 for dense graded mixes made with the softer asphalt.

Using a statistical test (Table 17), the null hypothesis that the slope of the regression lines for the studies reported herein are equal to 5 must be rejected at the significance level of 95. Thus the slopes of the lines resulting from tests performed in this study are not of the order of 5.0 to 6.0 as has been suggested by Pell. These differences moreover do not appear unreasonable in the light of the discussion presented herein.

Figs. 37 and 38 show comparisons of the fatigue relationships for the California medium-graded granite mix made with a 40-50 penetration asphalt and the granite mix graded according to the British requirements and tested in this laboratory. The British mix has a mean stiffness of 570,000 psi and an average air void content of 5.4 percent while the California mix has a stiffness of 656,000 psi and an air void content of 4.7 percent. However, the British mix, even with its lower stiffness and higher air void content, provides a longer fatigue life at strain levels expected in pavements. Part of the observed difference may be due to the lower asphalt content for the California mix. As suggested before, however, the structure of the air voids may also be an important factor leading to part of the difference in fatigue life observed between these two mixes.

It would appear that the British designed mix utilizing a harder asphalt and a larger asphalt content tends to give better fatigue response than a comparable American mix. While the effect of grading is not clearly defined; the British grading appears to produce an air void structure which does not influence the fatigue behavior of these mixes to the same degree as for the American dense graded mixes. These data would appear to be substantiated by the results of field trials in South Africa (41), accordingly, it would appear worthwhile to consider such a mix in an experimental paving project. * Because of the high asphalt content and the fine texture which results from rolling of this type of mixture, it should initially be considered for use as an asphalt bound base rather than as a surface course.

*Some care may be required in placing a mix of this type in the field since it appears to behave differently in the compaction process than mixes of the type normally used in California.

SUMMARY

In this report, a subsystem of the pavement design system has been presented to consider the fatigue mode of distress. The proposed procedure permits the incorporation of realistic material properties (in the engineering sense) within the framework of multi-layer elastic theory (at the present time) to define the potential for cracking of the pavement structure under repetitive loading. As indicated in the report, the procedure can be used either for design purposes or for checking the adequacy of existing pavements.

In using the procedure for checking the Morro Bay pavement, distress which had actually occurred was predicted. However, the time period in which cracking was estimated to develop was somewhat shorter than that which actually occurred in service, (approximately 2 years vs. some unknown time period in the range 3 to 3-1/2 years*).

The difference could be in part due to:

1. lack of precise truck traffic information for the pavement section;
2. the use of average conditions for the degree of saturation of the untreated base and subbase materials rather than considering potential seasonal variations in these characteristics;
3. the assumption that one fatigue curve is applicable for a range in temperatures rather than considering fatigue response to be dependent on stiffness (thereby permitting more realistic consideration of damage development associated with crack propagation).

In spite of these limitations, the system has been shown to be responsive to actual conditions since, as noted above, distress which was subsequently observed was predicted in advance. The strength of such a system would appear to lie in its usefulness as a design tool since it has the potential to consider a number of factors not utilized

*This is merely an estimate since no cracking was evident at the time of the first samples in December 1965 (about 2 years from the opening of the pavement). However, it could have occurred at any time thereafter.

in present day design procedures. It should also be emphasized that this type of approach has not been designed to replace existing techniques but rather to be used in conjunction with existing procedures.

Relative to the data on mix variables, in tests of the controlled-stress type, stiffness, as has already been emphasized, is an important mix variable. In the light of the Morro Bay project and from the data presented in the immediately preceding section it appears necessary to develop fatigue data at higher temperatures (lower stiffnesses) than those which have been utilized thus far in the project. This would appear particularly necessary in order to analyze the performance of comparatively thin pavements.

The data also indicate that a worthwhile field experiment would be to construct an asphalt-bound base course utilizing a mix similar to that suggested by the B. S. 594 specifications.

REFERENCES

1. Monismith, C. L., D. A. Kasianchuk, and J. A. Epps, Asphalt Mixture Behavior in Repeated Flexure: A Study of an In-Service Pavement Near Morro Bay, California. Report TE 67-4, University of California, Berkeley, Soil Mechanics and Bituminous Materials Research Laboratory, 1967.
2. Kasianchuk, D. A., Fatigue Considerations in the Design of Asphalt Concrete Pavements. Ph.D. Dissertation, University of California, Berkeley, 1968.
3. Epps, J. A., Influence of Mixture Variables on the Flexural Fatigue and Tensile Properties of Asphalt Concrete, Ph.D. Dissertation, University of California, Berkeley, 1968.
4. Finn, F. N., W. R. Hudson, B. F. McCullough, and K. Nair, "An Evaluation of Basic Material Properties Affecting Behavior and Performance of Pavement Systems." Paper presented at annual meeting of the Highway Research Board, 1968.
5. Hutchinson, B. F. and R. C. G. Haas, "A System Analysis of the Highway Pavement Design Process." in Design and Performance of Pavement Systems, Highway Research Record 239, Highway Research Board, 1968.
6. California Division of Highways, "Test Method No. 301" in Materials Manual 1, 1963.
7. U.S. Corps of Engineers, Flexible Airfield Pavements, EM 1110-45-302, Pt. 12, 1958.
8. The Asphalt Institute. Thickness Design, Manual Series No. 1, College Park, Maryland, 1963.
9. Factors Involved in the Design of Asphaltic Pavement Surfaces, NCHRP Report 39, Highway Research Board, 1967.
10. Barber, E. S., "Calculation of Maximum Pavement Temperatures from Weather Reports," in Fundamental and Practical Concepts of Soil Freezing, Bulletin 168, Highway Research Board, 1957.
11. Richards, B. G., Soil Water and its Effect on Soil Engineering Parameters, Research Paper 102, Australia, CSIRO, Div. of Soil Mechanics, 1968.
12. Sauer, E. K. and C. L. Monismith, "The Influence of Soil Suction on the Behavior of a Glacial Till Subjected to Repeated Loading," in Moisture Responses, Underclay Development, and Frost Action, Highway Research Record 215, Highway Research Board, 1968.
13. Dehlen, G. L., The Effect of Non-Linear Material Response on the Behaviour of Pavements Subjected to Traffic Loads. Ph.D. Dissertation, University of California, 1969.
14. Richards, B. G., "Moisture Flow and Equilibria in Unsaturated Soils for Shallow Foundations," in Permeability and Capillarity of Soils, STP 417, American Society for Testing and Materials, 1967.

15. Gusfeldt, K. H. and K. R. Dempwolff, "Stress and Strain Measurements in Experimental Road Sections Under Controlled Loading Conditions," Proceedings, Second International Conference on the Structural Design of Asphalt Pavements, University of Michigan, 1967.
16. Klomp, A. J. G. and Th. W. Neisman, "Observed and Calculated Strains at Various Depths in Asphalt Pavements," Proceedings, Second International Conference on the Structural Design of Asphalt Pavements, University of Michigan, 1967.
17. Nijboer, L. W. and J. Delcour, "Testing Flexible Pavements Under Normal Traffic Loadings by Means of Measuring Some Physical Quantities Related to Design Theories," Proceedings, Second International Conference on the Structural Design of Asphalt Pavements, University of Michigan, 1967.
18. Brown, S. F. and P. S. Pell, "An Experimental Investigation of the Stresses, Strains, and Deflections in a Layered Pavement Structure Subjected to Dynamic Loads," Proceedings, Second International Conference on the Structural Design of Asphalt Pavements, University of Michigan, 1967.
19. Seed, H. B., F. G. Mitry, C. L. Monismith, and C. K. Chan. Prediction of Flexible Pavement Deflections from Laboratory Repeated-Load Tests, NCHRP Report 35, Highway Research Board, 1967.
20. Seed, H. B. and J. W. N. Fead, "Apparatus for Repeated Loading Tests on Soils," Soils - 1959 Annual Meeting, STP, No. 254, American Society for Testing and Materials, 1959, pp. 78-87.
21. Kallas, B. F. and J. C. Riley, "Mechanical Properties of Asphalt Pavement Materials," Proceedings, Second International Conference on the Structural Design of Asphalt Pavements, University of Michigan, 1967.
22. Coffman, B. S., "Pavement Deflections from Laboratory Tests and Layer Theory," Proceedings, Second International Conference on the Structural Design of Asphalt Pavements, University of Michigan, 1967.
23. Shifley, L. H. and C. L. Monismith, Test Road to Determine the Influence of Subgrade Characteristics on the Transient Deflections of Asphalt Concrete Pavements, Report No. TE 68-5, University of California, Berkeley, August 1968.
24. van der Poel, C., "A General System Describing the Viscoelastic Properties of Bitumens and Its Relation to Routine Test Data," Journal of Applied Chemistry, May 4, 1954, pp. 221-236.
25. van der Poel, C., "Road Asphalt," in Building Materials - Their Elasticity and Inelasticity, M. Reiner, ed., New York, Interscience Publishers, 1954.
26. Heukelom, W. and A. J. G. Klomp, "Road Design and Dynamic Loading," Proceedings, Association of Asphalt Paving Technologists, v-1, 33, 1964, pp. 92-125.
27. Van Draat, W. E. F. and P. Sommer, "Ein Gerät zur Bestimmung der Dynamischen Elastizitätsmoduln von Asphalt," Strasse und Autobahn, Vol. 35, 1966.

28. Terrel, R. L. and C. L. Monismith, "Evaluation of Asphalt-Treated Base Course Materials," Proceedings, The Association of Asphalt Paving Technologists, vol. 37, 1968, pp. 159-199.
29. Monismith, C. L. and J. A. Deacon, "Fatigue of Asphalt Paving Mixtures," ASCE Transportation Engineering Journal, May, 1969. pp. 317-346.
30. Pell, P. S. and I. F. Taylor, "Asphaltic Road Materials in Fatigue", Proceedings, The Association of Asphalt Paving Technologists, vol. 38, 1969.
31. Warren, H. and W. L. Dieckmann, Numerical Computation of Stresses and Strains in a Multiple-Layer Asphalt Pavement System, International Report, Unpublished, Chevron Research Corporation, 1963.
32. Peutz, M. G. F., H. P. M. van Kempen, and A. Jones, "Layered Systems Under Normal Surface Loads," Highway Research Record 228, Highway Research Board, 1968.
33. Taragin, A., "Lateral Placement of Trucks in Two-Lane Highways and Four-Lane Divided Highways," Public Roads, Vol. 30, no. 3, 1958, pp. 71-75.
34. Bazin, P. and J. Saunier, "Deformability, Fatigue, and Heating Properties of Asphalt Mixes," Proceedings, Second International Conference on the Structural Design of Asphalt Pavements, University of Michigan, 1967.
35. California. Division of Highways. "Test Method No. 304," in Materials Manual, 1, 1963.
36. Saal, R. N. J. and P. S. Pell, "Fatigue of Bituminous Road Mixes," Kolloid-Zeitschrift (Darmstadt), vol. 171, 1960, pp. 61-71.
37. Tons, E. and E. M. Krokosky, "Effect of Microaggregates on Tensile Strength of Bituminous Concrete," Proceedings, Association of Asphalt Paving Technologists, Vol. 32, 1963.
38. Deacon, John A., Fatigue of Asphalt Concrete. Graduate Report, Institute of Transportation and Traffic Engineering, University of California, Berkeley, 1965.
39. Pell, P. S., "Fatigue of Asphalt Pavement Mixes," Proceedings, Second International Conference on the Structural Design of Asphalt Pavements, 1967.
40. Jimenez, R. A., An Apparatus for Laboratory Investigations of Asphalt Concrete Under Repeated Flexural Deformations. A report submitted to the Texas Highways Department, College Station, The Texas Transportation Institute, 1962.
41. Williams, A. A. B. and G. L. Dehlen, "The Performance of Full-Scale Base and Surfacing Experiments on National Route 3-1, at Key Ridge After the First Six Years," Proceedings, First Conference on Asphalt Pavements for Southern Africa, Durban, South Africa, August 1969.

TABLE 1 — DEFLECTION SURVEY RESULTS*

Location		Mean Deflection in.	Std. -Dev.	Eightieth Percentile Deflection	Near Sample Location No.
STA 620-630,	NBTL-IWT	.0229	.0042		
	NBTL-OWT	.0268	.0052	.0312	Loc. 1
	NBPL-LWT	.0197	.0023	.0216	Loc. 2
	NBPL-RWT	.0223	.0032		
STA 102-92,	SBTL-IWT	.0156	.0024		
	SBTL-OWT	.0163	.0020		
	SBPL-LWT	.0160	.0013		
	SBPL-RWT	.0165	.0020	.0181	Loc. 3
STA 715-725,	NBTL-IWT	.0159	.0009		
	NBTL-OWT	.0197	.0013	.0208	Loc. 4
For all data		.0192	.00452	.023	

*March 1964

TABLE 2 — TRAVELING DEFLECTOMETER DEFLECTIONS
AT SAMPLE LOCATIONS**

Sample Location Number	Location	Traveling Deflectometer Deflection, in.
1	Sta. 625+00, NBTL-RWT*	0.035
2	Sta. 626+00, NBPL-RWT	0.030
3	Sta. 100+00, SBPL-RWT	0.013
4	Sta. 718+00, NBTL-RWT	0.017
Mean deflection at sample locations		0.024

* In direction of travel.

**March 1964

TABLE 3 — IN SITU PHYSICAL PROPERTIES AND
STRUCTURAL SECTION*

Layer	Thickness ft	Unit Weight (lb. per cu. ft)	Water Content percent	Dry Density (lb. per cu. ft)	Degree of Saturation percent
Open- Graded Asphalt Concrete	0.06	Not included in structural section.			
Type B Asphalt Concrete	0.21	139.7			
Class 2 Aggregate Base	0.67	129.5	10.4	117.2	78.
Class 2 Aggregate Subbase	1.00	132.6	11.7	118.6	83.
Subgrade Soil	See Table 29, Report TE 66-6				

*December 1965

TABLE 4 — SUMMARY OF TEST RESULTS FOR ASPHALT CONCRETE
SAMPLED NEAR MORRO BAY, CALIFORNIA IN DECEMBER, 1965

Location	Number of Samples	Mean Stiffness (psi)	Standard Deviation	Coeff. of Variation percent
<u>Tests at 68°F</u>				
1	9	345,000	138,000	39.8
2	11	333,000	108,000	32.4
3	10	341,000	105,000	30.7
4	14	335,000	115,000	34.3
Grand Mean	44	338,000	112,000	33.1
<u>Tests at 40°F</u>				
1	4	1,130,000	715,000	63.2
2	14	943,000	396,000	42.0
3	16	965,000	400,000	41.4
4	9	1,235,000	506,000	40.9
Grand Mean	43	1,030,000	453,000	43.9

TABLE 5 — MONTHLY AXLE LOAD DISTRIBUTION,
MORRO BAY PAVEMENT

Axle Load Group kips	Axle Load kips	Number per Month
Under 3	3	245
3 - 7	5	4409
7 - 8	7.5	1236
8 - 12	10	2899
12 - 16	14	1344
16 - 18	17	1565
18 - 20	19	282
20 - 22	21	15.0
22 - 24	23	5.4
24 - 26	25	3.6
26 - 30	28	3.8
30 - 35	32.5	0.1

TABLE 6 — WEATHER RECORD DATA FOR MORRO BAY, CALIFORNIA

Month	Avg. Air Temp.	Daily Air Temp. Range	Avg. Wind Velocity	Solar Insol. *	Sky Cover
Jan.	51.0	24.	6.7	269	6.1
Feb.	52.0	23.	7.2	350	5.8
Mar.	54.0	23.	8.3	482	5.6
Apr.	56.0	22.	8.0	569	5.1
May	57.0	21.	8.3	631	4.8
June	58.0	20.	7.9	692	3.7
July	60.0	19.	6.5	681	3.0
Aug.	60.0	19.	6.2	612	3.4
Sept.	60.0	23.	5.9	520	3.1
Oct.	59.0	26.	6.2	413	4.1
Nov.	55.0	28.5	6.6	309	5.2
Dec.	50.0	25.	6.4	251	6.1

*Langley's per day.

TABLE 7 — TRAFFIC WEIGHTED MEAN STIFFNESSES FOR 2.5 INCH ASPHALT CONCRETE LAYER AT MORRO BAY

Month	Stiffness, psi
Jan.	1,053,000
Feb.	947,000
Mar.	799,000
Apr.	655,000
May	580,000
June	457,000
July	362,000
Aug.	406,000
Sept.	437,000
Oct.	577,000
Nov.	822,000
Dec.	1,094,000

TABLE 8 — LABORATORY TEST VARIABLES AFFECTING FATIGUE BEHAVIOR*

Load Variables	Mixture and Specimen Variables	Environmental Variables
1. Pattern of stressing	1. Asphalt	1. Temperature
2. Stress level	a. Type	2. Moisture
3. Testing Method	b. Hardness	3. Alteration of material properties during service life (e.g. aging)
a. Load history	2. Aggregate	
(1) Simple loading	a. Type	
(2) Compound loading	b. Gradation	
b. Mode of Loading	3. Specimen	
(1) Controlled-stress	a. Stiffness	
(2) Controlled-strain	b. Air void content	
(3) Intermediate	c. Asphalt content	

*Adapted from Reference (38).

TABLE 9 — MIXTURE VARIABLES

Aggregate	Asphalt	Asphalt Content (by dry wt. of aggregate)			
		State of Calif., 1/2-in. Max. Grading			British Standard
		Coarse	Medium	Fine	594
Crushed Basalt	60-70	-	5.3 to 8.7	-	-
Crushed Granite	40-50	-	6.0	-	7.9
	60-70	-	6.0	-	-
	85-100	6.0	5.2 and 6.0	6.0	-

TABLE 10 — PROPERTIES OF ORIGINAL ASPHALTS

Property	Asphalt Cement Classification		
	40-50	60-70	85-100
Penetration, dmm 100 gr. 5 sec, 77°F	33	67	92
Viscosity, cp 140°F	4.06×10^5	2.22×10^5	-
Viscosity, cs 275°F	375	369	238
Flash Point, PMCT, °F	-	-	460

TABLE 11 — RECOVERED PROPERTIES FOR ASPHALTS USED
IN LABORATORY STUDY

Mix Designation		Original Asphalt Cement	Properties of Recovered Asphalts	
Aggregate Type	Gradation		Penetration, dmm 100 gr., 5 sec, 77°F	Ring and Ball Softening Point, °F
Granite	Coarse	85-100	56	125
Granite	Medium	85-100	37	127
Granite	Fine	85-100	30	129
Granite	Medium	60-70	35	129
Basalt	Medium	60-70	32	136.5
Granite	Medium	40-50	26	132
Granite	British 594	40-50	21	140

TABLE 12 — AGGREGATE CHARACTERISTICS

Test Property	Crushed Granite	Crushed Basalt
LA Abrasion Loss - percent		--
After 100 rev.	6	--
After 500 rev.	24	18
Cleanness Value - percent	89	--
Sand Equivalent - percent	--	41
Oil Equivalent - percent	3.7	--
Centrifuge Kerosene Equivalent - percent		--
(at surface area of approx. 34 sq ft per lb.)	4.0	--

TABLE 13 — COMPARISON OF ASPHALT CONTENTS USED IN TEST SPECIMENS WITH THOSE ESTIMATED ACCORDING TO STATE OF CALIFORNIA METHOD OF MIX DESIGN

Mix Designation	Asphalt Content -- Percent (By Dry Wt. Aggregate)					
	85-100		60-70		40-50	
	Actual	Estimated	Actual	Estimated	Actual	Estimated
Granite British 594	-	-	-	-	7.9	6.3
Granite Coarse	6.0	5.5	-	-	-	-
Granite Fine	6.0	5.9	-	-	-	-
Granite Medium	6.0 5.2	5.8	6.0	6.1	6.0	6.6
Basalt	-	-	5.7 to 8.7	5.9	-	-

TABLE 14 -- AIR VOID CONTENTS FOR LABORATORY PREPARED SPECIMENS

Mix Designation	Asphalt Cement	Asphalt Content Percent	Percent Air Voids		
			Mean	Standard Deviation	Coefficient of Variation
Granite British 594	40-50	7.9	5.38	.69	12.8
Granite, Coarse	85-100	6.0	5.71	.59	10.3
Granite, Fine	85-100	6.0	5.71	.46	8.1
Granite, Medium	85-100	6.0	4.49	.55	12.2
Granite, Medium	60-70	6.0	4.80	.43	9.1
Granite, Medium	40-50	6.0	4.73	.50	10.6
Basalt	60-70	5.7	7.65	.46	6.0
Basalt	60-70	6.2	6.72	.62	9.3
Basalt	60-70	6.7	5.20	.34	6.6
Basalt	60-70	7.7	4.05	.26	6.5
Basalt	60-70	8.7	1.60	.14	8.8
Granite	85-100	5.2	7.16	.73	10.4

TABLE 15 - MEAN, STANDARD DEVIATION AND COEFFICIENT OF VARIATION OF STIFFNESS, STRAIN, AIR VOIDS AND FATIGUE LIFE FOR GRANITE AGGREGATE MIXES - LABORATORY STUDY

Mix Identification Grading & Asphalt Penetration	Stress Level psi	No. of Bars	Stiffness			Strain			Percent Air			Fatigue Life		
			Mean psi $\times 10^3$	Std. Dev. psi $\times 10^3$	C _v $\times 10^{-3}$	Mean in. $\times 10^{-6}$	Std. Dev. in. $\times 10^{-6}$	C _v $\times 10^{-6}$	Mean	Std. Dev.	C _v	Mean	Std. Dev.	C _v
British Standard	175	10	567	90	15.8	315	46	14.5	5.19	.84	16.2	67,385	48,625	72.1
594	150	14	565	80	14.2	271	37	13.6	5.42	.67	12.4	104,923	129,188	123.1
40-50 penetration	125	11	578	86	14.8	220	30	13.3	5.50	.58	10.5	175,032	107,347	61.3
7.9 percent	all	35	570	83	14.4				5.38	.69	12.8			
California Coarse	150	9	193	37	18.9	799	153	19.0	5.48	.58	10.7	1,605	571	35.5
Granite Aggregate	100	10	248	64	25.8	425	94	22.1	5.80	.63	10.9	7,885	3,054	38.7
85-100 penetration	75	9	239	45	18.8	322	48	15.0	5.85	.55	9.3	23,017	12,873	55.9
6.0 percent	all	28	228	54	23.8				5.71	.59	10.3			
California Fine	450	10	246	32	13.1	1860	272	14.6	5.72	.47	8.2	72	25	35.3
Granite Aggregate	250	10	254	60	23.4	1129	404	35.8	5.62	.57	10.1	836	435	52.0
85-100 penetration	150	11	257	52	20.0	611	163	26.5	5.64	.52	9.2	3,800	2,424	63.8
6.0 percent	100	11	284	83	29.3	376	94	25.1	5.82	.28	4.9	19,277	15,271	79.2
75	11	11	317	68	21.3	246	50	20.2	5.73	.49	8.5	72,059	97,541	135.3
all	53	53	273	65	23.8				5.71	.46	8.1			
California Medium	150	6	258	35	18.6	590	74	12.5	4.60	.38	8.3	3,509	1,274	36.3
Granite Aggregate	100	6	276	59	21.5	377	81	21.5	4.30	.52	12.1	21,193	8,038	37.9
85-100 penetration	75	7	325	44	13.6	234	31	13.3	4.57	.70	15.5	73,310	56,672	77.3
6.0 percent	all	19	288	53	18.5				4.49	.55	12.2			
California Medium	150	9	285	58	20.2	545	101	18.5	4.83	.48	10.2	6,592	4,419	67.0
Granite Aggregate	100	9	334	66	19.8	310	61	19.6	4.68	.50	10.7	28,812	13,974	48.4
60-70 penetration	75	9	335	30	8.9	226	20	9.0	4.87	.33	6.9	123,936	90,590	73.0
6.0 percent	all	27	318	57	17.8				4.80	.43	9.1			
California Medium	175	7	631	117	18.5	285	49	17.0	4.78	.52	10.8	22,944	19,345	84.3
Granite Aggregate	150	8	655	82	12.5	233	30	13.0	4.55	.53	11.8	42,818	25,383	59.2
40-50 penetration	125	2	590	33	5.5	212	11	5.3	5.55	.07	1.2	58,921	25,704	43.6
6.0 percent	100	6	708	71	10.0	142	14	9.6	4.63	.19	4.2	346,538	197,055	56.8
all	23	23	656	92	13.9				4.73	.50	10.6			
California Medium														
Granite Aggregate														
85-100 penetration	75	8	289	25	8.7	262	24	9.1	7.06	.73	10.4	19,925	13,231	66.4
5.2 percent														

TABLE 16 -- MEAN, STANDARD DEVIATION AND COEFFICIENT OF VARIATION OF STIFFNESS, STRAIN, AIR VOIDS AND FATIGUE LIFE FOR BASALT AGGREGATE -- LABORATORY PREPARED MIXES

Mix Identification Grading & Asphalt Percent	Stress Level psi	No. of Bars	Stiffness		Strain		Percent Air		Fatigue Life					
			Mean psi $\times 10^3$	Std. Dev. psi $\times 10^3$	Mean in. $\times 10^{-6}$	Std. Dev. in. $\times 10^{-6}$	Mean in. $\times 10^{-6}$	Std. Dev.	Mean	Std. Dev.	c_v			
California Medium														
Basalt Aggregate Type I (5.7%)	150	8	279	51	18.3	553	96	17.4	7.65	.46	6.0	4,878	3,270	67.0
California Medium														
Basalt Aggregate	150	8	318	27	8.5	475	41	8.6	6.17	.54	8.8	6,645	3,808	57.3
Type I (6.2%)	100	8	284	61	21.5	367	80	21.6	7.00	.45	6.5	21,512	11,562	53.7
	75	8	293	56	19.1	265	51	19.1	7.00	.51	7.3	54,968	16,672	30.3
	all	24	298	50	16.9				6.72	.62	9.3			
California Medium														
Basalt Aggregate Type I (6.7%)	150	4	380	40	10.5	398	40	10.0	5.20	.34	6.6	19,136	11,160	58.3
California Medium														
Basalt Aggregate Type I (7.7%)	150	4	301	22	7.2	500	35	7.0	4.05	.26	6.5	14,953	5,985	40.0
California Medium														
Basalt Aggregate Type I (8.7%)	150	4	190	4	2.2	789	20	2.4	1.60	.14	8.8	9,573	2,215	23.1
California Medium														
Basalt Aggregate Type II (5.3%)	150	4	223	55	24.5	705	173	24.5	8.77	.54	6.1	2,387	2,285	95.7
California Medium														
Basalt Aggregate Type II (5.7%)	150	4	278	20	7.2	539	35	6.4	8.10	.28	3.4	3,298	1,582	47.7
California Medium														
Basalt Aggregate Type II (6.2%)	150	4	277	38	13.8	549	74	13.4	7.20	.64	9.0	4,605	2,426	52.6

TABLE 17 — t TEST — TEST FOR HYPOTHESIS THAT SLOPE OF
POPULATION REGRESSION LINE HAS A VALUE OF FIVE — CALIFORNIA
GRADED GRANITE MIXES

Aggregate Grading	Asphalt Penetration	S_b	b	n	t	t^a	Reject	Accept or Reserve Judgment
Fine	85-100	.1357	2.952	53	15.1	2.01	x	
Coarse	85-100	.1899	2.486	28	13.2	2.06	x	
Medium	85-100	.3351	2.833	19	6.48	2.11	x	
Medium	60-70	.2105	3.256	27	8.28	2.06	x	
Medium	40-50	.2480	4.011	23	3.99	2.08	x	

a. $t_{\alpha/2, n-2}$

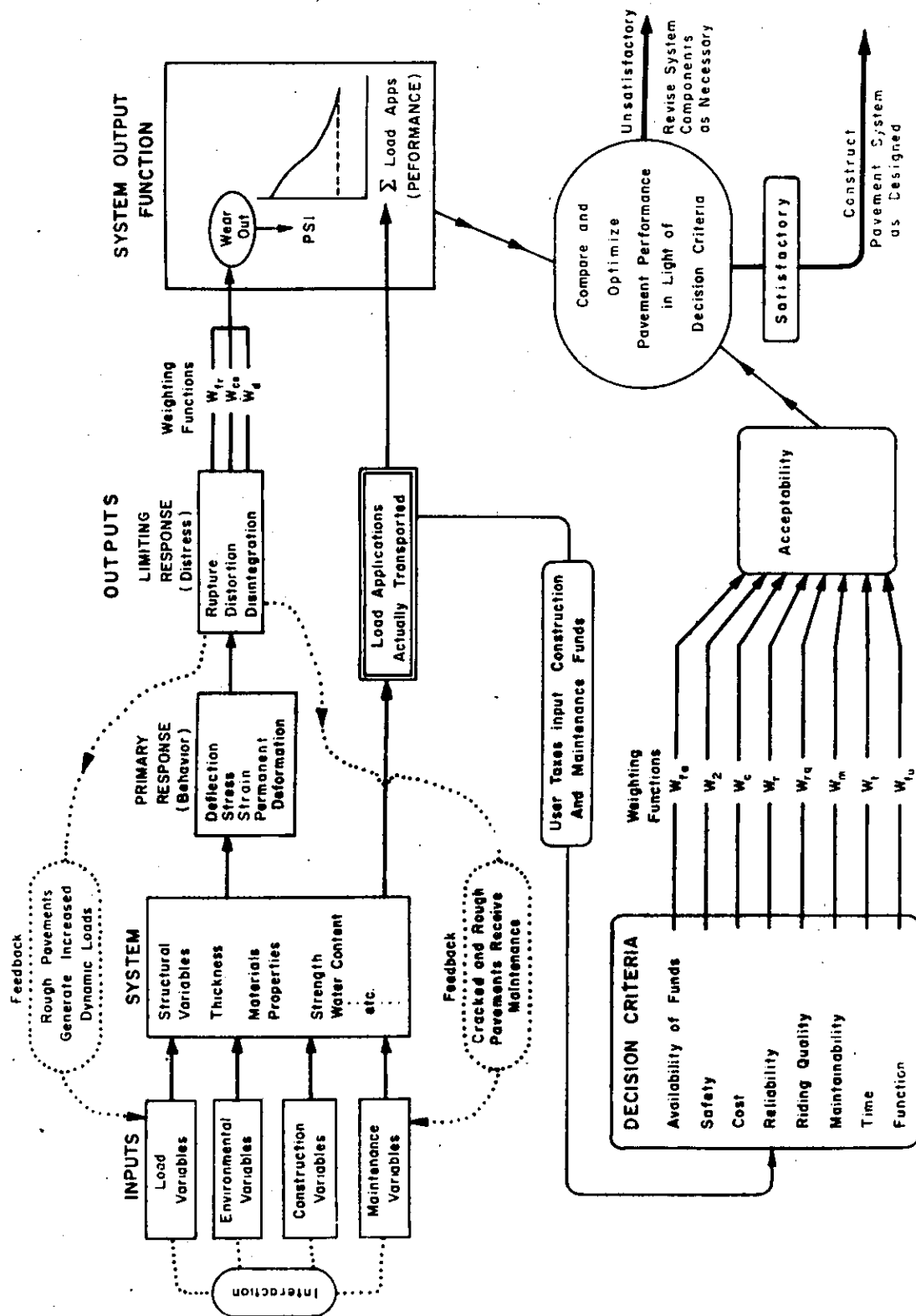


Fig. 1 — Block diagram of the pavement system. (After Finn, et al.)

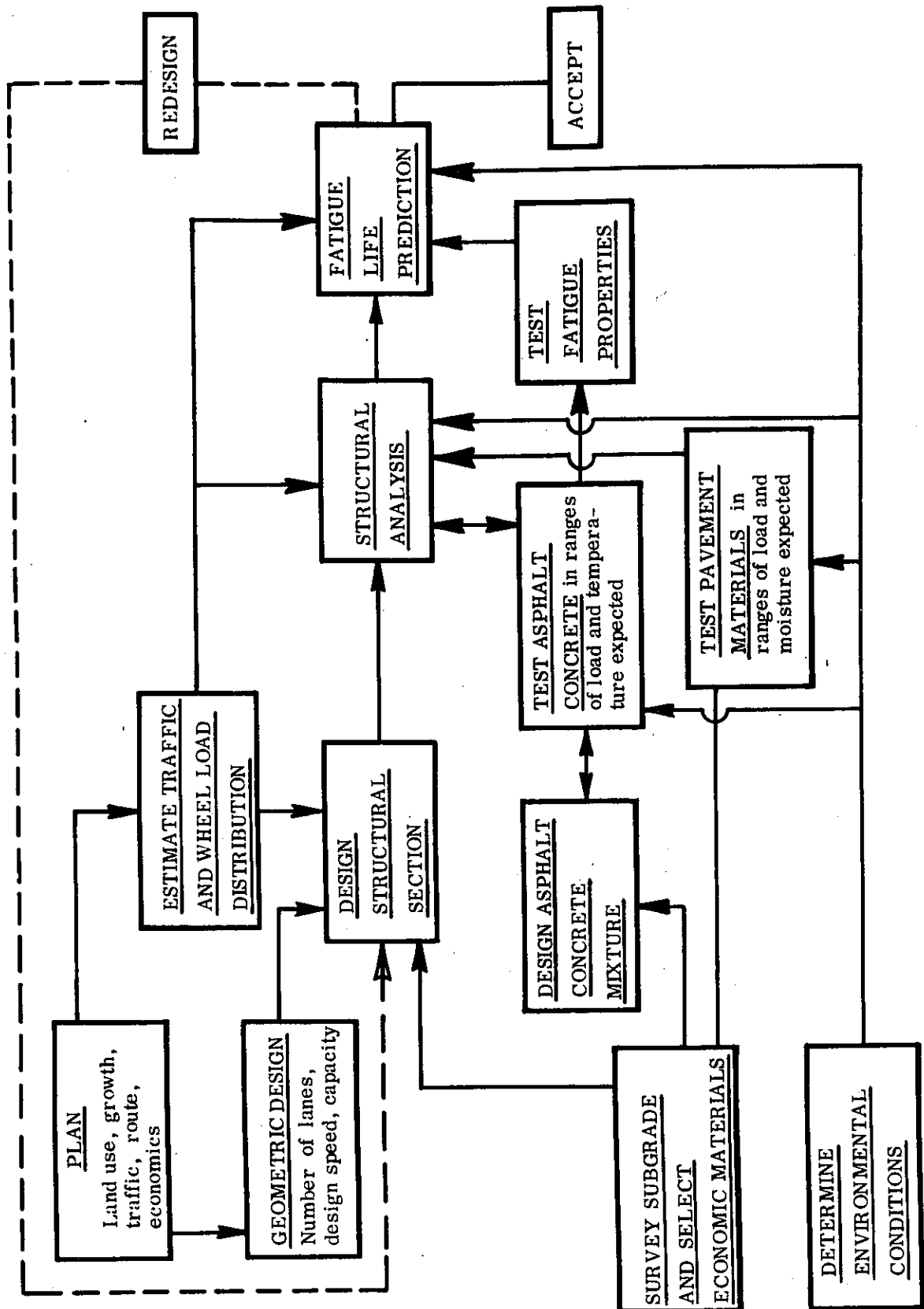


Fig. 2 — Block diagram of a fatigue subsystem.

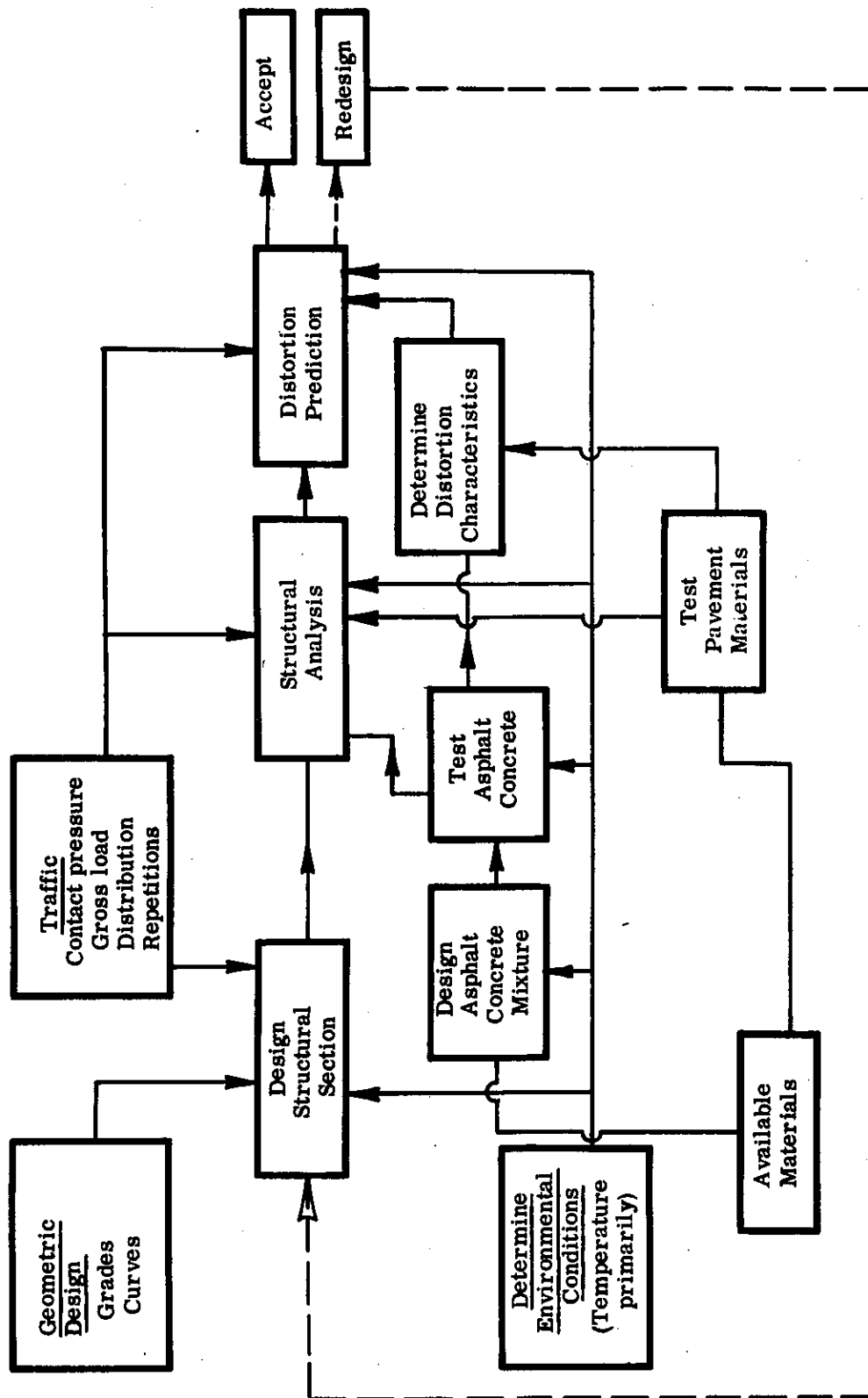
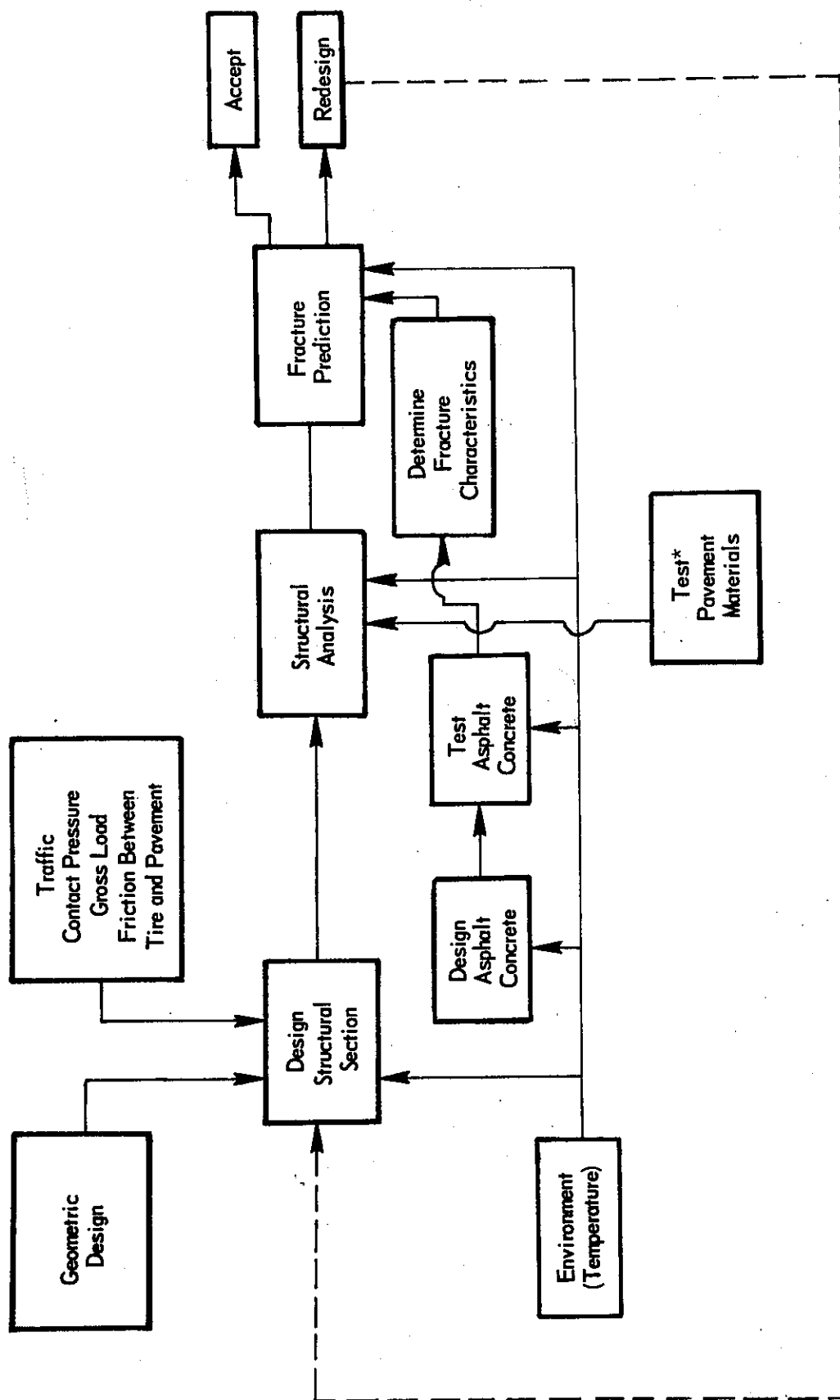
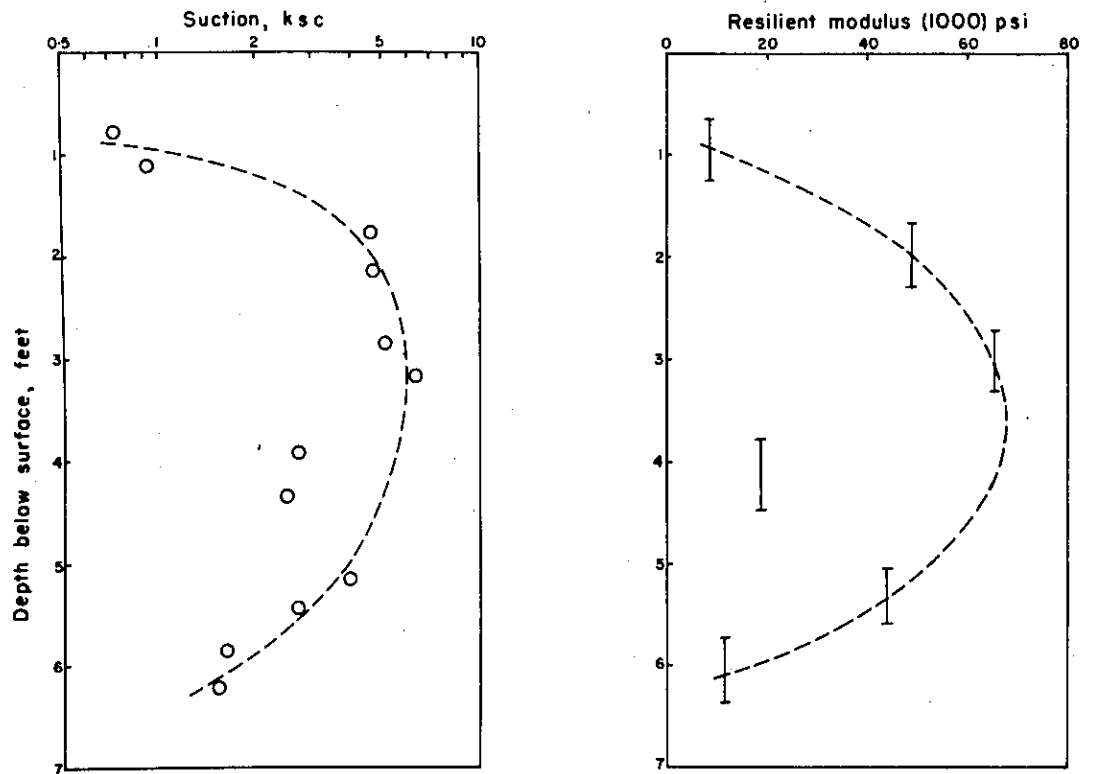


Fig. 3 — Block diagram of the distortion subsystem.

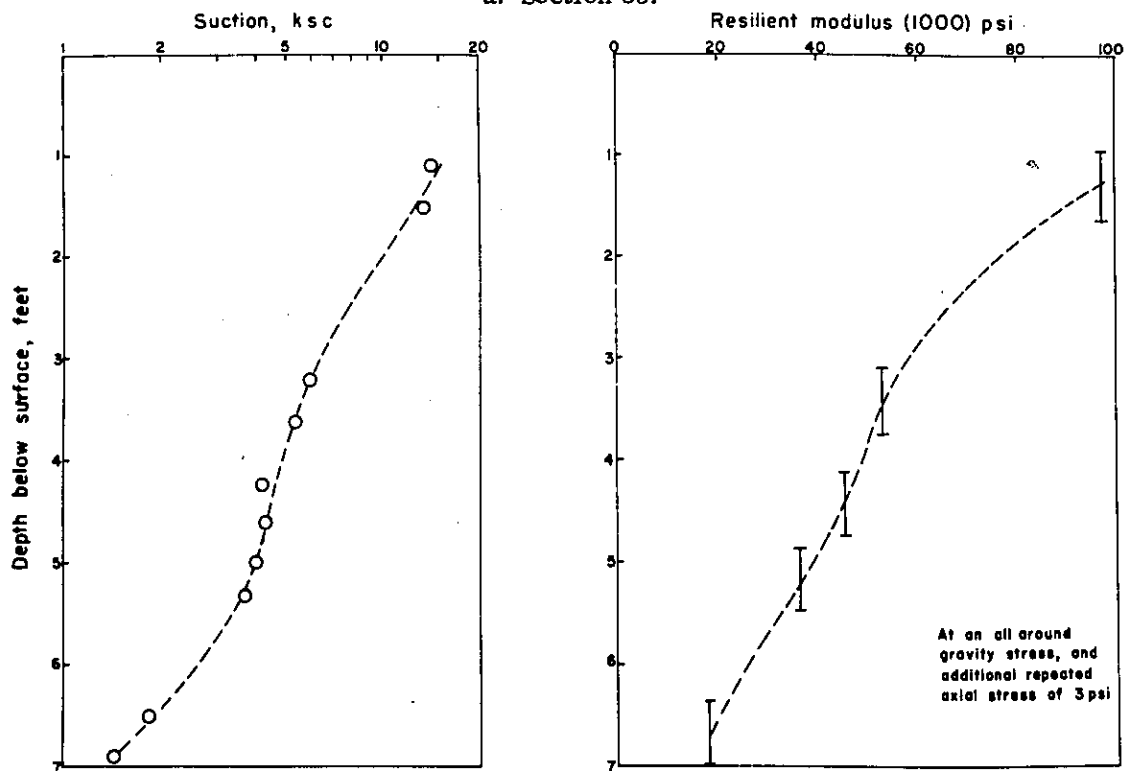


* Knowledge of bond between asphalt-bound layer and underlying layer required.

Fig. 4 -- Block diagram of a fracture subsystem.



a. Section 35.



b. Section 2.

Fig. 5 — Suction and resilient modulus.

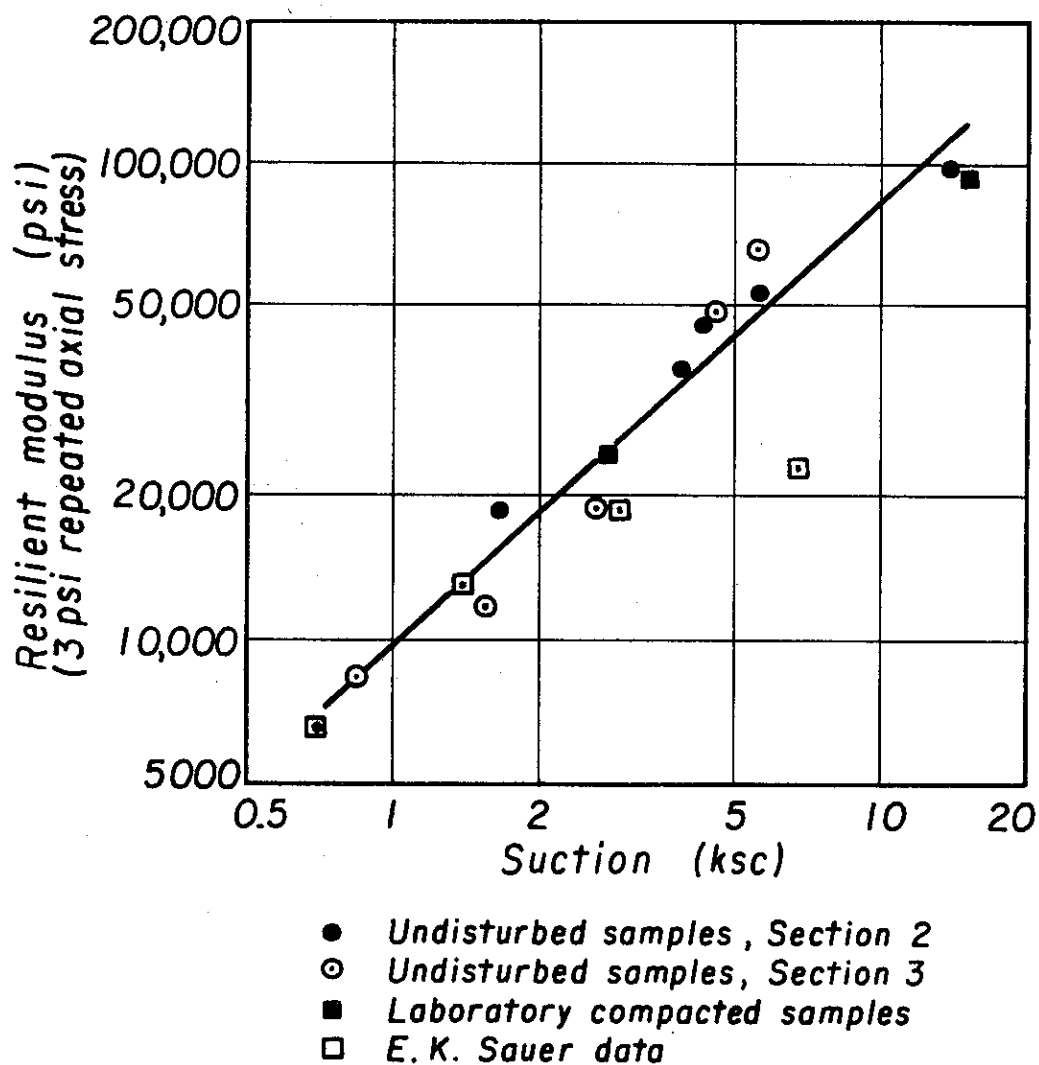


Fig. 6 — Relation between resilient modulus and suction, San Diego road test subgrade soil.

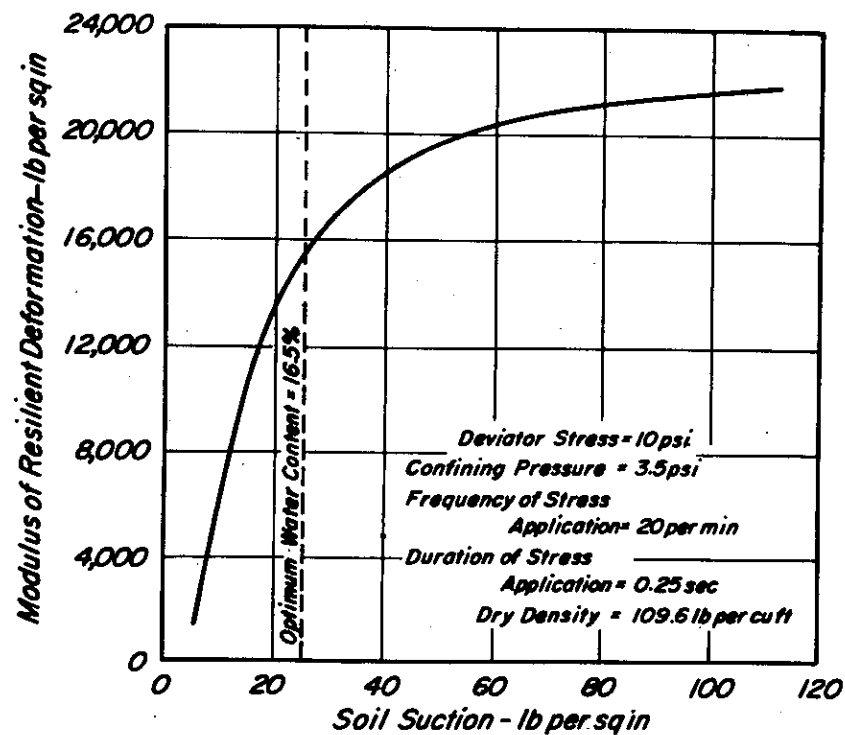


Fig. 7 — Relationship between modulus of resilient deformation and soil suction for laboratory compacted specimens of till from Qu'Appelle Moraine, Saskatchewan, Canada.

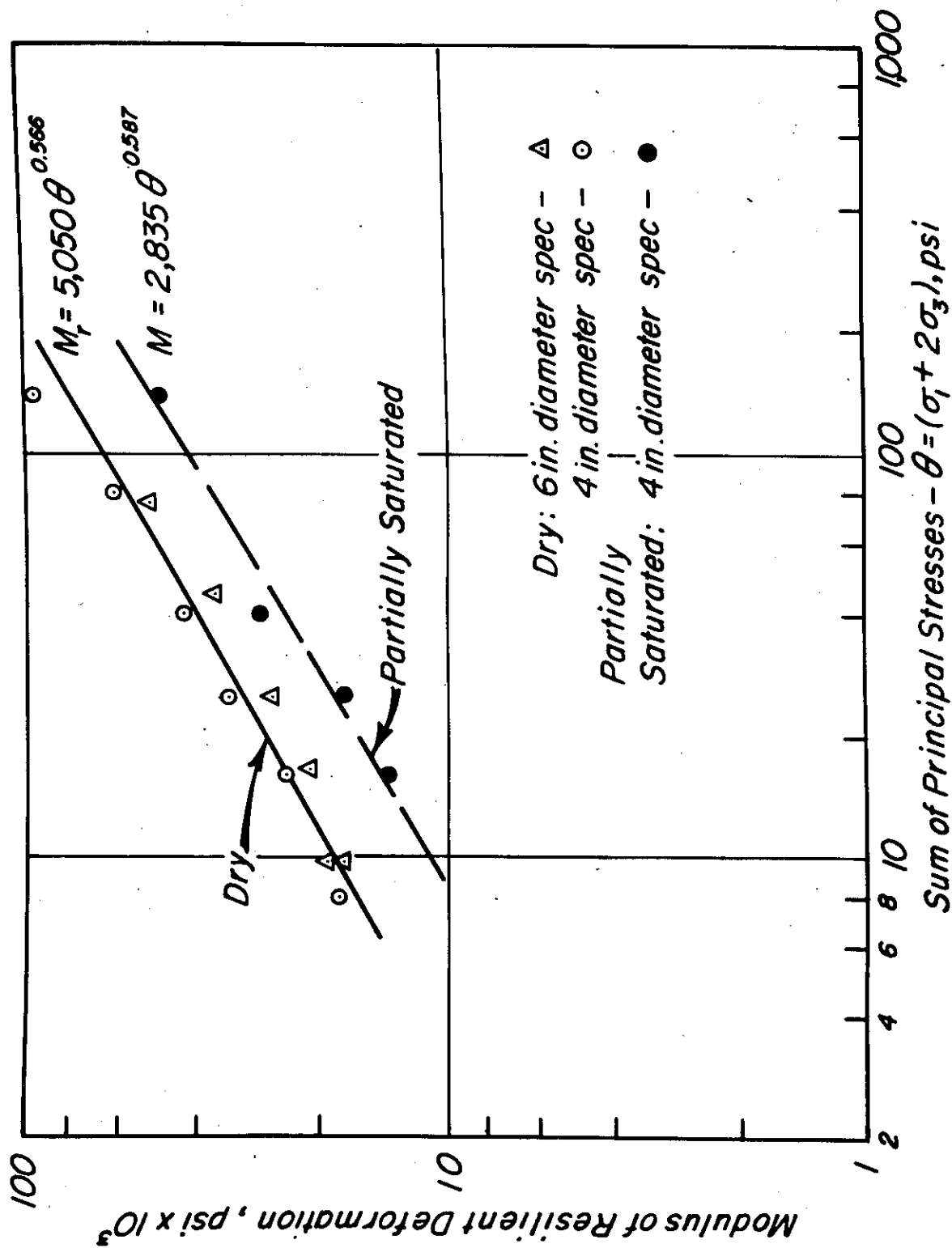


Fig. 8 - Relationship between resilient modulus and sum of principal stresses for untreated aggregate base.

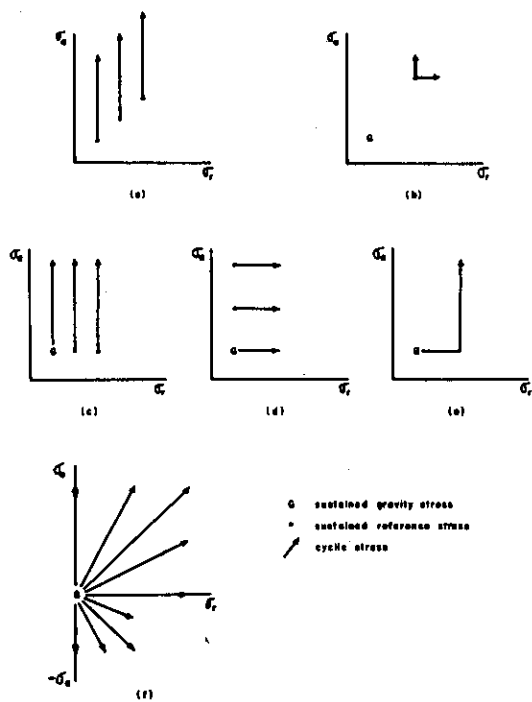


Fig. 9a — Stress paths in laboratory tests.

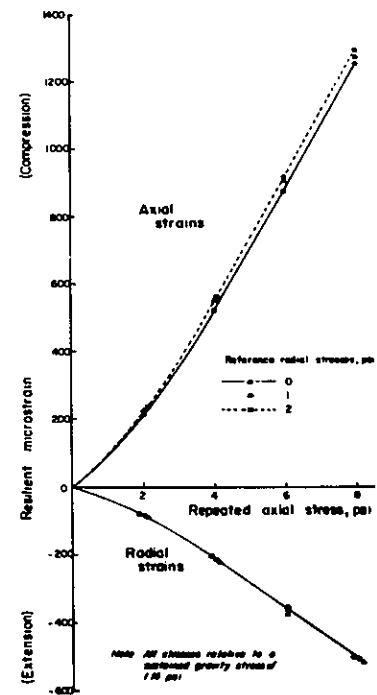


Fig. 9b — Variation of axial and radial strains with axial stress.

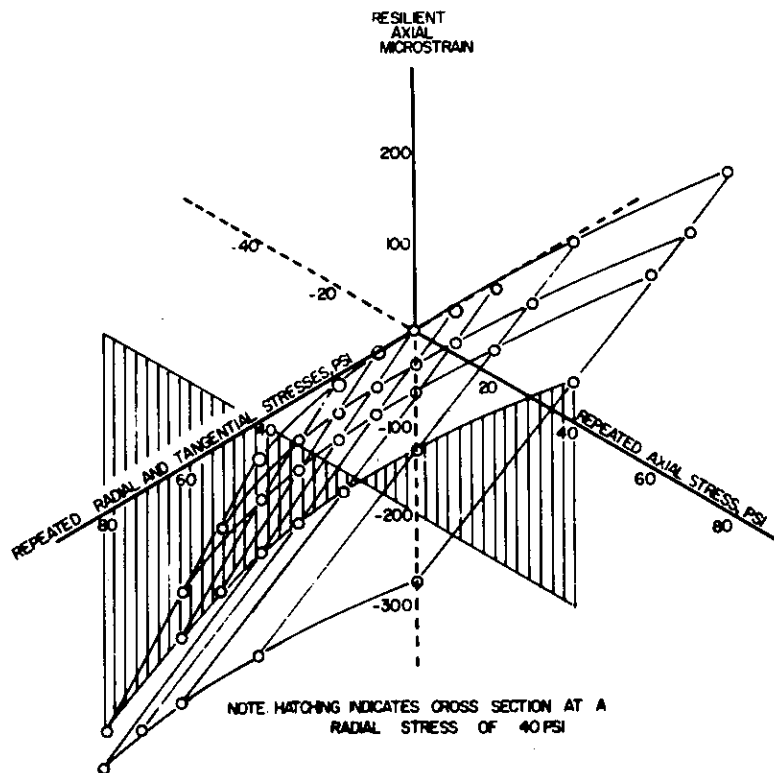


Fig. 10 — Three-dimensional surface - axial strains for various stress states in the triaxial apparatus (asphalt concrete core H2, 70°F).

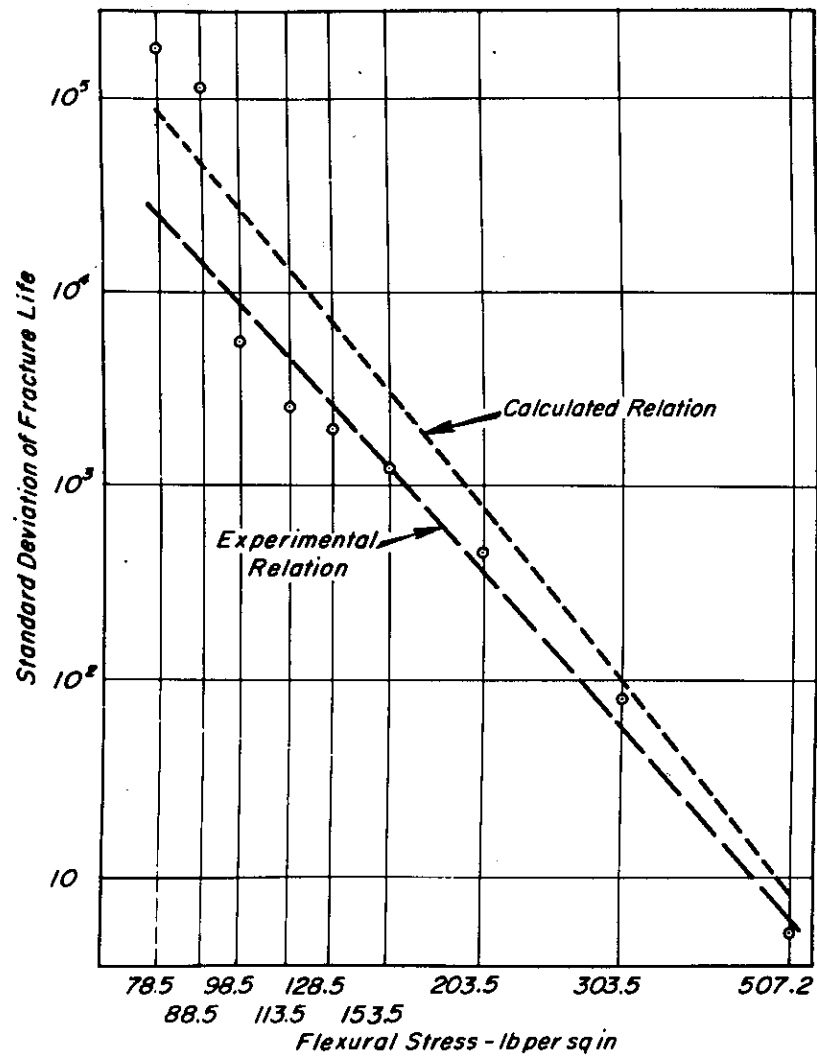


Fig. 11 — Standard deviation of fracture life against stress level.

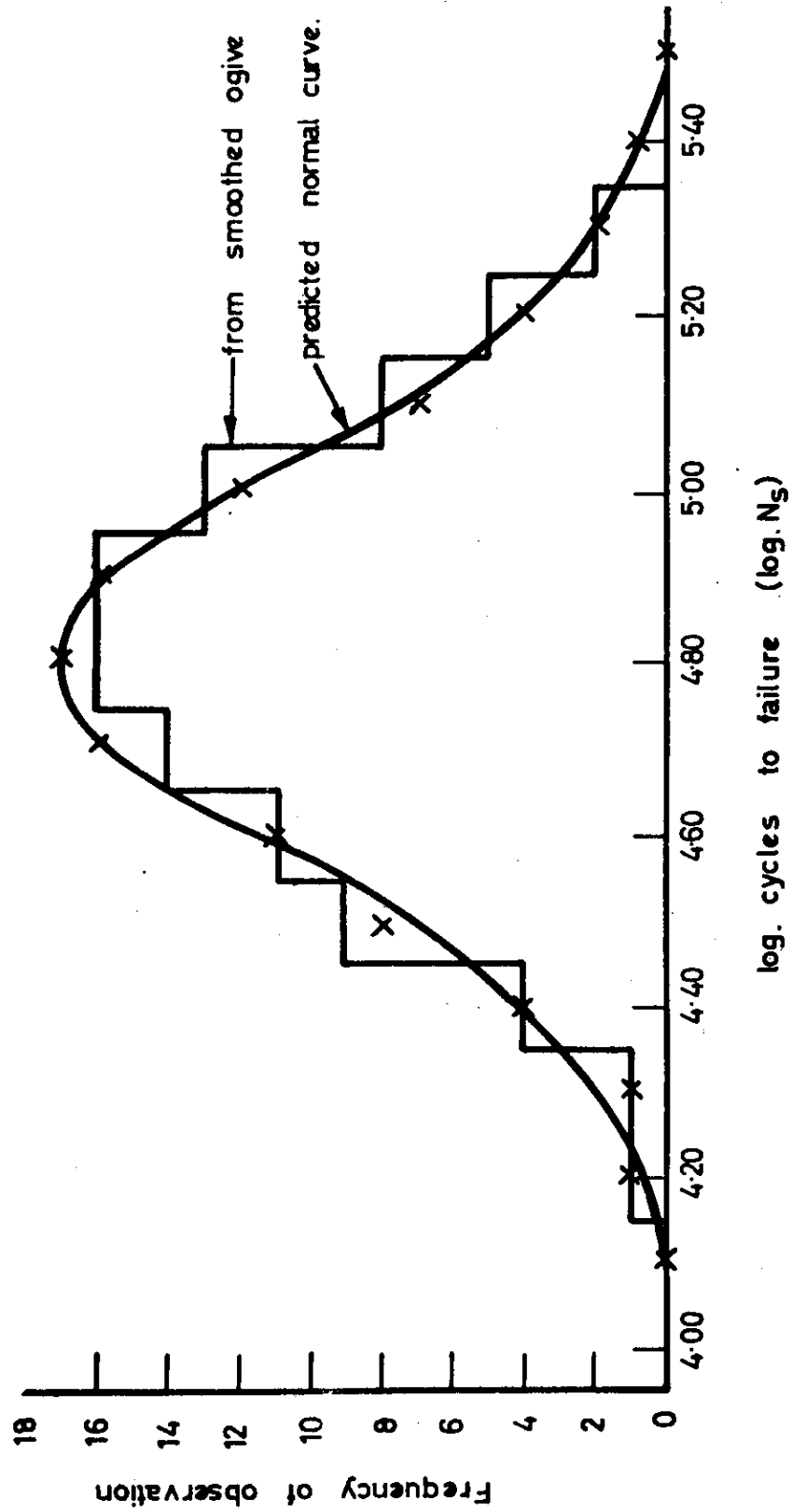


Fig. 12 — Histogram of 100 fatigue test results.

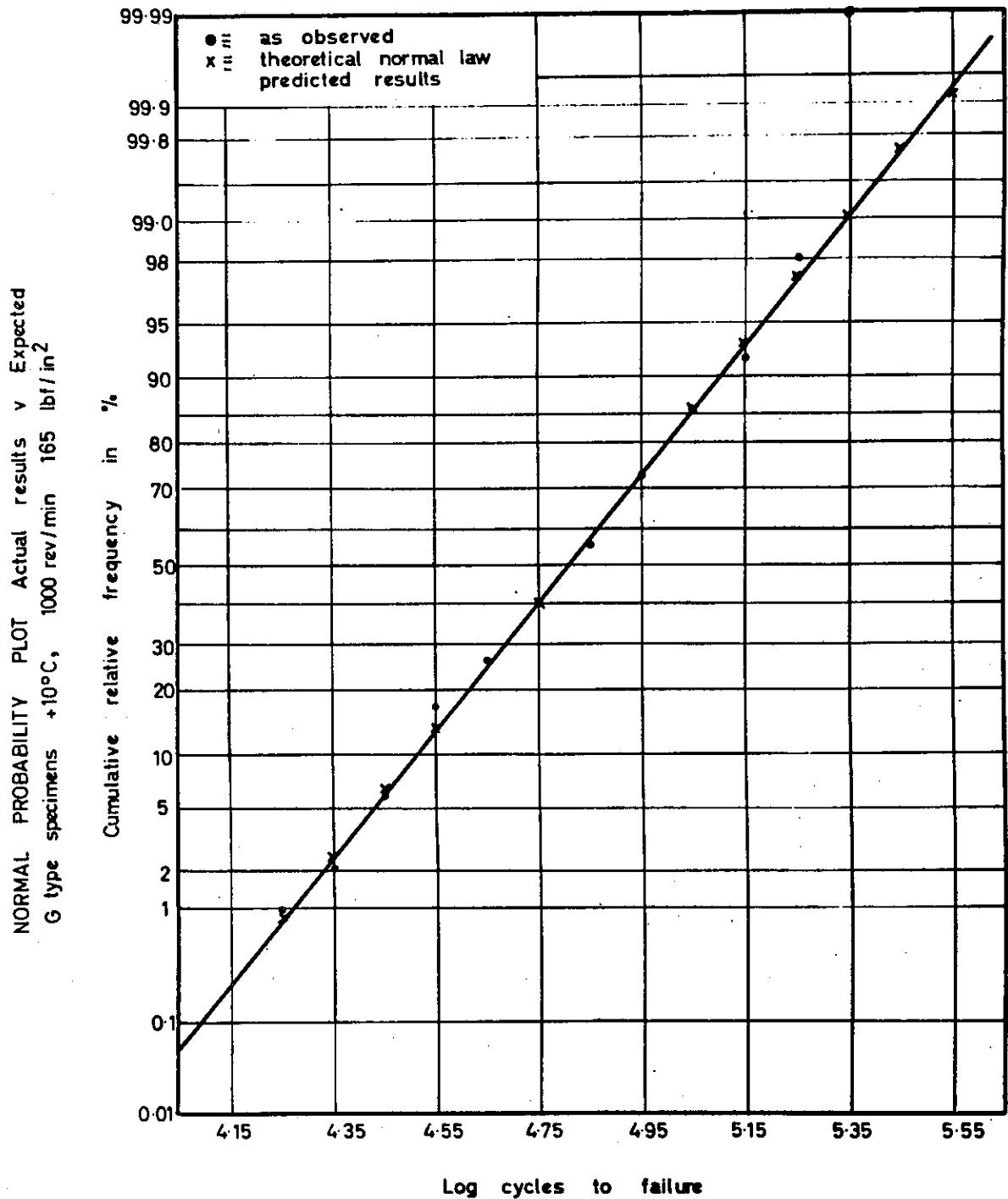


Fig. 13 — Normal probability plot of fatigue results.

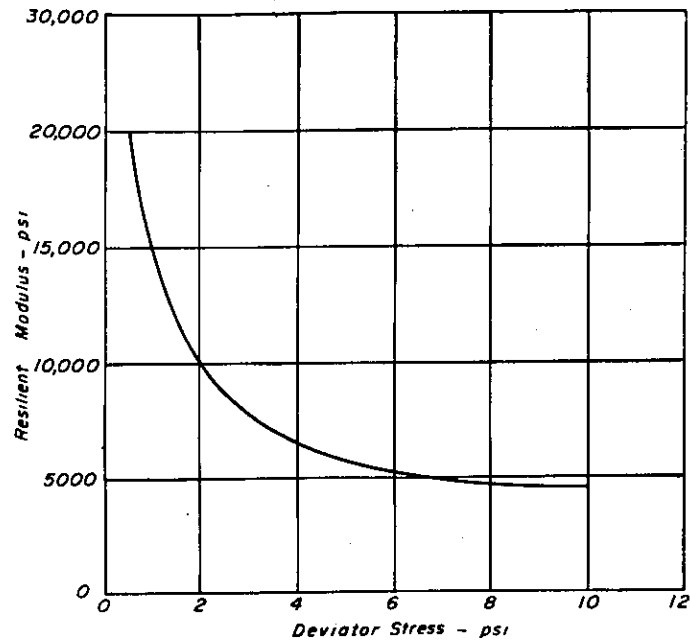


Fig. 14 — Resilient modulus vs. deviator stress — subgrade, Morro Bay.

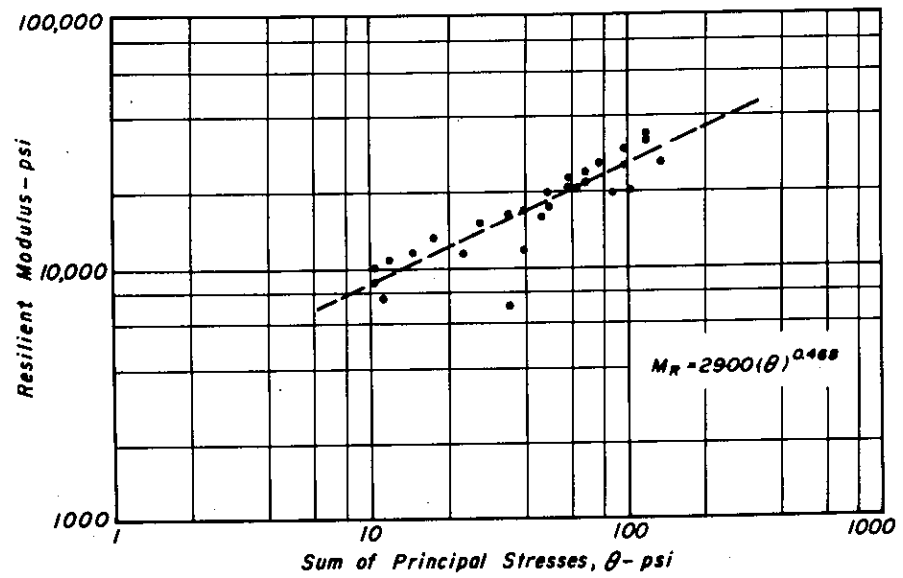


Fig. 15 — Resilient modulus vs. sum of principal stresses — subbase, Morro Bay.

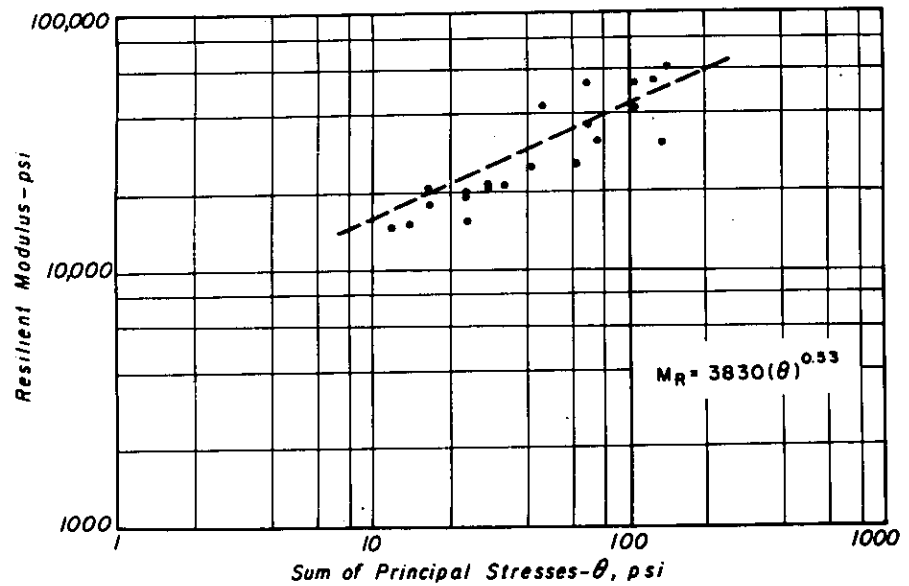


Fig. 16 — Resilient modulus vs. sum of principal stresses — base, Morro Bay.

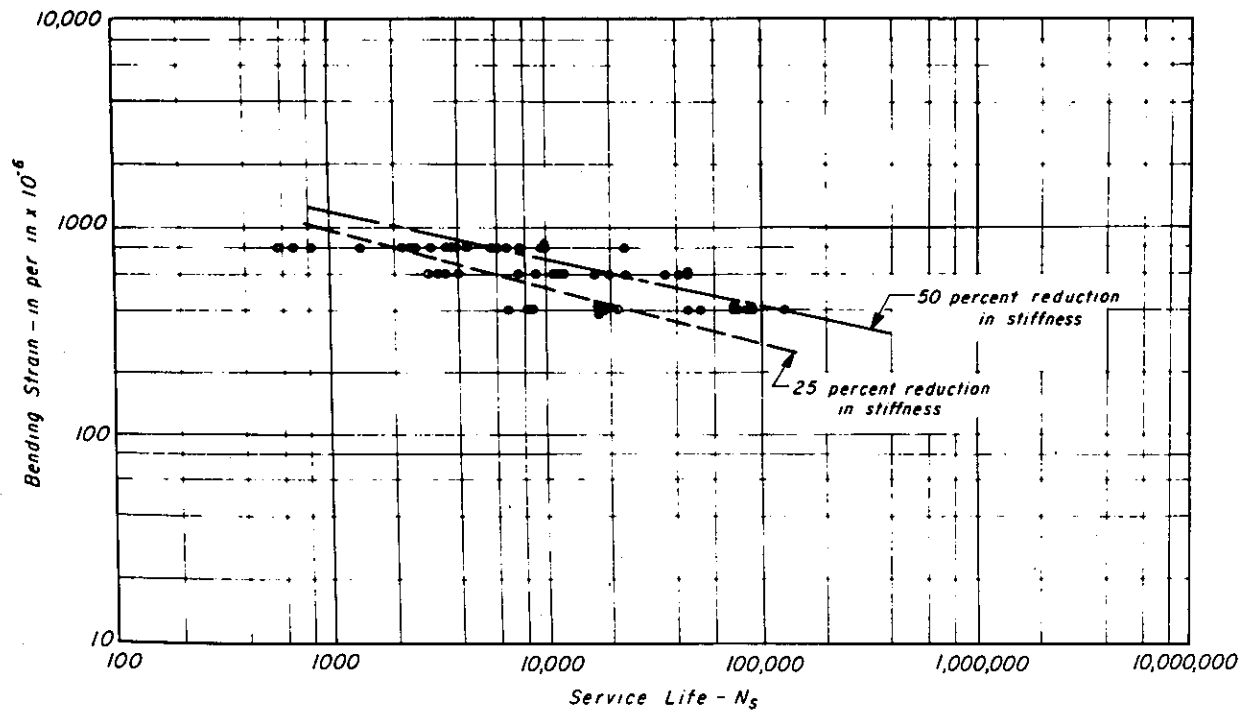


Fig. 17 — Controlled-strain fatigue tests on laboratory prepared specimens — 68°F.

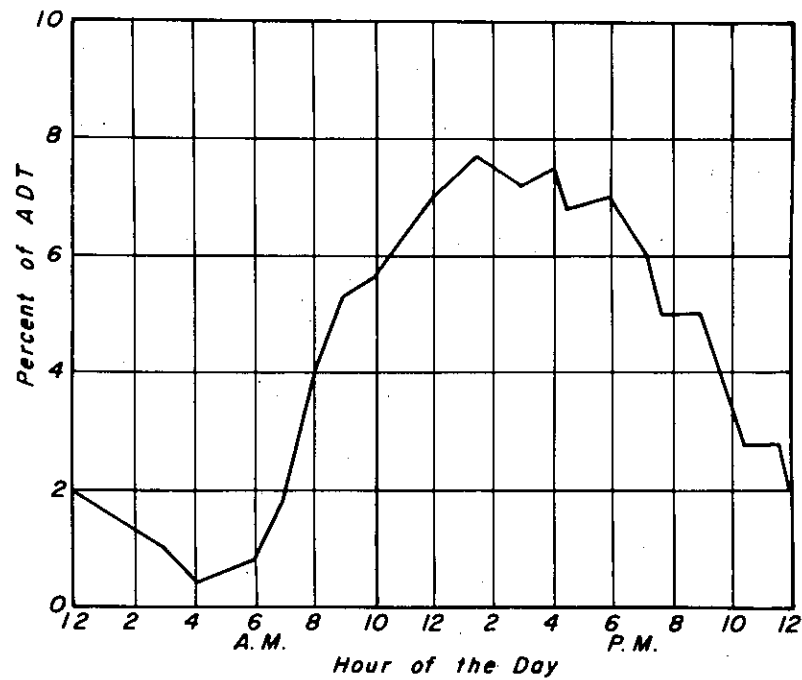
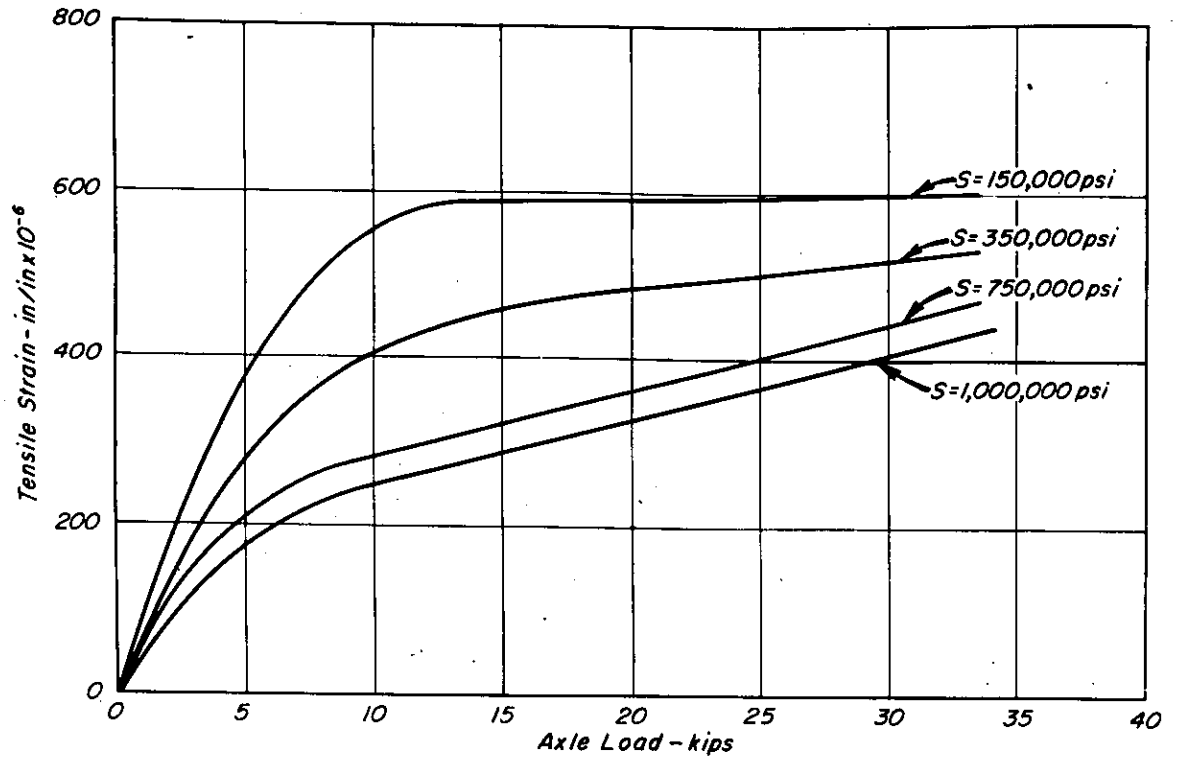
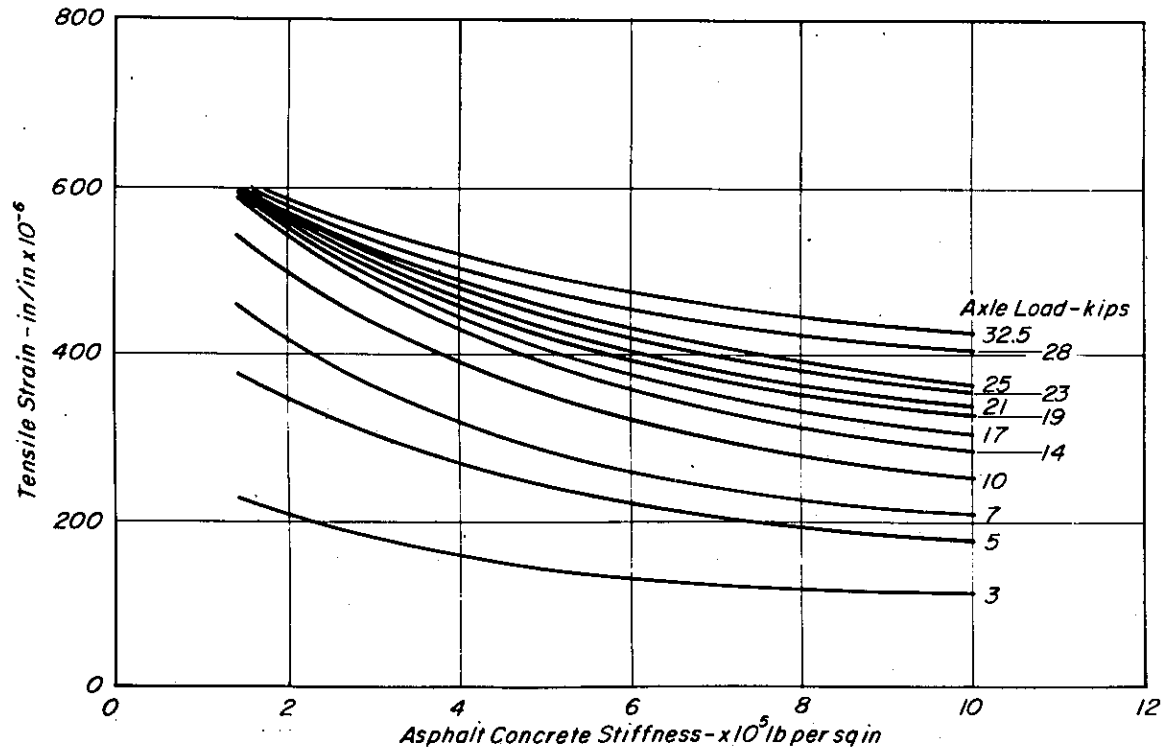


Fig. 18 — Hourly traffic variation, California General Purpose Interstate Route.



(a) Tensile Strain Against Axle Load.



(b) Tensile Strain Against Asphalt Concrete Stiffness

Fig. 19 — Results of structural analysis of Morro Bay pavement showing maximum tensile strain at the bottom of the asphalt concrete layer.

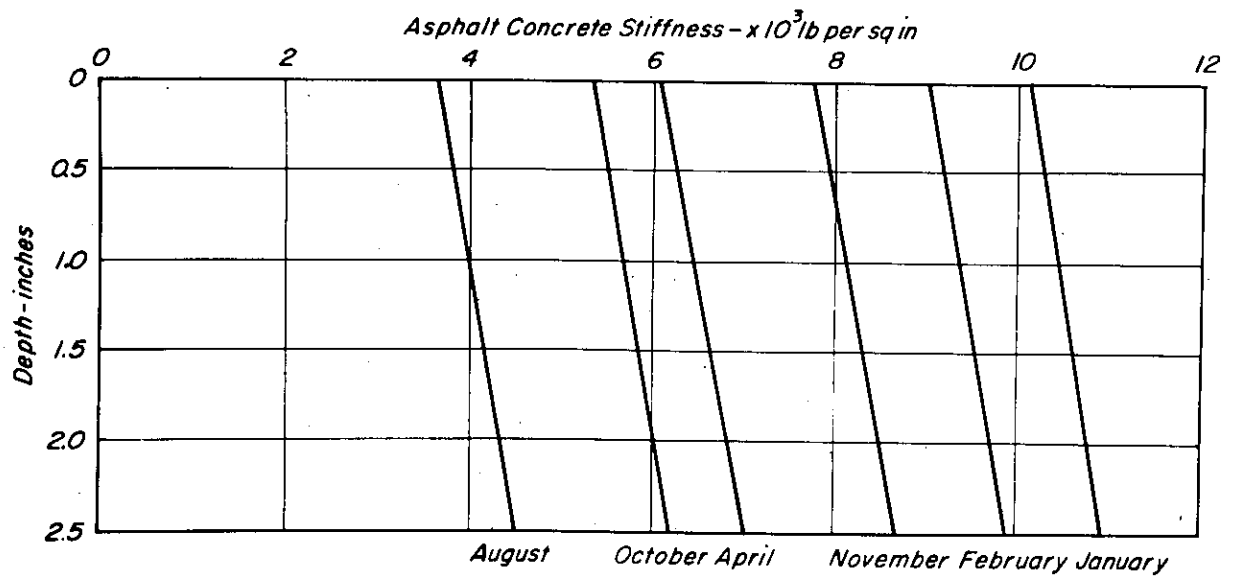


Fig. 20 — Traffic weighted mean stiffness profiles in several months, Morro Bay pavement.

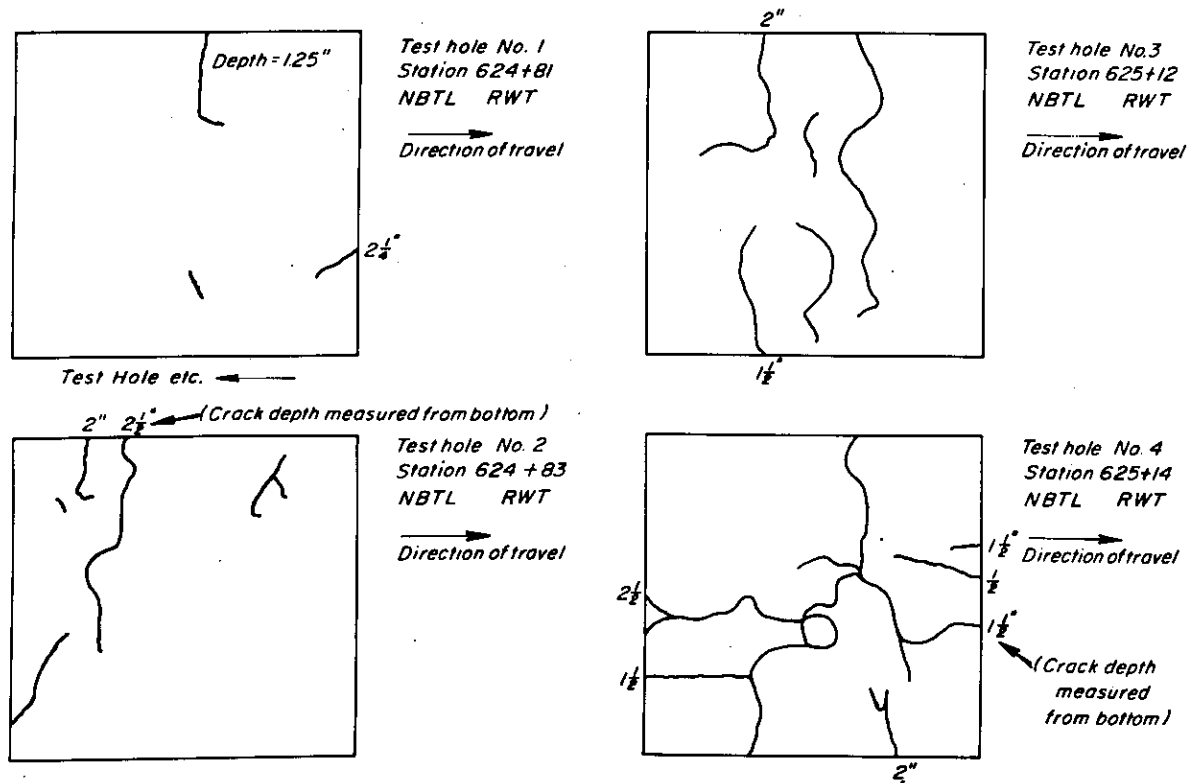


Fig. 21 — Crack patterns on bottom of slabs obtained in vicinity of Sta. 625+00.

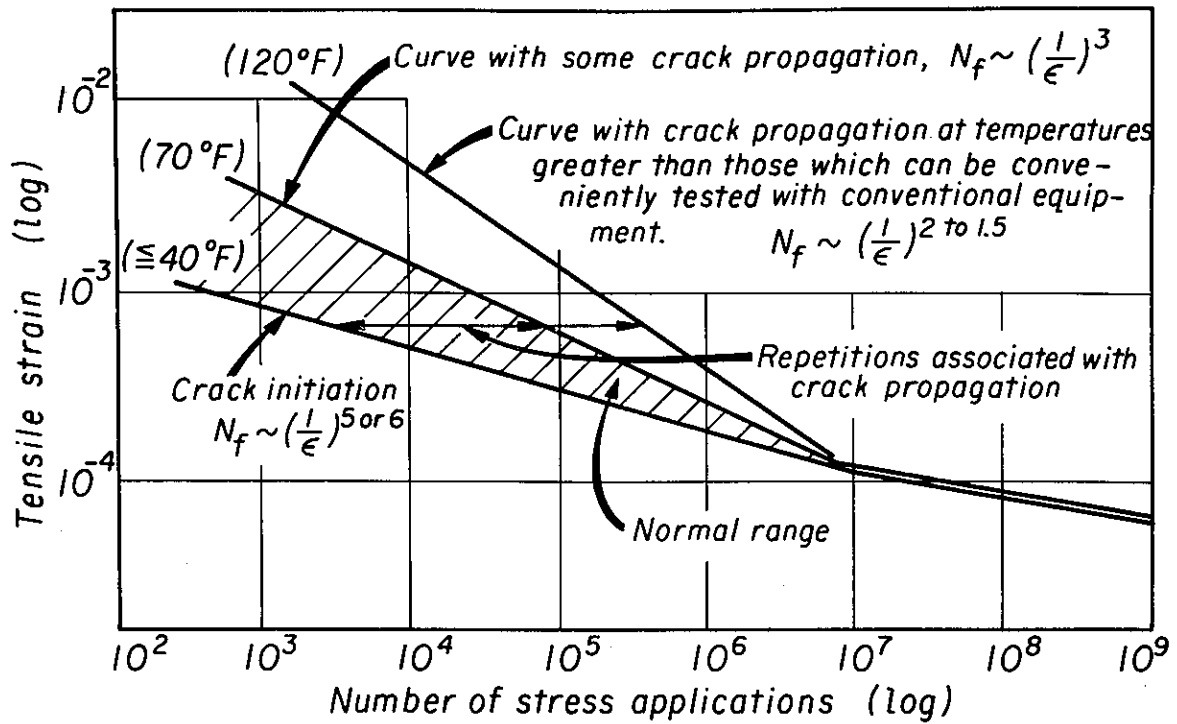


Fig. 22 — Influence of temperature (or mixture stiffness) on the strain vs. stress applications relationship for asphalt concrete.

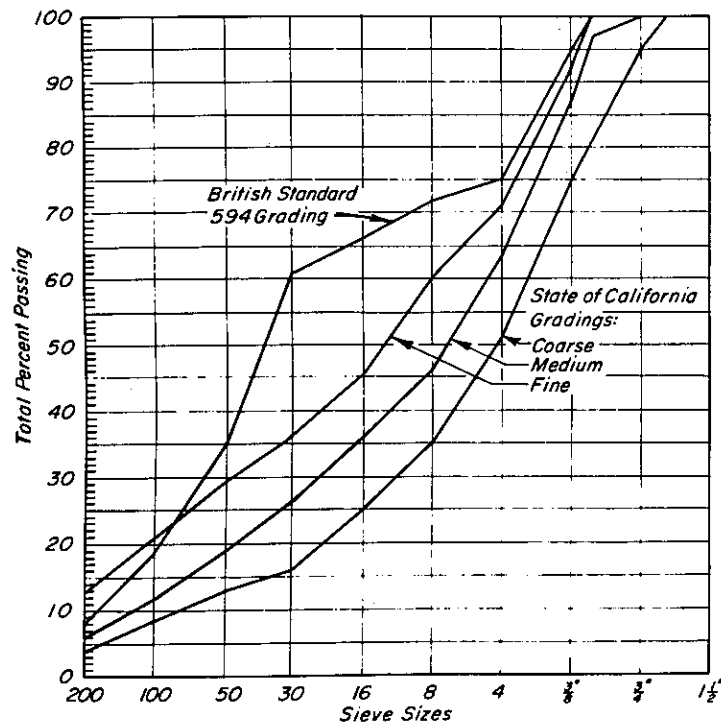
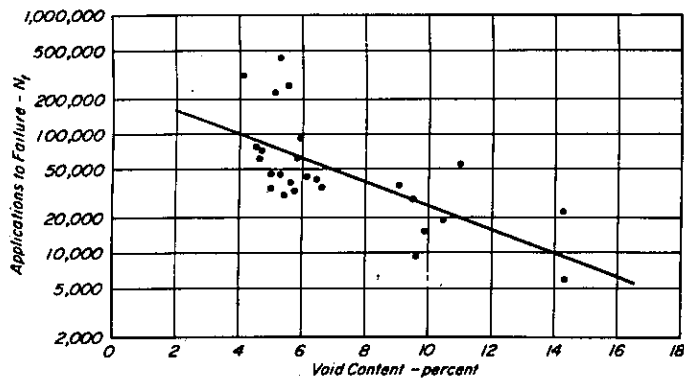
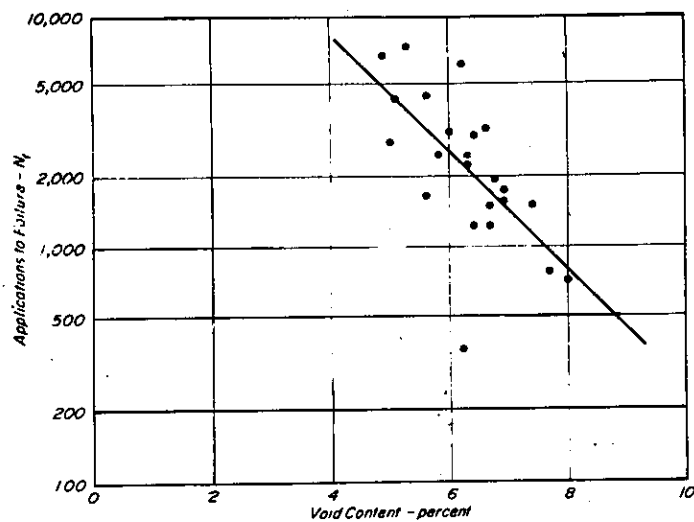


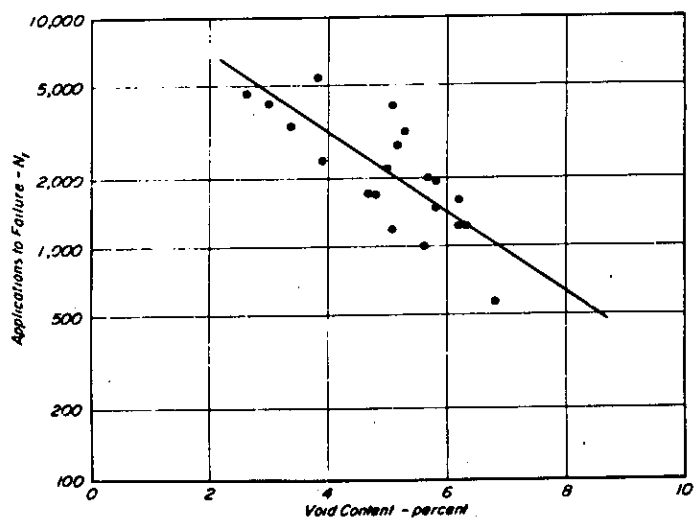
Fig. 23. — Aggregate grading curves, laboratory study.



a. British Standard 594 grading — 7.9 percent asphalt.



b. California fine grading — 6 percent asphalt.



c. California coarse grading — 6 percent asphalt.

Fig. 24 - The effect of voids content on fatigue life.

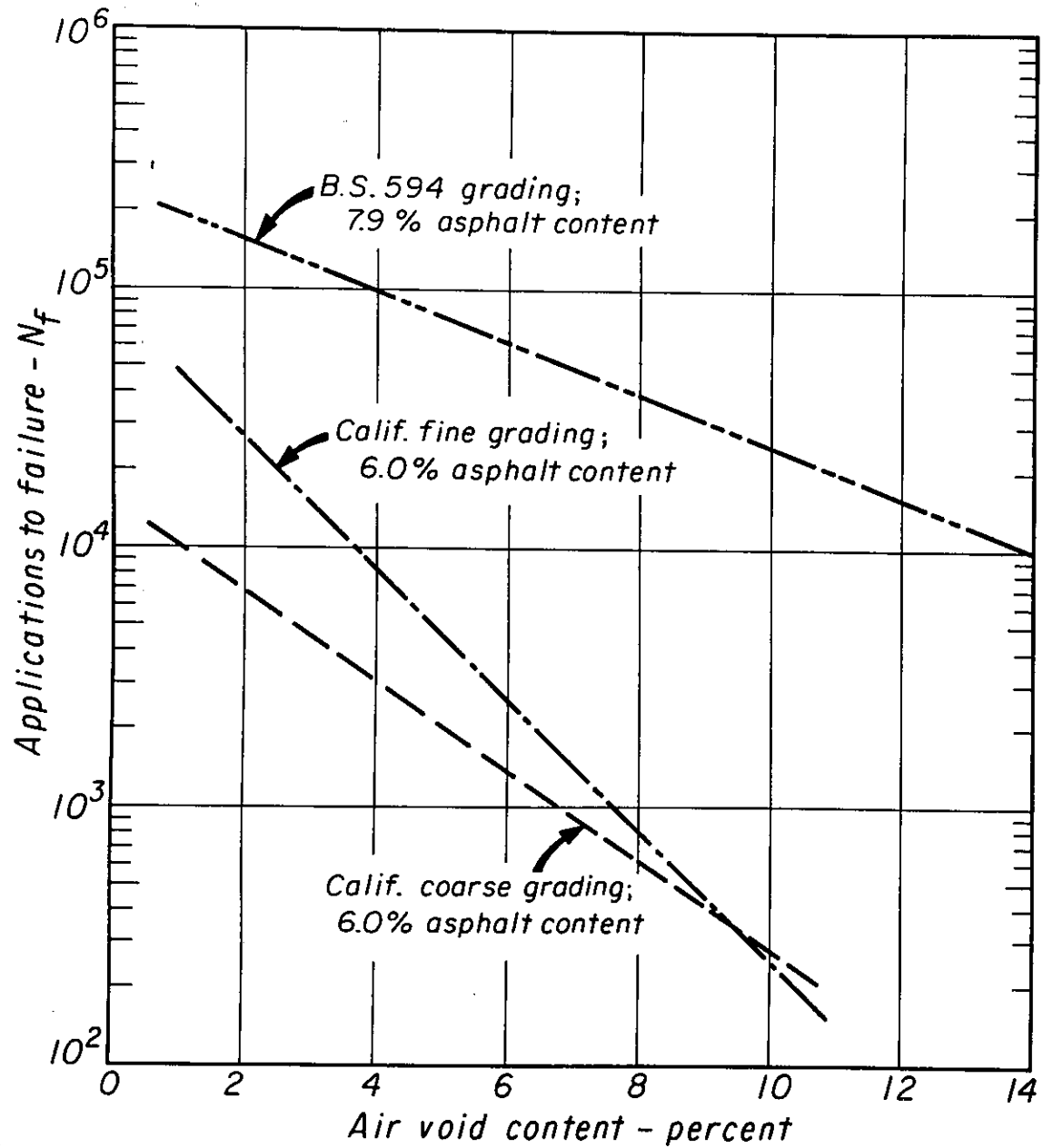
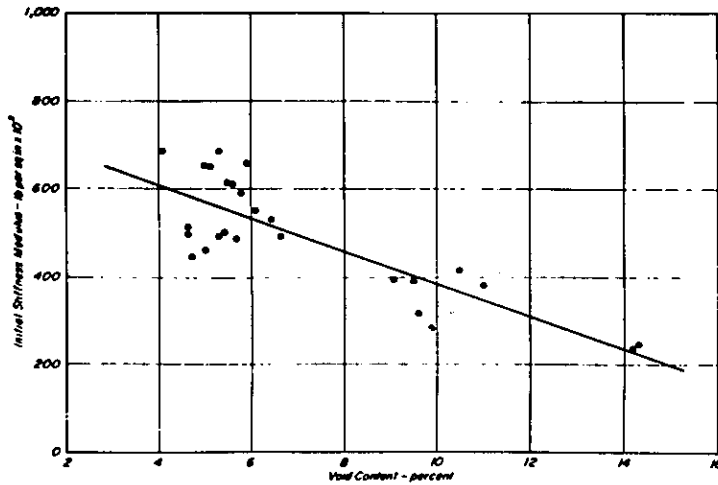
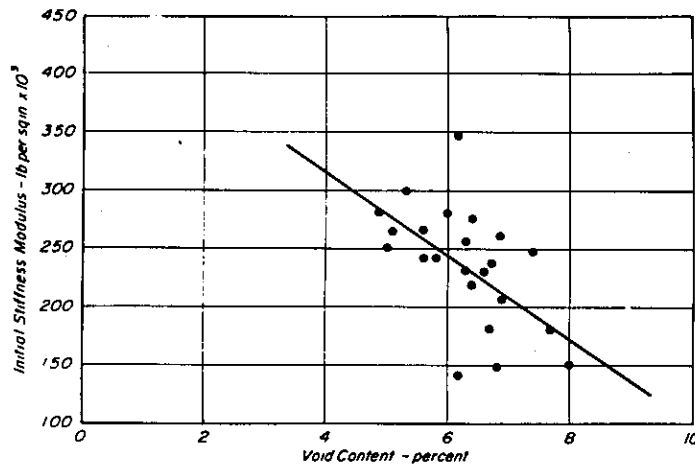


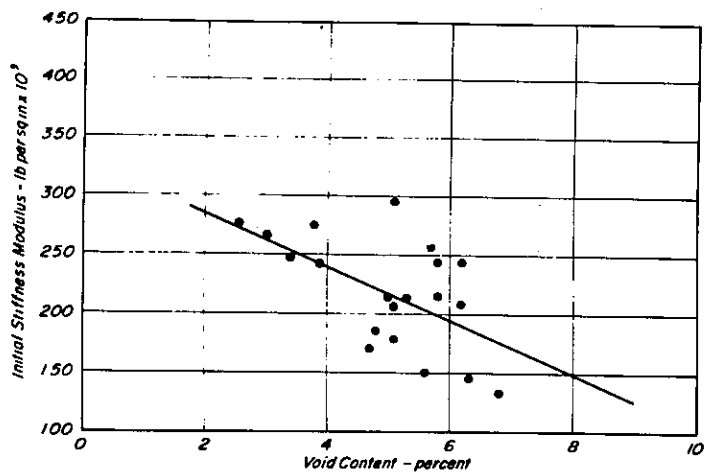
Fig. 25 - Effect of air void content on fatigue life, granite aggregate; stress level - 150 psi.



a. British Standard 594 grading — 7.9 percent asphalt.



b. California fine grading — 6 percent asphalt.



c. California coarse grading — 6 percent asphalt.

Fig. 26 — Relationships between initial stiffness modulus and air void content — granite aggregate.

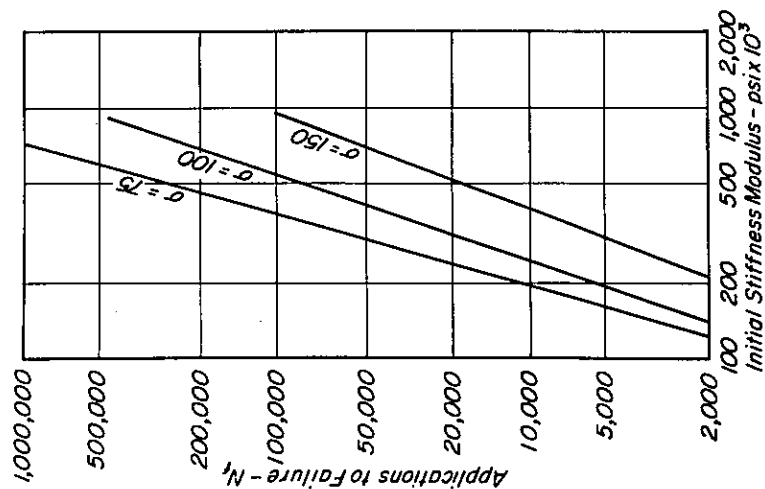


Fig. 27 - Relation between fatigue life and initial stiffness modulus California graded mixes, granite aggregates, 85-100, 60-70, and 40-50 penetration asphalts, 6 per cent asphalt content.

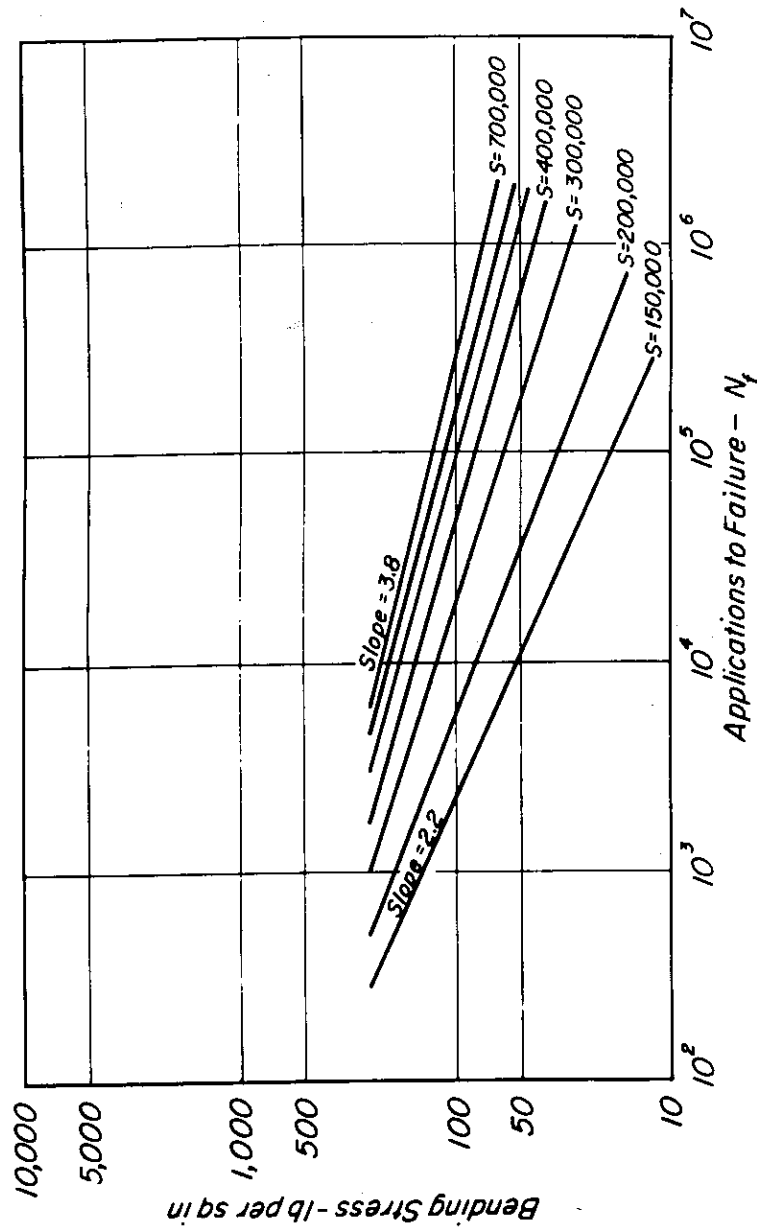


Fig. 28 - Bending stress vs. application to failure, for mixes of different stiffness - California graded mixes, granite aggregate, 85-100, 60-70, and 40-50 penetration asphalts, 6.0 per cent asphalt.

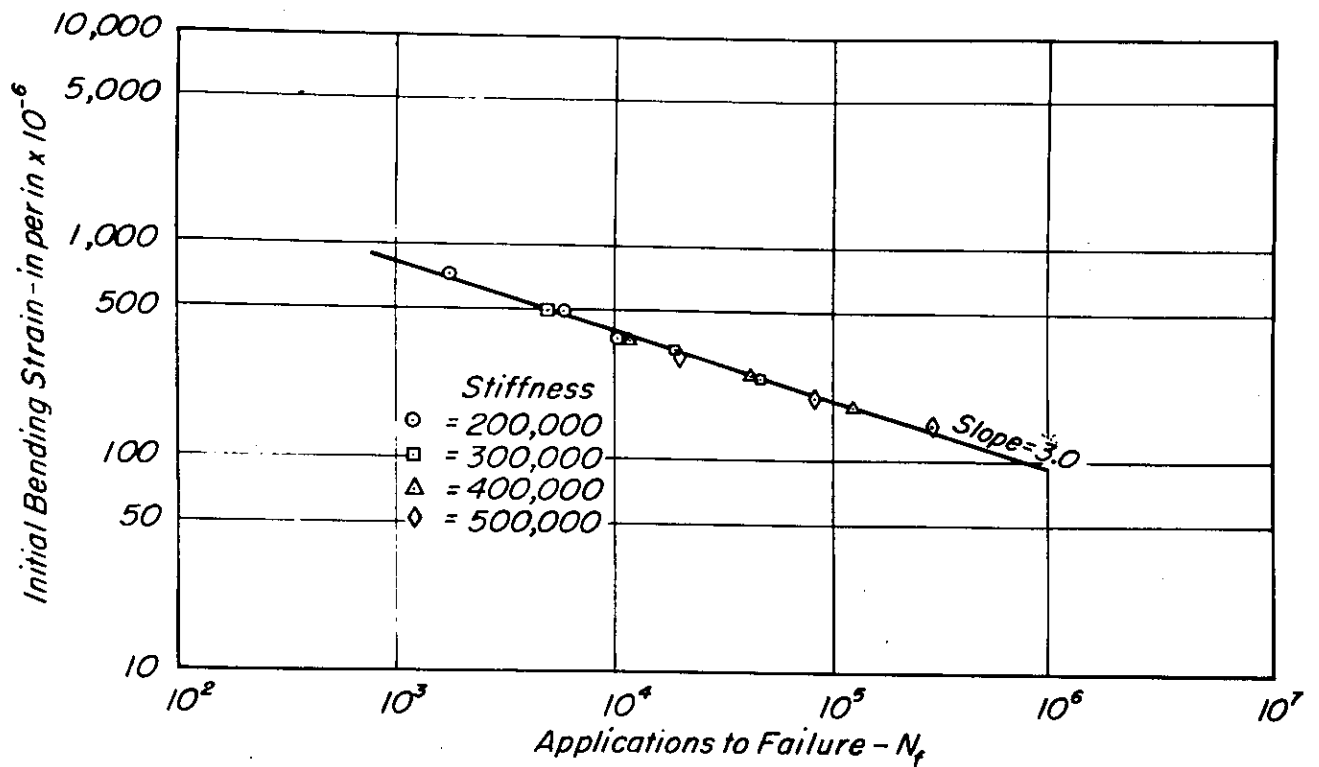


Fig.29 - Initial bending strain vs. application to failure, for mixes of different stiffness - California graded mixes, granite aggregate, 85-100, 60-70, and 40-50 penetration asphalts, 6.0 percent asphalt.

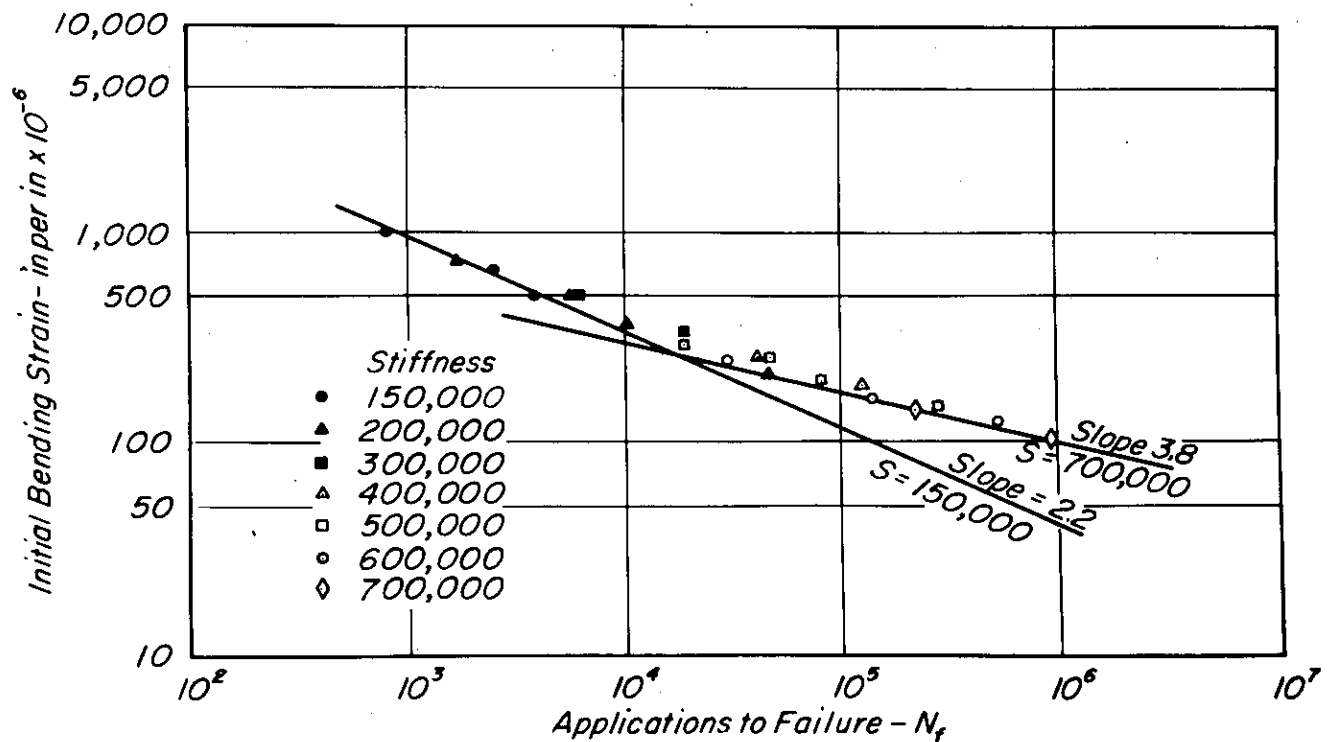


Fig. 30- Initial bending strain vs. application to failure, for mixes of different stiffness - California graded mixes, granite aggregate, 85-100, 60-70, and 40-50 penetration asphalts, 6.0 percent asphalt.

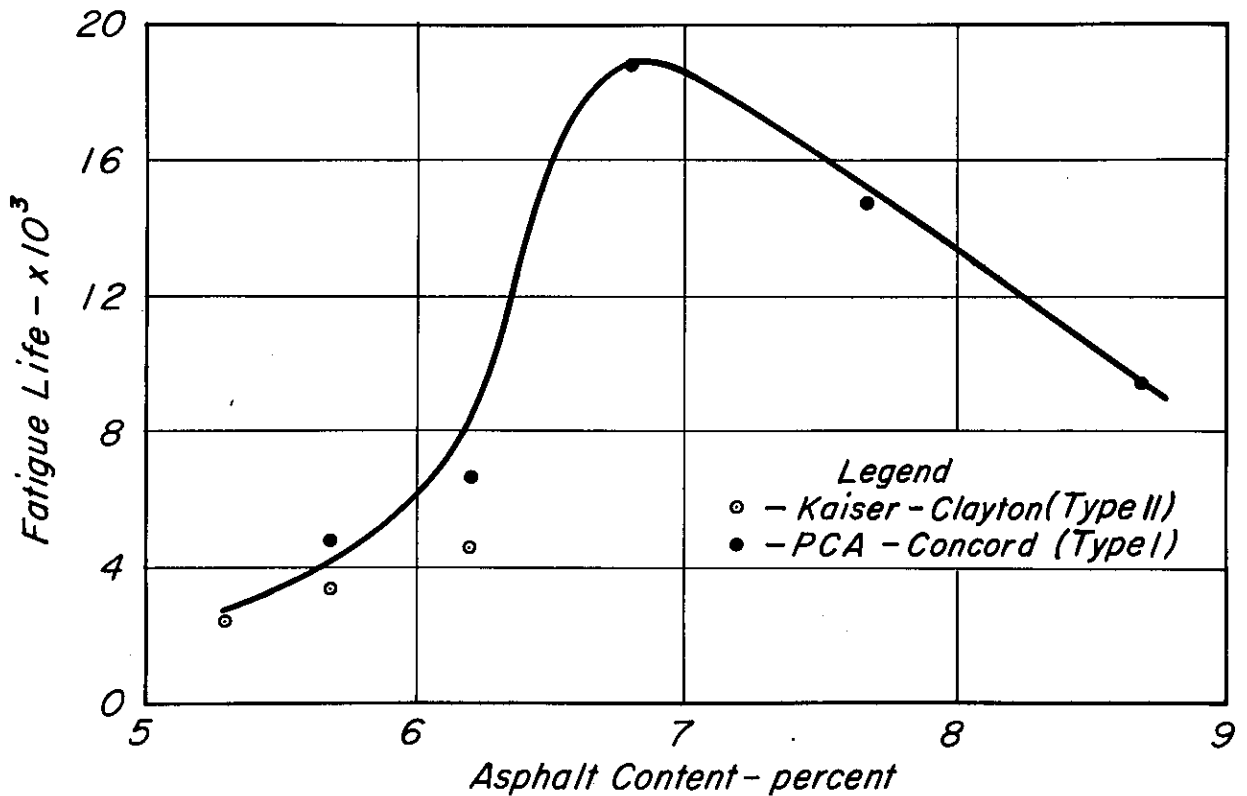


Fig. 31 - Effect of asphalt content on fatigue life - California medium grading, basalt aggregate, 60-70 penetration asphalt.

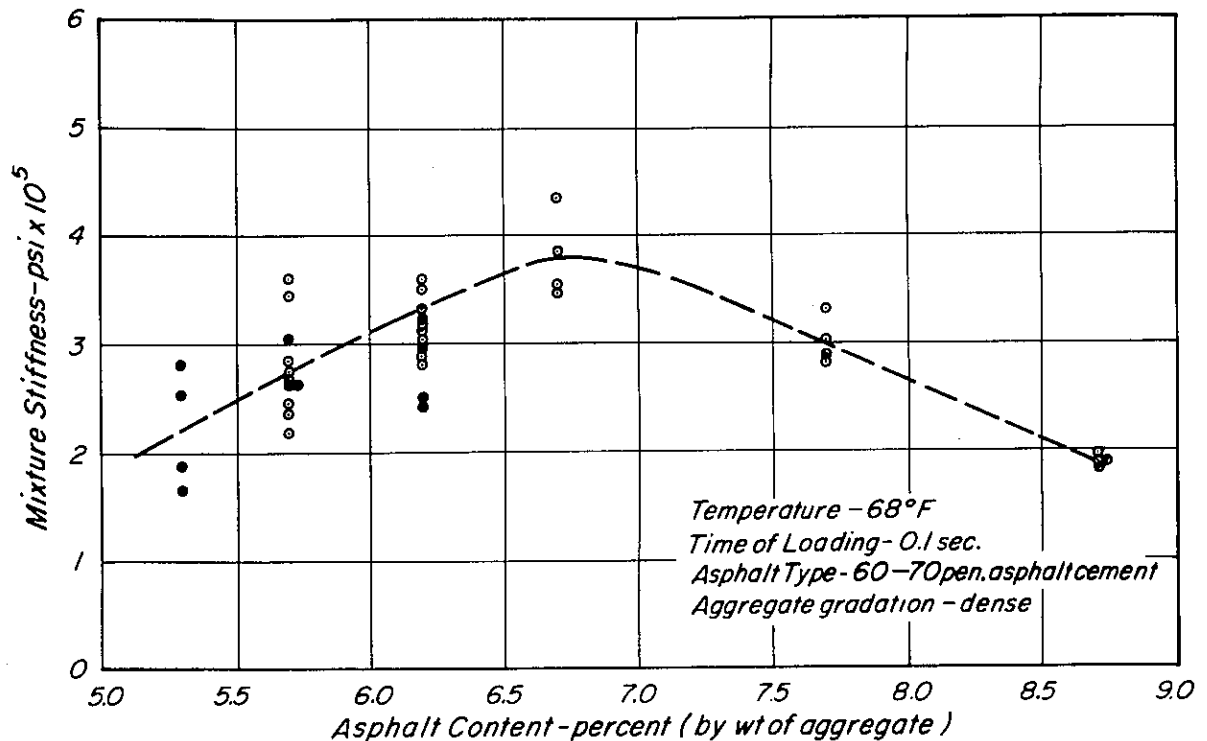


Fig. 32 - Relationship between initial stiffness modulus and asphalt content - California medium grading, basalt aggregate, 60-70 penetration asphalt.

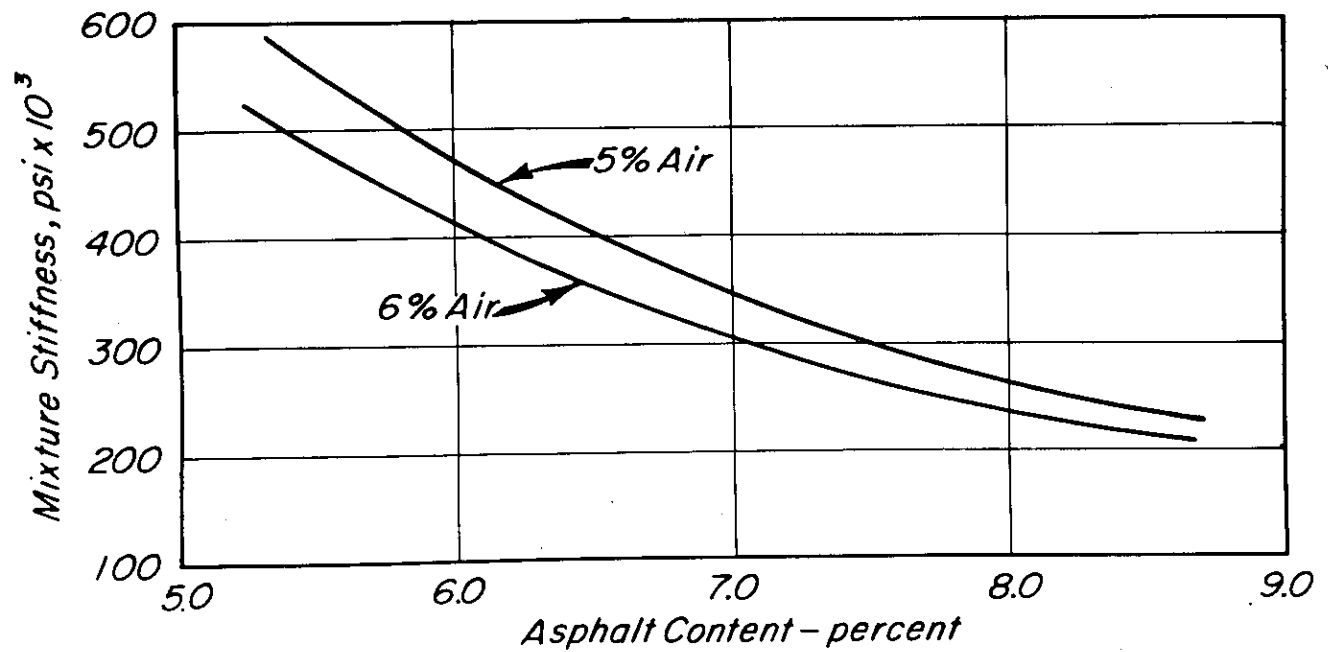


Fig. 33 — Estimated mixture stiffness from properties of recovered asphalt.

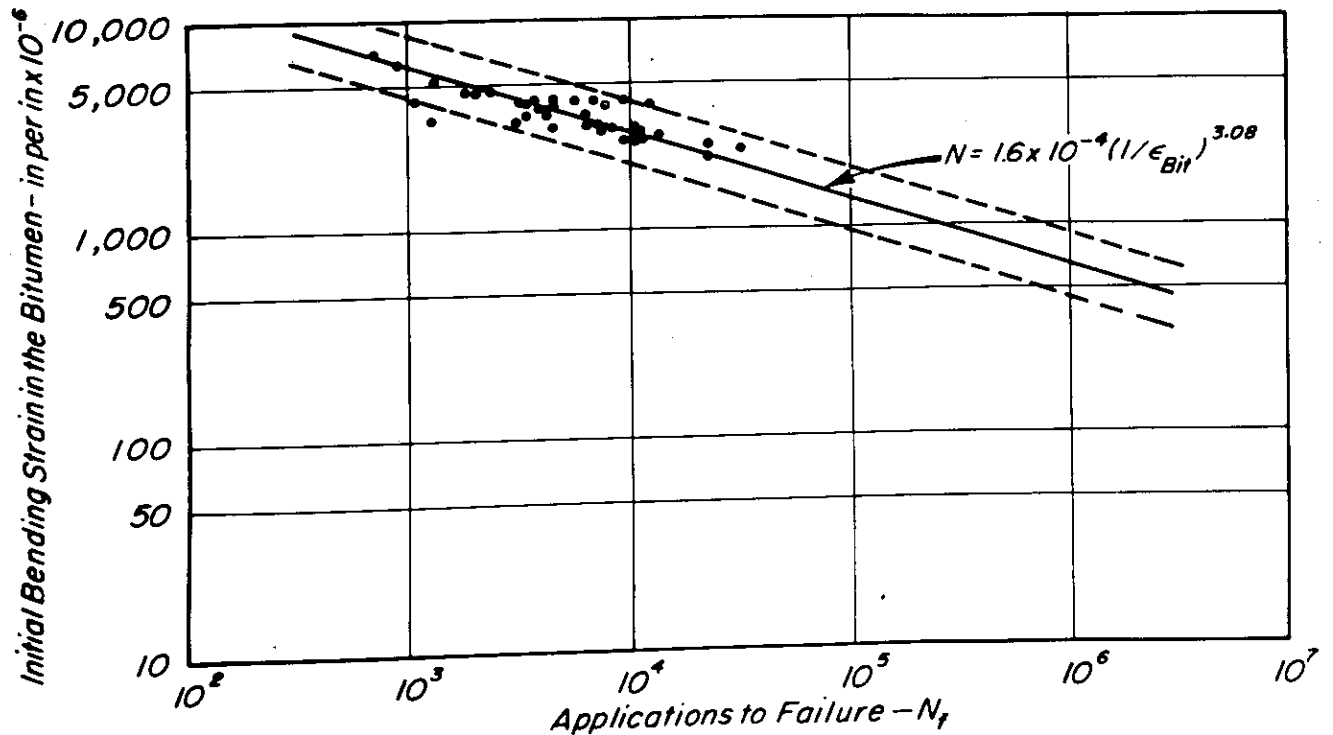


Fig. 34 — Initial bitumen bending strain vs. fatigue life — California medium grading, basalt aggregate, 60-70 penetration asphalt, 5.3 - 8.7 percent asphalt.

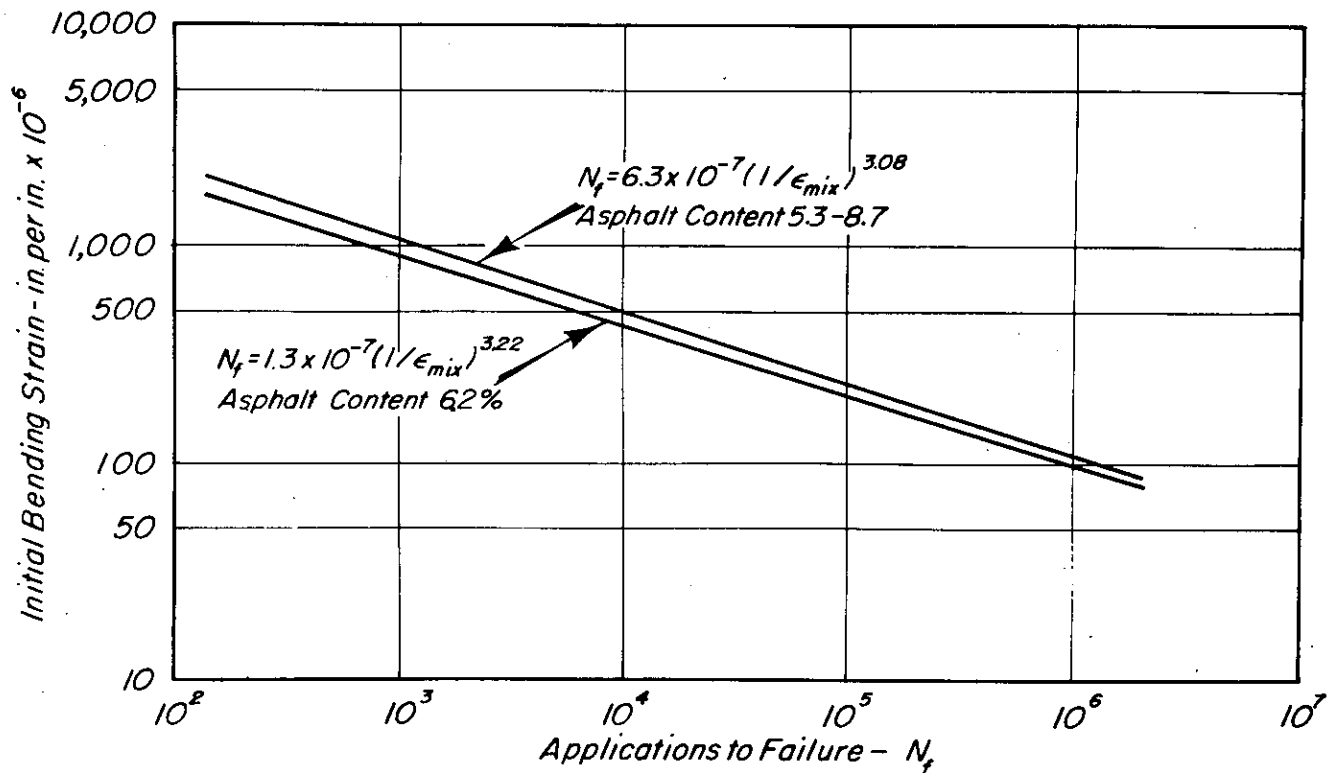


Fig. 35 — Comparison of calculated and measured fatigue behavior — California medium grading, basalt aggregate, 60-70 penetration asphalt, 5.3-8.7 percent asphalt.

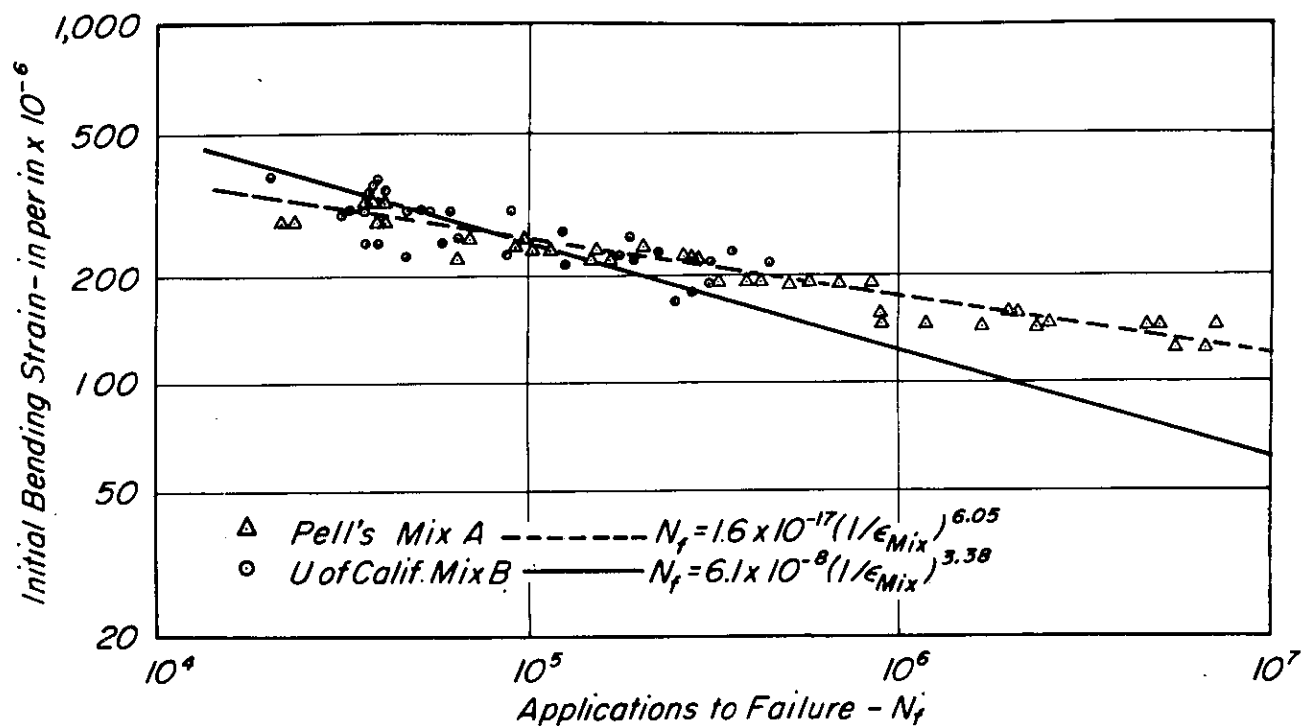


Fig. 36 — Comparison of individual test results of Pell's mix A and the British Standard 594 graded mix tested in the University of California Laboratory.

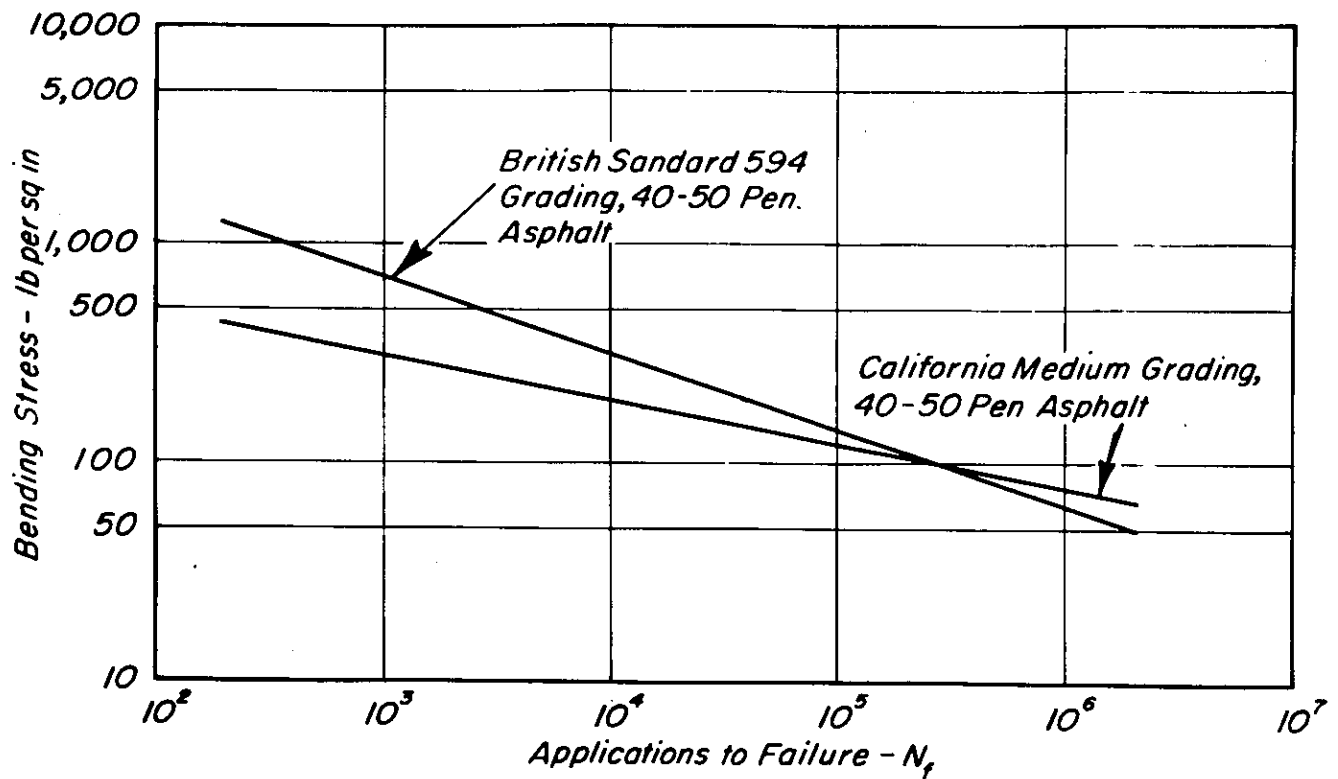


Fig. 37 — Comparison of fatigue results from British Standard 594 graded mix and California medium graded mix — mixture bending stress vs. N_f

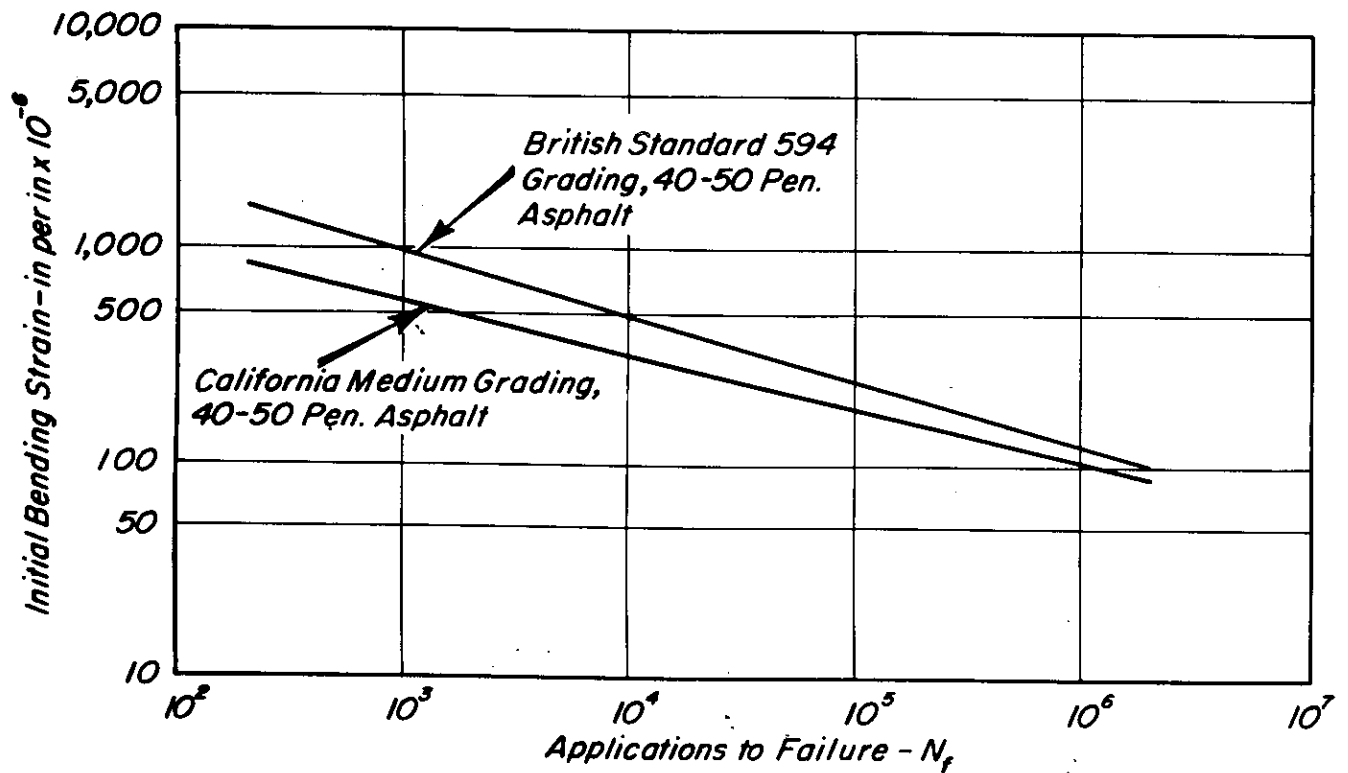


Fig. 38 — Comparison of fatigue results from British Standard 594 graded mix and California medium graded mix — initial mixture bending vs. fatigue life.

APPENDIX A

PROGRAM INSTRUCTIONS FOR MULTILAYERED ELASTIC SYSTEM USING THE CHEVRON FIVE-LAYER PROGRAM WITH ITERATION

Description

The Multilayered Elastic System computer program (CHEV5L with iteration) will determine the various component stresses and strains in a three dimensional ideal elastic layered system with two vertical uniform circular loads at the surface of the system. (The computer printout, however, lists the stresses and deformations resulting from one of the loads.) The bottom layer of the system is semi-infinite with all other layers of uniform thickness. All layers extend infinitely in the horizontal direction. The top surface of the system is free of shear and all interfaces between layers have full continuity of stresses and displacements.

With a vertical uniform circular load, the system is axi-symmetric with the Z axis perpendicular to the layers and extending through the center of the load. Using cylindrical coordinates, any point in the system may be described by an R and Z. R is the horizontal distance out from the center of the load and Z is the depth of the point measured vertically from the surface of the system.

The load is described by the total vertical load in pounds and the tire pressure in psi. The load radius is computed by the program. Each layer of the system is described by modulus of elasticity or stress-modulus relationship ($M_R = K_1 \theta^{K_2}$), Poisson's ratio, and thickness in inches. Each layer is numbered with the top layer as 1 and numbering each layer consecutively downward.

Program Operating Notes

The program operates with the various given R and Z values as follows:

Trial #1. For every R value a complete set of characterizing functions is developed for all layers, then the stresses and strains are computed at those points represented by that R and each of the given Z values. The program then steps to the next R value and computes the stresses and strains at those points represented by each of the given Z values and continues until all combinations of R and Z values are used.

Trial #2. The stresses calculated at each of these R and Z values are then used in determining the modulus for the respective points for trial 2. The stresses and strains for each R and Z are calculated as before. The stresses calculated from trial 2 are then used to determine the modulus for trial 3. This process is continued until the modulus assumed in trial n-1 is within a specified limit of that calculated in trial n. At this point, the stress and strains for each R and Z are then printed out.

When a given Z value is directly on an interface between two layers, the program will first compute the stresses and strains at this point using the functions for the upper of the two layers then will recompute the stresses and strains at this same point using the functions from the lower of the two layers. In the output of the program a negative Z value indicates that the stresses and strains have been computed at an interface and that the characteristics of the upper layer have been used.

Limitations

The following are limitations of the program and/or method.

1. Number of layers in the system; must be five.
2. Number of points in the system where stresses and strains are to be determined; refer to Fig. A1 for exact locations for which computations are required.
3. All data are positive, no negative values.
4. Poisson's ratio must not have a value of one.
5. Number of problems (pavement structures) to be solved.

Input Cards

The notation CC refers to card columns, with the range of columns being inclusive. All "Real" values (REAL) are punched with a decimal point as a part of the value and all "Integer" values (INTEGER) are to be punched without a decimal point and right justified in the data field.

- | | | |
|----------|---------------------------------|-------------|
| 1. CC1-5 | number of problems to be solved | FORMAT (I5) |
|----------|---------------------------------|-------------|

2. CC1-72 any combination of alphameric characters may be used to identify the problem to be solved. FORMAT (12 A6)
3. CC1-12 total load in pounds (REAL)
 CC13-24 tire pressure in psi (REAL)
 FORMAT (2F12.0)
4. CC1-2 number of layers in the system - must be five (INTEGER)
 CC3-10 initially assumed modulus of elasticity for layer 1 (REAL)
 CC11-16 Poisson's ratio for layer 1 (REAL)
 CC17-24 initially assumed modulus of elasticity for layer 2 (REAL)
 CC25-30 Poisson's ratio for layer 2 (REAL)
 etc. , FORMAT (I2, 5(F8.0, F6.0))
5. The data on this card is applicable for the top layer only. The data for the semi-infinite layer is loaded in card 6.
- CC1-10 coefficient K_1 in the relationship $M_R = K_1 \theta^{K_2}$ for layer 1. If layer 1 is linearly elastic then K_1 equals the modulus.
- CC11-20 coefficient K_2 in the relationship $M_R = K_1 \theta^{K_2}$ for layer 1. If layer is linearly elastic, $K_2 = 0$.
- CC21-30 coefficient K_1 in the relationship $M_R = K_1 \theta^{K_2}$ for layer 2. If layer 2 is linearly elastic then K_1 equals the modulus.
- CC31-40 coefficient K_2 in the relationship $M_R = K_1 \theta^{K_2}$ for layer 2. If layer 2 is linearly elastic then $K_2 = 0$.
 etc. , FORMAT (8 F10.0)
6. CC1-10 unit weight of material in layer 1
 CC11-20 unit weight of material in layer 2
 etc. , FORMAT (4F 10.0)

7. This card reads in the curve of resilient modulus vs. repeated vertical stress.

CC1-2 number of points in this data. (INTEGER)
 CC3-8 deviator stress for the first point (REAL)
 CC9-16 resilient modulus corresponding to the first point deviator stress
 (REAL)
 CC17-24 deviator stress for the second point
 CC25-32 resilient modulus corresponding to the second point deviator stress
 etc. , FORMAT (I2, F6.0, 9F8.0/(10F8.0))
 maximum of 20 points can be used.

8. CC1-6 thickness of layer 1 in inches (REAL)
 CC7-12 thickness of layer 2 in inches (REAL)
 etc. , FORMAT (4F6.0)

9. The radial distances read in on this card must correspond to those shown on Fig. A1. (0, 1, 1-1/2, 2, 3, and 4 radii).

CC1-6 number of R values on card (INTEGER)
 CC7-12 first R value (REAL) in inches
 CC13-18 19-24, 25-30 second, third, etc. , R value
 FORMAT (I6, 11F6.0)

10. The vertical distances read in on this card must correspond to those shown in Fig. A1.

CC1-6 number of Z values on card (INTEGER)
 CC7-12 first Z value (REAL) in inches
 CC13-18, 19-24, 25-30, second, third, etc. , Z value
 FORMAT (I6, 11F6.0)

CARDS 2 THROUGH 10 MAY BE REPEATED FOR EACH DIFFERENT SYSTEM TO BE SOLVED AS INDICATED ON CARD 1

Example of input cards for one five-layer system.

```

1      1
2 ***SAN DIEGO TEST ROAD--SECTION 1---CLASS 2 AGGREGATE BASE*****
3      4500.      70.      0  2
4 5 140000. .40 20000. .20 20000. .20 50000. .32 20000. .40
5      140000.      0.0      3800.      0.5      3800.      0.5      50000.      0.0
6      145.      138.      138.      120.
7 3 0. 20000. 5.0 20000. 10. 20000.
8 3.12 7.28 7.28 39.20
9      6 0.0 4.5 6.7 9.0 13.5 18.0
10     7 0.0 3.12 6.76 10.40 14.04 17.68 56.88

```

Sample Problems

Fig. A2 shows a typical problem to be solved with the CHEV5L (with iteration) program. As indicated, only layers two and three have relationship between stress level to resilient modulus. For many conditions, however, it may be that the bottom four layers will have relationships between stress level and resilient modulus.

The input data (cards 1 through 10) for a typical pavement section is shown in Table A1 and output for this problem is shown in Table A2.

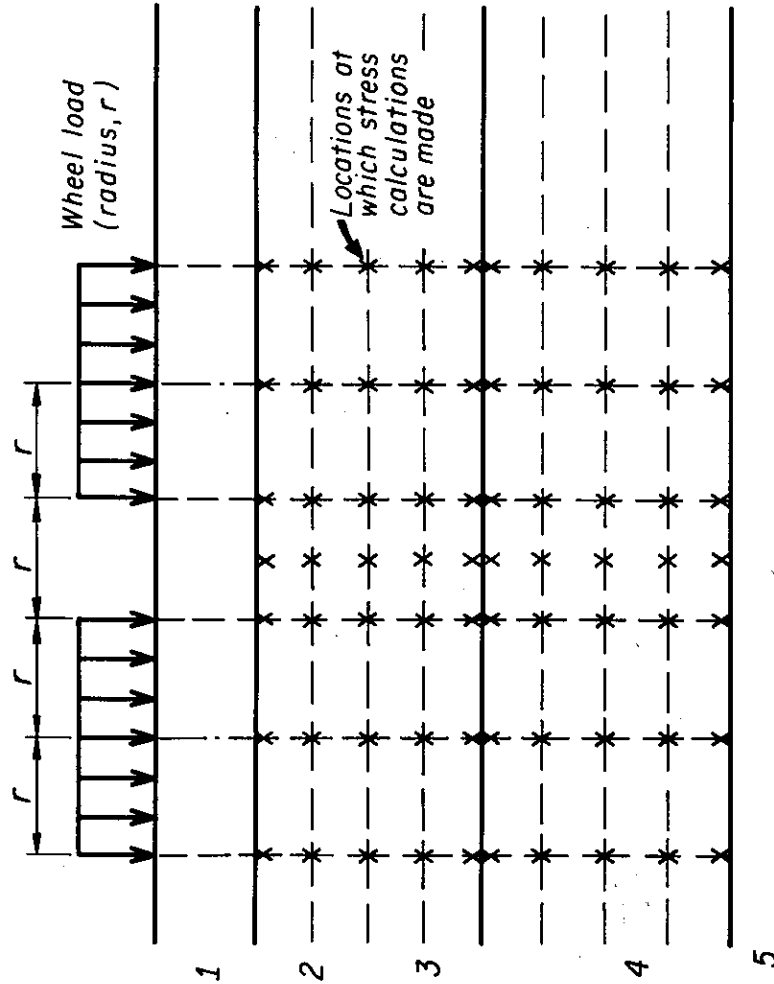


Fig. A-1 -- Computer representation of pavement structure.

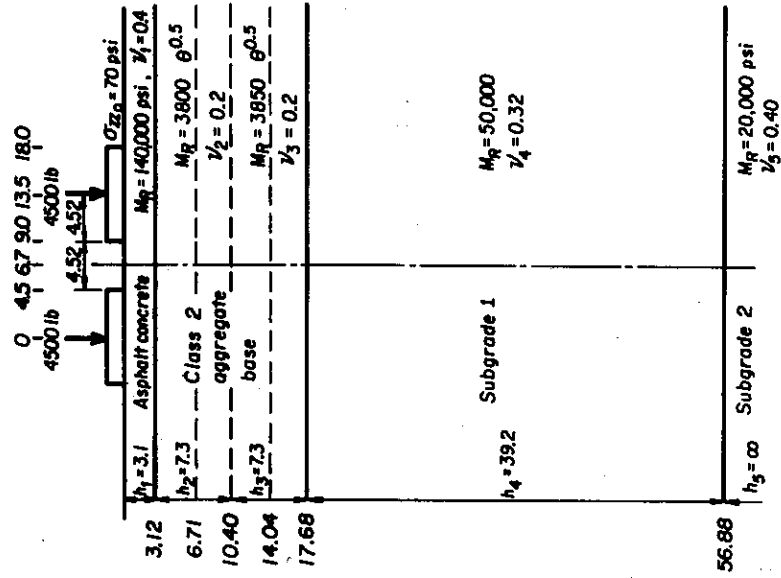


Fig. A-2 -- Pavement structure for sample problem Section 1, San Diego Test Road.

TABLE A1 — INPUT DATA FOR SAMPLE PROBLEM

FORTRAN Coding Form

IBM

PAGE		CHEV 5L w/Iteration		DATE		PURCHASER INSTRUCTIONS		GRAPHIC PURCH		PAGE OF		CERO ELECTRO NUMBER	
1		2		3		4		5		6		7	
8		9		10		11		12		13		14	
15		16		17		18		19		20		21	
22		23		24		25		26		27		28	
29		30		31		32		33		34		35	
36		37		38		39		40		41		42	
43		44		45		46		47		48		49	
50		51		52		53		54		55		56	
57		58		59		60		61		62		63	
64		65		66		67		68		69		70	
71		72		73		74		75		76		77	
78		79		80		81		82		83		84	
85		86		87		88		89		90		91	
92		93		94		95		96		97		98	
99		100		101		102		103		104		105	

As standard card form, BPA electric 488157, is available for purchase separately, for \$1.00.

TABLE A2- COMPUTER OUTPUT FOR TYPICAL PROBLEM

***** **SAN DIEGO TEST ROAD--SECTION 1---CLASS 2 AGGREGATE BASE***** *****

THE PROBLEM PARAMETERS ARE

TOTAL LOAD..	6500.00 LBS
TIRE PRESSURE..	70.00 PSI
LOAD RADIUS..	4.52 IN.
LAYER 1 HAS MODULUS	140000.
LAYER 2 HAS MODULUS	20000.
LAYER 3 HAS MODULUS	20000.
LAYER 4 HAS MODULUS	50000.
LAYER 5 HAS MODULUS	20000.
	POISSONS RATIO
	.400
	AND THICKNESS
	.200
	AND THICKNESS
	.200
	AND THICKNESS
	.320
	AND THICKNESS
	.400
	AND IS SEMI-INFINITE.

MODULUS-STRESS RELATIONSHIPS

MODULUS OF LAYER 1 =	140000.(THETA) ** 0.
MODULUS OF LAYER 2 =	3800.(THETA) ** .50
MODULUS OF LAYER 3 =	3800.(THETA) ** .50
MODULUS OF LAYER 4 =	50000.(THETA) ** 0.
MODULUS OF LAYER 5 IS INTERPOLATED FROM CURVE OF LABORATORY RESULTS	

AFTER TRIAL NO. 1		MODULUS USED	MODULUS REQUIRED
LAYER NO. 1	1	140000.	140000.
LAYER NO. 2	2	20000.	17307.
LAYER NO. 3	3	20000.	13449.
LAYER NO. 4	4	50000.	50000.
LAYER NO. 5	5	20000.	20000.

TABLE A2 (Continued)

***** SAN DIEGO TEST ROAD--SECTION 1--CLASS 2 AGGREGATE BASE***** *****

THE PROBLEM PARAMETERS ARE

TOTAL LOAD..	4500.00	LES			
TIRE PRESSURE..	70.00	PSI			
LOAD RADIUS..	4.72	IN.			
LAYER 1 HAS MODULUS	14000.		PCISSNS RATIO	.400	AND THICKNESS 3.1 IN.
LAYER 2 HAS MODULUS	18204.		PCISSNS RATIO	.200	AND THICKNESS 7.3 IN.
LAYER 3 HAS MODULUS	18786.		PCISSNS RATIO	.200	AND THICKNESS 7.3 IN.
LAYER 4 HAS MODULUS	50000.		PCISSNS RATIO	.320	AND THICKNESS 39.2 IN.
LAYER 5 HAS MODULUS	20000.		PCISSNS RATIO	.400	AND IS SEMI-INFINITE.

AFTER TRIAL NO. 2

MODULUS REQUIRED

MODULUS USED

LAYER NO. 1	14000.	14000.
LAYER NO. 2	18204.	16825.
LAYER NO. 3	18786.	13678.
LAYER NO. 4	50000.	50000.
LAYER NO. 5	20000.	20000.

TABLE A2 (Continued)

***** **SAN DIEGO TEST ROAD--SECTION 1---CLASS 2 AGGREGATE BASE***** *****

THE PROBLEM PARAMETERS ARE

TOTAL LOAD..	4500.00 LBS
TIRE PRESSURE..	70.00 PSI
LOAD RADII..	4.52 IN.
LAYER 1 HAS MODULUS	140000.
LAYER 2 HAS MODULUS	17251.
LAYER 3 HAS MODULUS	14374.
LAYER 4 HAS MODULUS	50000.
LAYER 5 HAS MODULUS	20000.
	PCISSENS RATIO
	400
	AND THICKNESS
	3.1 IN.
	AND THICKNESS
	7.3 IN.
	AND THICKNESS
	7.3 IN.
	AND THICKNESS
	39.2 IN.
	AND IS SEMI-INFINITE.

AFTER TRIAL NO. 3

MODULUS USED MODULUS REQUIRED

LAYER NO.	1	140000.	140000.
LAYER NO.	2	17251.	14668.
LAYER NO.	3	14374.	13693.
LAYER NO.	4	50000.	50000.
LAYER NO.	5	20000.	20000.

TABLE A2 (Continued)

***** SAN DIAGO TEST ROAD--SECTION 1---CLASS 2 AGGREGATE BASE***** *****

THE PROBLEM PARAMETERS ARE

TOTAL LOAD..	4500.00 LBS		
TIRE PRESSURE..	70.00 PSI		
LOAD RADII..	4.72 IN.		
LAYER 1 HAS MODULUS	140000.	POISSONS RATIO	.400 AND THICKNESS 3.1 IN.
LAYER 2 HAS MODULUS	16876.	POISSONS RATIO	.200 AND THICKNESS 7.3 IN.
LAYER 3 HAS MODULUS	13920.	POISSONS RATIO	.200 AND THICKNESS 7.3 IN.
LAYER 4 HAS MODULUS	50000.	POISSONS RATIO	.320 AND THICKNESS 39.2 IN.
LAYER 5 HAS MODULUS	20000.	POISSONS RATIO	.400 AND IS SEMI-INFINITE.

	AFTER TRIAL NO. 4	
	MODULUS USED	MODULUS REQUIRED
LAYER NO. 1	140000.	140000.
LAYER NO. 2	16876.	16621.
LAYER NO. 3	13920.	13702.
LAYER NO. 4	50000.	50000.
LAYER NO. 5	20000.	20000.

TABLE A2 (Continued)

***** SAN DIEGO TEST ROAD--SECTION 1--CLASS 2 AGGREGATE BASE***** *****

THE PROBLEM PARAMETERS ARE

TOTAL L JAC..	4500.00	LPS
TIRE PRESSURE..	70.00	PSI
LOAD RADII..	4.32	IN.
LAYER 1 HAS MODULUS	140000.	POISSONS RATIO .400 AND THICKNESS 3.1 IN.
LAYER 2 HAS MODULUS	16706.	POISSONS RATIO .200 AND THICKNESS 7.3 IN.
LAYER 3 HAS MODULUS	13775.	POISSONS RATIO .200 AND THICKNESS 7.3 IN.
LAYER 4 HAS MODULUS	50000.	POISSONS RATIO .320 AND THICKNESS 39.2 IN.
LAYER 5 HAS MODULUS	20000.	POISSONS RATIO .400 AND IS SEMI-INFINITE.

	AFTER TRIAL NO. 5	MODULUS USED	MODULUS REQUIRED
LAYER NO. 1		140000.	140000.
LAYER NO. 2		16706.	16310.
LAYER NO. 3		13775.	13707.
LAYER NO. 4		50000.	50000.
LAYER NO. 5		20000.	20000.

MODULUS ITERATION CLOSURES IN TRIAL NO. 5

TABLE A2 (Continued)

***** **SAN DFGO TEST FGAC--SECTION 1---CLASS 2 AGGREGATE BASE***** *******

THE PROBLEM PARAMETERS ARE

TOTAL LOAD.. 500.00 LBS

TIRE PRESSURE.. 70.00 PSI

LOAD RADII.. 4.12 IN.

LAYER 1 HAS MODULUS 140000. PCISSONS RATIO .400 AND THICKNESS 3.1 IN.
 LAYER 2 HAS MODULUS 16700. PCISSONS RATIO .200 AND THICKNESS 7.3 IN.
 LAYER 3 HAS MODULUS 13775. PCISSONS RATIO .200 AND THICKNESS 7.3 IN.
 LAYER 4 HAS MODULUS 50000. PCISSONS RATIO .320 AND THICKNESS 39.2 IN.
 LAYER 5 HAS MODULUS 20000. PCISSONS RATIO .400 AND IS SEMI-INFINITE.

R	Z	S T R E S S E S				D I S P L A C E M E N T				S T R A I N S			
		VERTICAL	TANGENTIAL	RADIAL	SHEAR	BULK	VERTICAL	RADIAL	TANGENTIAL	SHEAR			
0.	0.	-7.000E+01	-1.627E+02	-1.627E+01	0.	-3.954E+02	1.721E-02	-4.974E-04	-4.974E-04	0.			
0.	-3.1	-3.523E+01	9.385E+01	5.385E+01	0.	1.524E+02	1.656E-02	5.030E-04	5.030E-04	0.			
0.	3.1	-3.523E+01	1.683E+00	1.683E+00	0.	-3.191E+01	1.656E-02	5.030E-04	5.030E-04	0.			
0.	5.3	-1.845E+01	1.933E+00	1.933E+00	0.	-1.458E+01	1.076E-03	3.135E-04	3.135E-04	0.			
0.	10.4	-1.097E+01	1.744E+00	1.744E+00	0.	-7.485E+00	7.516E-03	2.148E-04	2.148E-04	0.			
0.	10.4	-1.097E+01	9.364E-01	9.364E-01	0.	-5.059E+00	7.516E-03	2.148E-04	2.148E-04	0.			
0.	14.0	-7.613E+00	1.572E-01	1.572E-01	0.	-7.301E+00	5.051E-03	1.197E-04	1.197E-04	0.			
0.	17.7	-5.345E+00	-5.292E-01	-5.292E-01	0.	-7.542E+00	3.344E-03	2.856E-05	2.856E-05	0.			
0.	35.9	-3.567E-01	-5.748E-01	-5.748E-01	0.	-6.833E+00	3.344E-03	2.856E-05	2.856E-05	0.			
0.	55.9	-1.347E-01	-3.060E-02	-3.060E-02	0.	3.997E-01	1.771E-03	9.777E-06	9.777E-06	0.			
4.5	0.	-5.324E+01	-1.023E+02	-7.747E+01	-3.630E-13	-2.230E+02	1.310E-02	-1.375E-04	-3.859E-04	-1.737E-03	SLOW		
4.5	-3.1	-2.037E+01	3.253E+01	2.315E+01	-1.054E+01	5.595E+01	1.281E-02	7.766E-05	3.658E-04	1.646E-03			
4.5	3.1	-2.037E+01	1.544E+00	-2.667E+00	-1.094E+00	-2.129E+01	1.281E-02	7.766E-05	3.658E-04	1.646E-03			
4.5	5.3	-1.0310E+01	1.529E+00	4.301E-02	-5.005E+00	-1.161E+01	9.206E-03	1.359E-04	2.489E-04	1.119E-03			
4.5	10.4	-3.895E+00	1.533E+00	5.687E-01	-2.335E+00	-6.793E+00	6.777E-03	1.294E-04	1.843E-04	8.296E-04			
4.5	10.4	-3.895E+00	7.923E-01	1.612E-01	-2.335E+00	-7.943E+00	6.777E-03	1.294E-04	1.843E-04	8.296E-04			
4.5	14.0	-3.895E+00	1.207E-01	-1.522E-01	-1.274E+00	-6.627E+00	4.731E-03	8.271E-05	1.067E-04	4.803E-04			
4.5	17.7	-1.092E+00	-5.343E-01	-8.853E-01	-5.688E-01	-6.811E+00	3.237E-03	2.177E-05	2.621E-05	1.180E-04			
4.5	35.9	-7.092E+00	-5.478E-01	-7.150E-01	-5.688E-01	-6.355E+00	3.237E-03	2.177E-05	2.621E-05	1.180E-04			
4.5	55.9	-3.273E-01	-6.500E-01	-6.500E-01	-3.609E-02	3.892E-01	1.763E-03	9.483E-06	9.678E-06	4.355E-05			
4.5	55.9	-3.273E-01	-3.082E-02	-3.082E-02	-3.509E-02	-5.918E-01	1.763E-03	9.483E-06	9.678E-06	4.355E-05			
5.7	0.	3.573E-01	-1.561E+01	-1.483E+00	-3.155E-13	-3.674E+01	9.651E-03	9.012E-05	-2.511E-04	-1.683E-03	SLOW		
5.7	-3.1	-9.407E+00	2.625E+01	1.804E+01	-3.474E+00	-7.608E+00	9.769E-03	-1.588E-04	2.243E-04	1.503E-03			
5.7	3.1	-9.407E+00	3.987E-01	-4.235E+00	-8.474E+00	-1.334E+01	9.769E-03	-1.588E-04	2.243E-04	1.503E-03			
5.7	5.3	-1.133E+00	1.159E+00	-1.291E+00	-5.133E+00	-9.027E+00	7.743E-03	1.534E-05	1.914E-04	1.282E-03			
5.7	10.4	-7.092E+00	1.153E+00	-1.815E-01	-2.720E+00	-6.032E+00	5.954E-03	5.917E-05	1.550E-04	1.039E-03			
5.7	10.4	-7.092E+00	5.435E-01	-4.849E-01	-2.720E+00	-6.816E+00	5.954E-03	5.917E-05	1.550E-04	1.039E-03			
5.7	14.0	-1.555E+00	3.127E-02	-4.213E-01	-1.667E+00	-5.894E+00	4.344E-03	4.886E-05	9.353E-05	6.266E-04			

TABLE A2 (Continued)

***** **SAN DING TEST ROAD--SECTION 1---CLASS 2 AGGREGATE BASE*****									

APPENDIX B

The appendix consists of three parts, each of which is the Fortran IV listing of a computer program used to perform calculations to which reference has been made in the body of the dissertation. These programs have been heavily annotated making use of comment (C) statements in order to define the variable names employed and to indicate the nature of the computation being carried out. The three parts of the appendix are:

Part 1. Determination of the Traffic Weighted Mean Stiffness.

Part 2. Stress-Modulus Iteration in the Chevron Five-Layer Program.

Part 3. Fatigue Life Prediction.

PART 1. DETERMINATION OF TRAFFIC WEIGHTED MEAN STIFFNESS

THIS PROGRAM DETERMINES THE TRAFFIC WEIGHTED MEAN STIFFNESS AT
 ARBITRARILY SELECTED DEPTHS WITHIN AN ASPHALT CONCRETE LAYER ON A
 DAY WITH GIVEN WEATHER AND TRAFFIC VARIATIONS. THE PROGRAM CONSISTS
 OF THE MAIN PROGRAM AND ONE SUBROUTINE. THE FUNCTION OF THE SUBROUTINE
 IS SOLELY TO PRINT A TITLE PAGE FOR EACH SERIES OF CALCULATIONS.

PROGRAM LIST

THE FOLLOWING DATA IS READ AND STORED

- MBIG - THE NUMBER OF PAVEMENTS TO BE CONSIDERED. EACH DIFFERENT
 TRAFFIC VARIATION, ASPHALT TYPE, OR SET OF MIXTURE PROPERTIES
 DEFINES A SEPARATE PAVEMENT.
- NRUN - THE NUMBER OF DAYS ON WHICH THE CALCULATIONS ARE TO BE PER-
 FORMED. SUBROUTINE FIRST IS CALLED ONCE FOR EACH DAY AND A NEW
 TITLE PAGE PRODUCED.
- TITLE - THE IDENTIFICATION OF THE PROBLEM
- LOCAT - THE IDENTIFICATION OF THE TYPE OF TRAFFIC VARIATION BEING CON-
 sidered.
- TRAFF - THE HOURLY VALUES OF THE DAILY TRAFFIC VARIATION AS
 PER CENT OF DAILY TRAFFIC
- PEN - STANDARD PENETRATION TEST RESULT ON RECOVERED ASPHALT
- RANDB - RING AND BALL SOFTENING POINT OF THE RECOVERED ASPHALT

```

MAIN PROGRAM      KASIANCHUK
DIMENSION Z(10),TEMP(25),TRAFF(24),T(25),S(25),SMIX(25),TITLE( 8),
1 MONTH(4), LOCAT( 8)
COMMON TA,TR,WIND,ELL,B,SS,W,COND,CV,AIR,PEN,RANDB,TEMP,TITLE,
1 MONTH, LOCAT,SKY
READ 208, MBIG
DO 207 MBI = 1,MBIG
READ 208, NRUN
208 FORMAT (I5)
READ 79,(TITLE(I) , I = 1, 8)
READ 79,(LOCAT(I), I = 1,8)
79 FORMAT(8A10)
READ 10,TRAFF
10 FORMAT(12F6.0/12F6.0)
READ 89,PEN,RANDB
89 FORMAT(2F10.0)
  
```



```

C      FOR THESE VALUES OF THE ASPHALT PROPERTIES, A TEMPERATURE-
C      STIFFNESS RELATION CAN BE OBTAINED FROM THE HEUKELOM NOMOGRAPH AT SOME
C      PARTICULAR TIME-OF-LOADING.  THE TEMPERATURE RANGE OVER WHICH THIS
C      DEFINITION IS DETERMINED SHOULD BE AS GREAT AS THE EXPECTED RANGE IN
C      DAILY PAVEMENT TEMPERATURES.  THESE VALUES WILL BE USED LATER IN A
C      NUMERICAL INTERPOLATION TO OBTAIN A STIFFNESS OF THE ASPHALT AT ANY
C      ARBITRARY TEMPERATURE.
C
C      NVAL  - THE NUMBER OF POINTS OBTAINED IN THE TEMPERATURE - STIFFNESS
C              RELATIONSHIP
C      T(I)  - THE I-TH VALUE OF TEMPERATURE-DEG.F.
C      S(I)  - THE 3ORRESPONDING I-TH VALUE OF STIFFNESS - KG/SQCM
C
C      READ 21,NVAL,(T(I),S(I), I = 1,NVAL)
C      21 FORMAT(I5,5(F4.0,F10.0) / (5X,5(F4.0,F10.0)))
C
C      THE STIFFNESS OF THE ASPHALT CONCRETE AND THE TEMPERATURE DIST-
C      RIBUTION INVOLVE CALCULATIONS WHICH REQUIRE THE FOLLOWING MIXTURE
C      PROPERTIES.
C
C      B      - ABSORPTIVITY OF THE SURFACE TO SOLAR INSOLATION
C      SS     - SPECIFIC HEAT OF THE MIXTURE - BTU/DEG.F.,LB
C      W      - UNIT WEIGHT OF MIXTURE - LB/CU. FT.
C      COND   - THERMAL CONDUCTIVITY - BTU-FT/SQ FT,DEG F,HR
C      CV     - VOLUME CONCENTRATION OF AGGREGATE - AS A DECIMAL
C      AIR    - AIR VOIDS CONTENT - AS A DECIMAL
C
C      READ 321,B,SS,W,COND,CV,AIR
C      321 FORMAT(6F10.0)
C
C      THE DEPTHS AT WHICH THE CALCULATIONS ARE TO BE CARRIED OUT ARE
C      THEN LOADED.
C
C      NZ     - THE NUMBER OF SUCH DEPTHS
C      Z(KZ)  - THE KZ-TH VALUE OF THE DEPTH-INCHES
C
C      READ 15,NZ,(Z(KZ),KZ = 1,NZ)
C      15 FORMAT(I5,10F6.0)
C      DO 207 MMM= 1,NRUN
C
C      SUBROUTINE FIRST IS THEN CALLED TO PROVIDE A TITLE PAGE SHOWING
C      THIS INFORMATION.  THIS SUBROUTINE ALSO READS THE DATA CARD CONTANING
C      THE WEATHER RECORDS FOR THE PARTICULAR DAY BEING CONSIDERED.  ONE CARD
C      IS REQUIRED FOR EACH SUCH DAY.
C
C      MONTH  - THE DATE BEING CALCULATED
C      TA     - THE AVERAGE AIR TEMPERATURE - DEG.F.
C      TR     - THE DAILY RANGE IN AIR TEMPERATURE - DEG. F.
C      WIND   - THE AVERAGE WIND VELOCITY ON THIS DAY - MPH
C      ELL    - THE SOLAR INSOLATION - LANGLEYS PER DAY
C      SKY    - THE PROPORTION OF DAYLIGHT HOURS IN WHICH CLOUDS OBSCURETHE SUN
C
C      CALL FIRST
C
C      DO 65 KZ = 1,NZ

```


DEPTH = Z(KZ)/12.

THE OUTPUT PAGE AT EACH DEPTH IS APPROPRIATELY TITLED AND HEADINGS PLACED.

```
PRINT 97, (TITLE(I), I = 1, 8)
97 FORMAT(8A10)
PRINT 96, (MONTH(I), I = 1, 4)
96 FORMAT(/ 30X, 4A6, //)
PRINT 98, Z(KZ)
98 FORMAT(30X, F5.1, 11H INCH DEPTH. //)
PRINT 100
100 FORMAT(15X, 4HTIME, 10X, 11HTEMPERATURE, 4X, 9HSTIFFNESS  /)
```

VALUES TO BE USED IN THE SIMULATION OF TEMPERATURES USING THE BARBER METHOD ARE CALCULATED.

```
CA = CV/(1.0 + AIR - 0.03)
SMALH = 1.3 + 0.62 * WIND **0.75
RELL = ELL - (SKY * 0.10 * ELL)
R = 0.103 * B * RELL/SMALH
SMALC = COND/(SS*W)
CAPC = (0.131/SMALC)**0.5
AYCH = SMALH/COND
SURD = (((AYCH+CAPC)**2.) + (CAPC**2.))**0.5
FNUM = AYCH * EXP (-DEPTH*CAPC)
```

FOR EACH HOUR OF THE DAY, THE TEMPERATURE AT THE POINT IN QUESTION IS CALCULATED.

```
DO 50 J=1, 25
TT = J-9
OUR = SIN ((0.262*TT) - (DEPTH*CAPC) - ATAN (CAPC/(CAPC+AYCH)))
TM = TA + R
IF(OUR) 49, 48, 48
49 TV = TR*0.5
GO TO 47
48 TV = (TR*0.5) + (3.0*R)
47 TEMP(J) = TM + TV * (FNUM/SURD) * OUR
IF(TEMP(J).LT.T(1).OR. TEMP(J).GT. T(NVAL)) GO TO 19
```

THE STIFFNESS OF THE ASPHALT AT THE CALCULATED TEMPERATURE IS INTERPOLATED. A STRAIGHT LINE IS ASSUMED IN THE LOG STIFFNESS - TEMPERATURE RELATION BETWEEN THE INPUT DATA POINTS.

```
22 DO 24 I=1, NVAL
IF(T(I)-TEMP(J)) 26, 53, 19
26 IF(T(I+1)-TEMP(J)) 24, 52, 25
24 CONTINUE
25 SLOW = S(I)
HIGH = S(I+1)
DIFF = T(I+1)-T(I)
SDIFF = ALOG10(SLOW) - ALOG10(HIGH)
SADD = ((T(I+1)-TEMP(J))/DIFF)*SDIFF
STIFL = ALOG10(HIGH) + SADD
```



```

      STIFF = 10.0 ** STIFL
      GO TO 75
53  STIFF    = S(I)
      GO TO 75
52  STIFF    = S(I+1)
C
C      THE STIFFNESS OF THE ASPHALT CONCRETE IS COMPUTED.
C
75  ENN = 0.83 * ALOG10(400000./STIFF)
      SMIX(J)=(STIFF *(1.0+(2.5/ENN)*(CA/(1.0-CA)))*ENN)*14.22344
C
C      THE OUTPUT DATA (TIME,TEMPERATURE,MIXTURE STIFFNESS) IS PRINTED.
C
      GO TO(1,2,2,2,2,2,2,2,2,2,2,2,3,4,4,4,4,4,4,4,4,4,4,1),J
1  PRINT 104,TEMP(J),SMIX(J)
104 FORMAT(15X,7H12 A.M. F15.2,F15.1)
      GO TO 50
2  JT = J-1
      PRINT 105,JT,TEMP(J),SMIX(J)
105 FORMAT(15X12,5X,F15.2,F15.1)
      GO TO 50
3  PRINT 106,TEMP(J),SMIX(J)
106 FORMAT(15X,7H12 NOON , F15.2,F15.1)
      GO TO 50
4  JT = J-13
      PRINT 105,JT,TEMP(J),SMIX(J)
      GO TO 50
C
C      AN ERROR MESSAGE IS PRINTED AND THE CALCULATION ABANDONED IF THE
C      TEMPERATURE AT THE POINT IS OUTSIDE THE RANGE OF THE INPUT DATA.
C
19  PRINT 17
17  FORMAT(31H TEMPERATURE OUT OF RANGE GIVEN )
      GO TO 207
50  CONTINUE
C
C      THE ORDINARY AND THE TRAFFIC WEIGHTED MEANS OF BOTH TEMPERATURE
C      AND STIFFNESS AT THE POINT ARE CALCULATED AND PRINTED.
C
      TRSUM = 0.0
      WTSUM = 0.0
      TSUM = 0.0
      STSUM = 0.0
      STITT = 0.0
      DO 11 J=1,24
      HRTEM = (TEMP(J)+TEMP(J+1))/2.0
      TRSUM = TRSUM + TRAFF(J)
      TSUM = TSUM + HRTEM
      WITEM = HRTEM*TRAFF(J)
      WTSUM = WTSUM + WITEM
      HRSTIF = (SMIX(J) + SMIX(J+1))/2.0
      STSUM = STSUM + HRSTIF
      WTSTIF = HRSTIF * TRAFF(J)
      STITT = STITT + WTSTIF
11  CONTINUE

```



```

TAVE = TSUM/24.
WTAVE = WTSUM/TRSUM
STAVE = STSUM/24.
WSTAVE = STITT/TRSUM
PRINT 30,TAVE
PRINT 31,WTAVE
PRINT 32,STAVE
PRINT 33,WSTAVE
30 FORMAT(////,15X,16HMEAN TEMPERATURE ,F8.1,6H DEG.F  //)
31 FORMAT(15X,21HTRAFFIC WEIGHTED MEAN ,F8.1,6H DEG.F  ///)
32 FORMAT(15X,14HMEAN STIFFNESS ,F15.0,3HPSI //)
33 FORMAT(15X,21HTRAFFIC WEIGHTED MEAN , F15.0,3HPSI )
PRINT 66
66 FORMAT(1H1)
65 CONTINUE
207 CONTINUE
STOP
END

C
C
C
C
SUBROUTINE FIRST

DIMENSION TEMP(25),TITLE( 8), MONTH(4),LOCAT(8)
COMMON TA,TR,WIND,ELL,B,SS,W,COND,CV,AIR,PEN,RANDB,TEMP,TITLE,
1 MONTH, LOCAT,SKY
PRINT 77
77 FORMAT(////,15X,50HTRAFFIC WEIGHTED MEAN TEMPERATURE AND STIFFNES
1S  ///)
PRINT 78 ,(TITLE(I), I = 1,8)
78 FORMAT(10X,22HPAVEMENT LOCATION....., 8A10, //)
PRINT 80, (LOCAT(I), I = 1,8)
80 FORMAT(/,10X,18HTRAFFIC DATA FOR ,8A10, //)
READ 20,(MONTH(I),I = 1,4),TA,TR,WIND,ELL, SKY
20 FORMAT(4A6,5F10.0)
PRINT 82, (MONTH(I), I = 1,4)
82 FORMAT(/,10X,22HWEATHER DATA FOR..... ,4A6, ///)
SAIR = AIR *100.
PRINT 84, TA
PRINT 85, TR
PRINT 86,WIND
PRINT 87,ELL
84 FORMAT(/,15X,20HMEAN AIR TEMPERATURE ,F5.1,6H DEG.F )
85 FORMAT(15X,13HDIURNAL RANGE ,7X,F5.1,6H DEG.F )
86 FORMAT(15X,20HMEAN WIND VELOCITY ,F5.1,4H MPH )
87 FORMAT(15X,18HSOLAR INSOLATION ,F7.1,21H LANGLEYS PER DAY )
PRINT 188, SKY
188 FORMAT(15X, 15HMEAN SKY COVER 5X,F5.1)
PRINT 88
88 FORMAT(/,10X,21HASPHALT CONCRETE DATA ///)
PRINT 90, PEN
PRINT 91,RANDB
90 FORMAT(15X,30HRECOVERED ASPHALT PENETRATION ,F6.0 )
91 FORMAT(15X,30HRRING AND BALL SOFTENING POINT F6.0,6H DEG.F )
PRINT 92, W

```



```
PRINT 93, SAIR
PRINT 94, CV
PRINT 95, COND
PRINT 96, SS
PRINT 97, B
92 FORMAT(15X,11HUNIT WEIGHT ,19X,F7.1,12H LBS/CU.FT. )
93 FORMAT(15X,16HAIR VOID CONTENT ,14X,F7.1 )
94 FORMAT(15X,25HVOLUME CONC. OF AGGREGATE ,5X,F8.2 )
95 FORMAT(15X,20HTHERMAL CONDUCTIVITY ,10X,F8.2 )
96 FORMAT(15X,13HSPECIFIC HEAT ,17X,F8.2 )
97 FORMAT(15X,19HSURFACE COEFFICIENT ,11X,F8.2 )
PRINT 397
397 FORMAT(1H1)
RETURN
END
```


PART 2. STRESS-MODULUS ITERATION IN THE CHEVRON FIVE-LAYER PROGRAM

THE CHEVRON FIVE-LAYER PROGRAM WILL SOLVE FOR THE STATE OF STRESS AT ANY POINT WITHIN THE STRUCTURAL SECTION UNDER THE ACTION OF A SINGLE CIRCULAR LOADED AREA OF UNIFORM CONTACT PRESSURE. IN ORDER TO CARRY OUT THE ITERATION REQUIRED TO OBTAIN COMPATIBILITY BETWEEN THE RESILIENT MODULUS AND THE STRESS LEVELS CALCULATED TO ACT IN THE GRANULAR AND FINE-GRAINED SOILS, SUBROUTINE LYDIA WAS ADDED TO THE PROGRAM.

AT THE SAME TIME THE SURFACE LOAD CONDITION WAS TAKEN TO BE A SET OF DUAL TIRES WITH THE INDIVIDUAL TIRES SEPARATED BY ONE LOAD RADIUS. THE POINTS AT WHICH THE STRESSES (AND THE RESULTING MODULI) WERE CALCULATED IS SHOWN IN FIGURE 1 OF APPENDIX A. SINCE THIS LOAD SYSTEM IS SYMMETRICAL ABOUT THE CENTRE-LINE OF THE DUAL TIRES, THE ITERATION IS CARRIED OUT OVER ONLY ONE-HALF OF THE SYSTEM.

***** MAIN ROUTINE - N-LAYER ELASTIC SYSTEM *****

THE COMMON BLOCK EFFECTS COMMUNICATION BETWEEN ALL OF THE SUB-ROUTINES OF THE PROGRAM.

```
PROGRAM PSAD(INPUT,OUTPUT)
  DIMENSION RR(100),ZZ(100),E(5),V(5),HH(4),H(4),AZ(400),A(400,5),
1    B(400,5),C(400,5),D(400,5),AJ(400),RJ1(400),RJ0(400)
  COMMON RR,ZZ,E,V,HH,H,AZ,A,B,C,D,AJ,RJ1,RJ0
  COMMON R,Z,AR,NS,N,L,ITN,P,RSZ,RST,RSR,RTR,ROM,RMU,SF
  DIMENSION TITLE(12), BZ(100), X(5,4,4), SC(4), PM(4,4,4), FM(2,2),
1 TEST(11)
  COMMON TITLE, PSI, NLINE, NOUTP, NTEST, TEST,
1 ITN4, LC, JT, TZZ, PR, PA, EP, T1P, T1M, T1, T2, T3, T4,
2 T5, T6, T2P, T2M, WA, BJ1, BJ0, BZ, ZF, SZ1, SZ2, PM, SG1, SG2,
3 PH, PH2, VKP2, VKP4, VKP4, VKK8, X, SC, FM
  COMMON EBS(6,12), VERT(6),CONST(15),DEV(20),RMOD(20),IRT,IZT,IZ
  COMMON FRONT(4),POWER(4),UNIT(5),NZT,DEPTH(20),MARK,ITER,KARL
```

```
  READ 403,NMARK
403 FORMAT(I5)
```

NMARK - THE NUMBER OF PAVEMENT PROBLEMS TO BE SOLVED.

```
DO 404 NMA= 1,NMARK
  ITER = 0
  MARK = 0
  ITN = 46
  ITN4 = ITN*4
```

EACH PROBLEM IS THEN DEFINED BY THE FOLLOWING DATA.

```
10 READ 310, (TITLE(I), I=1,12)
```



```

310 FORMAT (12A6)
C
C      TITLE      - IDENTIFICATION OF THE PAVEMENT.
C
      READ 311,WGT,PSI,NOUTP,KARL
311 FORMAT (2F12.0, I12,I4)
C
C      WGT      - THE TOTAL LOAD ON EACH TIRE - LBS.
C      PSI      - THE TIRE OR CONTACT PRESSURE - PSI.
C      NOUTP    - ABSOLUTE OR RELATIVE OUTPUT DATA SELECTOR.
C      KARL     - THE NUMBER OF LAYERS ABOVE THE SUBGRADE IN WHICH ITERATION
C                IS TO BE CARRIED OUT.
C
      READ      312, NS, (E(I),V(I), I=1,NS)
312 FORMAT(I2,5(F8.0,F6.0))
      N = NS - 1
C
C      NS      - THE NUMBER OF LAYERS IN THE PAVEMENT - (MAXIMUM - FIVE)
C      E(I)    - THE INITIALLY ASSUMED MODULUS OF THE I-TH LAYER
C      V(I)    - THE POISSONS RATIO OF THE I-TH LAYER
C
C      THE GRANULAR LAYERS ARE CHARACTERIZED BY THE EQUATION DETERMINED
C      FROM LABORATORY TESTS ON EACH OF THE MATERIALS RELATING THE RESILIENT
C      MODULUS AND THE SUM OF THE PRINCIPAL STRESSES.
C
      READ 405,(FRONT(I),POWER(I), I=1,N)
405 FORMAT(8F10.0)
C
C      FRONT(I) - THE COEFFICIENT IN THE EQUATION RELATING THE RESILIENT MOD-
C                  ULUS AND THE SUM OF PRINCIPAL STRESSES FOR THE I-TH LAYER.
C      POWER(I) - THE EXPONENT ON THE SUM OF PRINCIPAL STRESSES IN THAT
C                  EQUATION.
C
C
      READ 22,(UNIT(I),I = 1,N)
22 FORMAT(4F10.0)
C
C      UNIT(I) - THE UNIT WEIGHT OF THE MATERIAL IN THE I-TH LAYER.
C
C      THE CURVE OF RESILIENT MODULUS AGAINST REPEATED VERTICAL STRESS
C      IS THEN LOADED.
C
      READ 406,JMD,(DEV(J),RMOD(J), J = 1,JMD)
406 FORMAT(I2,F6.0,9F8.0/ (10F8.0))
C
C      JMD      - THE NUMBER OF POINTS IN THIS DATA.
C      DEV(J)   - THE J-TH VALUE OF DEVIATOR STRESS.
C      RMOD(J)  - THE RESILIENT MODULUS CORRESPONDING TO THAT STRESS LEVEL.
C
      JMD1 = JMD + 1
      DO 23 J = JMD1,20
      DEV(J) = 0.0
      23 RMOD(J) = 0.0
C

```



```

      READ          313, (HH(I), I=1,N)
313 FORMAT (4F6.0)

```

```

      HH(I)      - THICKNESS OF THE I-TH LAYER.

```

```

      THE POINTS AT WHICH THE STRESSES ARE TO BE CALCULATED ARE THEN
      DEFINED.

```

```

      7 READ          301, IR,(RR(I),I=1,IR)
      READ          301, IZ,(ZZ(I),I=1,IZ)
301 FORMAT(I6,11F6.0)

```

```

      IR      - THE NUMBER OF RADIAL DISTANCES.

```

```

      RR(I)   - THE I-TH VALUE OF RADIALDISTANCE IN INCHES MEASURED FORM
                THE AXIS OF THE LOADED AREA.

```

```

      IZ      - THE NUMBER OF DEPTHS.

```

```

      ZZ(I)   - THE ITH VALUE OFDEPTH IN INCHES MEASURED DOWN FROM THE
                SURFACE.

```

```

      FOR THIS VERSION OF THE PROGRAM, THESE POINTS MUST CORRESPOND TO
      THOSE SHOWN IN FIGURE 1 OF APPENDIX A.

```

```

      PRINT OUT PROBLEM PARAMETERS

```

```

      AR = SQRT (0.31830987*WGT/PSI)

```

```

400 PRINT 401

```

```

401 FORMAT(1H1)

```

```

      NLINE = 17+NS

```

```

      NPAGE = 1

```

```

      PRINT 350, (TITLE(I), I = 1,12 ), NPAGE

```

```

350 FORMAT( /1H0,18H***** ,1X,12A6,1X,18H*****

```

```

2**** 10X, 7H PAGE 13 )

```

```

      PRINT          351, WGT, PSI, AR, (I,E(I),V(I),HH(I),I=1,N)

```

```

351 FORMAT(1H0, 40X, 26HTHE PROBLEM PARAMETERS ARE/

```

```

2      1H0, 20X, 12HTOTAL LOAD.., 8X, F10.2, 5H LBS/

```

```

3      1H0, 20X, 15HTIRE PRESSURE.., 5X, F10.2, 5H PSI/

```

```

4      1H0, 20X, 13HLOAD RADIUS.., 7X, F10.2, 5H IN./ 1H /

```

```

5      ( 1H , 20X, 5HLAYER, 13, 14H HAS MODULUS , F10.0,

```

```

6      18H POISSONS RATIO , F6.3, 17H AND THICKNESS , F5.1,

```

```

7      4H IN.))

```

```

      PRINT          354, NS, E(NS), V(NS)

```

```

354 FORMAT (1H , 20X, 5HLAYER, 13, 14H HAS MODULUS ,F10.0,

```

```

1      18H POISSONS RATIO , F6.3, 24H AND IS SEMI-INFINITE. )

```

```

      SATISFY STRESS-MODULUS RELATIONSHIP FOR AGGREGATE BASE AND SUBGRADE

```

```

      THE STRESSES ARE THEN CALCULATED WITHOUT PRINTING AND THE SUM OF
      PRINCIPAL STRESSES AT EACH POINT STORED IN THE COMMON BLOCK FOR USE IN

```


SUBROUTINE LYDIA.

```

C
C      IF(MARK .GT.0) GO TO 54
      PRINT 50,(I,FRONT(I),POWER(I),I = 1,N)
50  FORMAT(/// 40X *MODULUS-STRESS RELATIONSHIPS* ///
1    (20X *MODULUS OF LAYER* I3, * = *,F10.0,*(THETA)* 4H ** ,F5.2/))
      PRINT 51,NS
51  FORMAT(20X *MODULUS OF LAYER * I3, * IS INTERPOLATED FROM CURVE OF
1    LABORATORY RESULTS* /)
      MIKE = 7 + 2*NS
      NLINE = NLINE + MIKE
54  CONTINUE
      IF(MARK .LT. 2) GO TO 53
      PRINT 352
352  FORMAT(1H0,34X,15HS T R E S S E S,28X,12HDISPLACEMENT,13X,
113HS T R A I N S /13X,62H.....
2.....3..... 3X,12H..... ,3X,34H.....
3..... /
45H      R,5X,1HZ,5X,8HVERTICAL,3X,10HTANGENTIAL,4X,6HRADIAL,6X,
55HSHEAR,8X,4HBULK,10X,8HVERTICAL,7X,6HRADIAL,4X,10HTANGENTIAL,4X,
65HSHEAR /1H )
C  ** ADJUST LAYER DEPTHS **
53  H(1)=HH(1)
      DO 25 I=2,N
25  H(I)=H(I-1)+HH(I)
      IRT=0
C  ** START ON A NEW R **
100  IRT=IRT+1
      NZT = 0
      IF (IRT-IR) 105,105,402
105  R=RR(IRT)
      DO 31 I =1,IZ
      DO 31 J=1,N
      TZ = ABS (H(J) - ZZ(I))
      IF(TZ - .0001) 32,32,31
32  ZZ(I) = -H(J)
31  CONTINUE
      PRINT 355
      NLINE = NLINE+1
355  FORMAT(1H )
C  ** CALCULATE THE PARTITION **
      CALL PART
C  ** CALCULATE THE COEFFICIENTS **
      DO 125 I=1,ITN4
      P=AZ(I)
107  CALL COEE (I)
109  IF (R) 115,115,110
110  PR = P*R
      CALL BESSEL (0,PR,Y)
      RJ0(I) = Y
      CALL BESSEL (1,PR,Y)
      RJ1(I) = Y
115  PA=P*AR
      CALL BESSEL (1,PA,Y)
      AJ(I)=Y

```



```

125 CONTINUE
195 IZT=0
C ** START ON A NEW Z **
200 IZT=IZT+1
    NZT = NZT + 1
    IF (IZT-IZ) 205,205,100
205 Z=ABS (ZZ(IZT))
    IF ( NLINE - 54 ) 207,206,206
206 NPAGE = NPAGE + 1
    NLINE = 8
    PRINT 350, (TITLE(I), I = 1,12 ), NPAGE
    PRINT 352
207 CONTINUE
C ** FIND THE LAYER CONTAINING Z **
    TZZ = 0.0
    DO 210 J1=1,N
        J=NS-J1
        IF (Z-H(J)) 210,215,215
210 CONTINUE
    L = 1
    GO TO 34
215 L=J+1
    IF (ZZ(IZT)) 33,34,34
33 L = J
    TZZ = 1.0
34 CONTINUE
    CALL CALCIN
    IF (TZZ) 36,36,35
35 ZZ(IZT) = -ZZ(IZT)
    IZT = IZT-1
36 CONTINUE
    GO TO 200
402 CALL LYDIA
    IF (MARK .EQ. 1 .OR. MARK .EQ. 2) GO TO 400
404 CONTINUE
    STOP
    END
    SUBROUTINE CALCIN
CCALCIN *****SUBROUTINE CALCIN - N-LAYER ELASTIC SYSTEM *****
    DIMENSION RR(100),ZZ(100),E(5),V(5),HH(4),H(4),AZ(400),A(400,5),
1      B(400,5),C(400,5),D(400,5),AJ(400),RJ1(400),RJ0(400)
    COMMON RR,ZZ,E,V,HH,H,AZ,A,B,C,D,AJ,RJ1,RJ0
    COMMON R,Z,AR,NS,N,L,ITN,P,RSZ,RST,RSR,RTR,ROM,RMU,SF
    DIMENSION TITLE(12), BZ(100), X(5,4,4), SC(4), PM(4,4,4), FM(2,2),
1  TEST(11)
    COMMON TITLE, PSI, NLINE, NOUTP, NTEST, TEST,
1  ITN4, LC, JT, TZZ, PR, PA, EP, T1P, T1M, T1, T2, T3, T4,
2  T5, T6, T2P, T2M, WA, BJ1, BJ0, BZ, ZF, SZ1, SZ2, PM, SG1, SG2,
3  PH, PH2, VK2, VKP2, VK4, VKP4, VKK8, X, SC, FM
    COMMON EBS(6,12), VERT(6),CONST(15),DEV(20),RMOD(20),IRT,IZT,IZ
    COMMON FRONT(4),POWER(4),UNIT(5),NZT,DEPTH(20),MARK,ITER,KARL
    DIMENSION W(4)
1  W(1) = 0.34785485
    W(2) = 0.65214515
    W(3) = W(2)

```



```

      W(4) = W(1)
2  VL=2.0*V(L)
   EL=(1.0+V(L))/E(L)
   VL1=1.0-VL
   CSZ=0.0
   CST=0.0
   CSR=0.0
   CTR=0.0
   COM=0.0
   CMU=0.0
   NTS1 = NTEST + 1
   ITS = 1
   JT = 0
   ARP = AR
   IF (NOUTP) 4,4,5
4  ARP = ARP*PSI
5  CONTINUE
10 DO 40 I=1,ITN
C   INITIALIZE THE SUB-INTEGRALS
   RSZ=0.0
   RST=0.0
   RSR=0.0
   RTR=0.0
   ROM=0.0
   RMU=0.0
C   COMPUTE THE SUB-INTEGRALS
      K = 4*(I-1)
   DO 30 J=1,4
      J1 = K + J
      P=AZ(J1)
      FP=EXP (P*Z)
      T1=R(J1,L)*EP
      T2=D(J1,L)/EP
      T1P=T1+T2
      T1M=T1-T2
      T1=(A(J1,L)+B(J1,L)*Z)*EP
      T2=(C(J1,L)+D(J1,L)*Z)/EP
      T2P=P*(T1+T2)
      T2M=P*(T1-T2)
      WA=AJ(J1)*W(J)
      IF (R) 20,20,15
15  BJ1=RJ1(J1)*P
      BJ0=RJ0(J1)*P
      RSZ=RSZ+WA*P*BJ0*(VL1*T1P-T2M)
      ROM=ROM+WA*EL*BJ0*(2.0*VL1*T1M-T2P)
      RTR=RTR+WA*P*BJ1*(VL*T1M+T2P)
      RMU=RMU+WA*EL*BJ1*(T1P+T2M)
      RSR=RSR+WA*(P*BJ0*((1.0+VL)*T1P+T2M)-BJ1*(T1P+T2M)/R)
      RST=RST+WA*(VL*P*BJ0*T1P+BJ1*(T1P+T2M)/R)
      GO TO 30
C   SPECIAL ROUTINE FOR R = ZERO
20  PP=P*P
      RSZ=RSZ+WA*PP*(VL1*T1P-T2M)
      ROM=ROM+WA*EL*P*(2.0*VL1*T1M-T2P)
      RST=RST+WA*PP*((VL+0.5)*T1P+0.5*T2M)

```


RSR=RST
30 CONTINUE

C

SF = (AZ(K+4) - AZ(K+1))/1.7222726
CSZ=CSZ+RSZ*SF
CST=CST+RST*SF
CSR=CSR+RSR*SF
CTR=CTR+RTR*SF
COM=COM+ROM*SF
CMU=CMU+RMU*SF

RSZ = 2.0*RSZ*AR*SF
TESTH = ABS (RSZ)-10.0**(-4)
IF (ITS-NTS1) 31,32,32

31 CONTINUE
TEST(ITS) = TESTH
ITS = ITS+1
GO TO 40

32 CONTINUE
TEST(NTS1) = TESTH
DO 33 J = 1,NTEST
IF (TESTH-TEST(J)) 35,36,36

35 CONTINUE
TESTH = TEST(J)

36 CONTINUE
TEST(J) = TEST(J+1)

33 CONTINUE
IF (TESTH) 50,50,40

40 CONTINUE
JT = 1

50 CSZ=CSZ*ARP
CST=CST*ARP
CTR=CTR*ARP
CSR=CSR*ARP
COM=COM*ARP
CMU=CMU*ARP
BSTS = CSZ+CST+CSR
RSTN = (CSR - V(L)*(CST+CSZ))/E(L)
TSTN = (CST - V(L)*(CSR+CSZ))/E(L)
IF (TZZ) 72,72,71

71 Z = -Z

72 CONTINUE
DEPTH(NZT) = Z
EBS(IRT,NZT) = -BSTS
IF (IZT .EQ. IZ) VERT(IRT) = -CSZ

IF (MARK .LT. 2) GO TO 99

PRINT 315,R,Z,CSZ,CST,CSR,CTR,BSTS,COM,RSTN,TSTN,CMU

315 FORMAT(1H ,F5.1,F6.1,1X,1P5E12.3,3H * ,E12.3,3H * ,3E12.3)
NLINE = NLINE + 1

16 IF (JT) 99,99,60

60 PRINT 316

316 FORMAT (1H+,126X,4HSLOW)

99 RETURN

END

SUBROUTINE PART

CPART *****SUBROUTINE PART - 5-LAYER ELASTIC SYSTEM *****


```

DIMENSION RR(100),ZZ(100),E(5),V(5),HH(4),H(4),AZ(400),A(400,5),
1 B(400,5),C(400,5),D(400,5),AJ(400),RJ1(400),RJ0(400)
COMMON RR,ZZ,E,V,HH,H,AZ,A,B,C,D,AJ,RJ1,RJ0
COMMON R,Z,AR,NS,N,L,ITN,P,RSZ,RST,RSR,RTR,ROM,RMU,SF
DIMENSION TITLE(12), BZ(100), X(5,4,4), SC(4), PM(4,4,4), FM(2,2),
1 TEST(11)
COMMON TITLE, PSI, NLINE, NOUTP, NTEST, TEST,
1 ITN4, LC, JT, TZZ, PR, PA, EP, TIP, T1M, T1, T2, T3, T4,
2 T5, T6, T2P, T2M, WA, BJ1, BJ0, BZ, ZF, SZ1, SZ2, PM, SG1, SG2,
3 PH, PH2, VK2, VKP2, VK4, VKP4, VKK8, X, SC, FM
COMMON EBS(6,12), VERT(6),CONST(15),DEV(20),RMOD(20),IRT,IZT,IZ
COMMON FRONT(4),POWER(4),UNIT(5),NZT,DEPTH(20),MARK,ITER,KARL

```

C ** COMPUTE ZEROS OF J1(X) AND J0(X). SET UP GAUSS CONSTANTS **

```

1 RZ(1) = 0.0
  BZ(2) = 1.0
  BZ(3) = 2.4048
  BZ(4) = 3.8317
  BZ(5) = 5.5201
  BZ(6) = 7.0156
  K = ITN+1
    DO 2 I=7,K,2
      T = I/2
      TD = 4.0*T - 1.0
2      BZ(I) = 3.1415927*(T - 0.25 + 0.050661/TD
1      -0.053041/TD**3 + 0.262051/TD**5)
      DO 3 I=8,ITN,2
        T = (I-2)/2
        TD = 4.0*T + 1.0
3      BZ(I) = 3.1415927*(T + 0.25 - 0.151982/TD
1      + 0.015399/TD**3 - 0.245270/TD**5)
      G1=0.86113631
      G2=0.33998104
4 ZF = AR
  NTEST = 2
  IF (R) 8,8,9
9 CONTINUE
  NTEST = AR/R + .0001
  IF (NTEST) 6,6,5
6 CONTINUE
  NTEST = R/AR + .0001
  ZF = R
5 CONTINUE
  NTEST = NTEST + 1
  IF (NTEST-10) 8,8,7
7 CONTINUE
  NTEST = 10
8 CONTINUE

```

C ** COMPUTE POINTS FOR LEGENDRE-GAUSS INTEGRATION **

```

15 K = 1
  ZF = 2.0*ZF
  SZ2 = 0.0
  DO 28 I=1,ITN
    SZ1 = SZ2
    SZ2 = BZ(I+1)/ZF
    SF = SZ2 - SZ1
  28

```



```

      PM = SZ2 + SZ1
      SG1=SF*G1
      SG2=SF*G2
      AZ(K)=PM-SG1
      AZ(K+1)=PM-SG2
      AZ(K+2)=PM+SG2
      AZ(K+3)=PM+SG1
      K = K + 4
28 CONTINUE
40 RETURN
END
SUBROUTINE COEE (KIN)
CCOEE *****SUBROUTINE COEE - 5-LAYER ELASTIC SYSTEM *****
      DIMENSION RR(100),ZZ(100),E(5),V(5),HH(4),H(4),AZ(400),A(400,5),
1      B(400,5),C(400,5),D(400,5),AJ(400),RJ1(400),RJ0(400)
      COMMON RR,ZZ,E,V,HH,H,AZ,A,B,C,D,AJ,RJ1,RJ0
      COMMON R,Z,AR,NS,N,L,ITN,P,RSZ,RST,RSR,RTR,ROM,RMU,SF
      DIMENSION TITLE(12), BZ(100), X(5,4,4), SC(4), PM(4,4,4), FM(2,2),
1      TEST(11)
      COMMON TITLE, PSI, NLINE, NOUTP, NTEST, TEST,
1      ITN4, LC, JT, TZZ, PR, PA, EP, T1P, T1M, T1, T2, T3, T4,
2      T5, T6, T2P, T2M, WA, BJ1, BJ0, BZ, ZF, SZ1, SZ2, PM, SG1, SG2,
3      PH, PH2, VK2, VKP2, VK4, VKP4, VKK8, X, SC, FM
      COMMON EBS(5,12), VERT(6),CONST(15),DEV(20),RMOD(20),IRT,IZT,IZ
      COMMON FRONT(4),POWER(4),UNIT(5),NZT,DEPTH(20),MARK,ITER,KARL
      DIMENSION SV1(4,2),CV1(2,1),SV2(4,4),CV2(2,2),SV3(4,8),CV3(2,4),
1      SV4(4,16),CV4(2,8),T(8),NT(4)
      COMMON SV1,CV1,SV2,CV2,SV3,CV3,SV4,CV4,T,NT
      LC = KIN
CS-MX      SET UP MATRIX X =DI*MI*KI*K*M*D
C      COMPUTE THE MATRICES X(K)
      DO 10 K=1,N
      T1=E(K)*(1.0+V(K+1))/(E(K+1)*(1.0+V(K)))
      T1M=T1-1.0
      PH=P*H(K)
      PH2=PH*2.0
      VK2=2.0*V(K)
      VKP2=2.0*V(K+1)
      VK4=2.0*VK2
      VKP4=2.0*VKP2
      VKK8=8.0*V(K)*V(K+1)
C
      X(K,1,1)=VK4-3.0-T1
      X(K,2,1)=0.0
      X(K,3,1)=T1M*(PH2-VK4+1.0)
      X(K,4,1)=-2.0*T1M*P
C
      T3=PH2*(VK2-1.0)
      T4=VKK8+1.0-3.0*VKP2
      T5=PH2*(VKP2-1.0)
      T6=VKK8+1.0-3.0*VK2
C
      X(K,1,2)=(T3+T4-T1*(T5+T6))/P
      X(K,2,2)=T1*(VKP4-3.0)-1.0
      X(K,4,2)=T1M*(1.0-PH2-VKP4)

```



```

C      X(K,3,4)=(T3-T4-T1*(T5-T6))/P
C      T3=PH2*PH-VKK8+1.0
      T4=PH2*(VK2-VKP2)
C      X(K,1,4)=(T3+T4+VKP2-T1*(T3+T4+VK2))/P
      X(K,3,2)= (-T3+T4-VKP2+T1*(T3-T4+VK2))/P
C      X(K,1,3)=T1M*(1.0-PH2-VK4)
      X(K,2,3)=2.0*T1M*P
      X(K,3,3)=VK4-3.0-T1
      X(K,4,3)=0.0
C      X(K,2,4)=T1M*(PH2-VKP4+1.0)
      X(K,4,4)=T1*(VKP4-3.0)-1.0
      K = K
10  CONTINUE
C      COMPUTE THE PRODUCT MATRICES PM
      SC(N)=4.0*(V(N)-1.0)
      IF (N-2) 13,11,11
11  DO 12 K1=2,N
      M=NS-K1
      SC(M)=SC(M+1)*4.0*(V(M)-1.0)
12  CONTINUE
13  CONTINUE
C      K = N
      DO 15 I=1,4
      DO 14 J=1,2
14  SV1(I,J) = X(K,I,J+2)
15  CONTINUE
      CV1(1,1) = -2.0*P*H(K)
      CV1(2,1) = 0.0
      K = K-1
      IF(K) 50,50,20
C
20  CONTINUE
      DO 22 J=1,2
      J1 = J+J
      T(1) = SV1(1,J)
      T(2) = SV1(2,J)
      T(3) = SV1(3,J)
      T(4) = SV1(4,J)
      DO 21 I=1,4
      SV2(I,J1-1) = X(K,I,1)*T(1)+X(K,I,2)*T(2)
21  SV2(I,J1) = X(K,I,3)*T(3)+X(K,I,4)*T(4)
22  CONTINUE
      T(1) = CV1(1,1)
      T(2) = -2.0*P*H(K)
      CV2(1,1) = T(1)
      CV2(1,2) = T(2)
      CV2(2,1) = T(1)-T(2)
      CV2(2,2) = 0.0
      K = K-1

```



```

      IF (K) 50,50,30
C
30 CONTINUE
   DO 34 J=1,4
      J1 = J
      IF (J1-2) 32,32,31
31 J1 = J1+2
32 CONTINUE
      T(1) = SV2(1,J)
      T(2) = SV2(2,J)
      T(3) = SV2(3,J)
      T(4) = SV2(4,J)
   DO 33 I=1,4
      SV3(I,J1) = X(K,I,1)*T(1)+X(K,I,2)*T(2)
33 SV3(I,J1+2) = X(K,I,3)*T(3)+X(K,I,4)*T(4)
34 CONTINUE
      T(1) = -2.0*P*H(K)
   DO 35 J=1,2
      CV3(1,J) = CV2(1,J)
      CV3(2,J) = CV2(1,J)-T(1)
      CV3(1,J+2) = CV2(2,J)+T(1)
      CV3(2,J+2) = CV2(2,J)
35 CONTINUE
      K = K-1
      IF (K) 50,50,40
C
40 CONTINUE
   DO 42 J=1,4
      T(1) = SV3(1,J)
      T(2) = SV3(2,J)
      T(3) = SV3(3,J)
      T(4) = SV3(4,J)
      T(5) = SV3(1,J+4)
      T(6) = SV3(2,J+4)
      T(7) = SV3(3,J+4)
      T(8) = SV3(4,J+4)
   DO 41 I=1,4
      SV4(I,J) = X(K,I,1)*T(1)+X(K,I,2)*T(2)
      SV4(I,J+4) = X(K,I,3)*T(3)+X(K,I,4)*T(4)
      SV4(I,J+8) = X(K,I,1)*T(5)+X(K,I,2)*T(6)
41 SV4(I,J+12) = X(K,I,3)*T(7)+X(K,I,4)*T(8)
42 CONTINUE
      T(1) = -2.0*P*H(K)
   DO 43 J=1,4
      CV4(1,J) = CV3(1,J)
      CV4(2,J) = CV3(1,J)-T(1)
      CV4(1,J+4) = CV3(2,J)+T(1)
      CV4(2,J+4) = CV3(2,J)
43 CONTINUE
C
50 CONTINUE
      NT(1) = 1
   DO 51 K=2,N
51 NT(K) = NT(K-1)+NT(K-1)
   DO 80 K=1,N

```



```

K1 = NS-K
DO 52 I=1,4
PM(K1,I,1) = 0.0
PM(K1,I,2) = 0.0
52 CONTINUE
I1 = NT(K)
DO 80 I=1,I1
I2 = I+I1
GO TO (61,62,63,64),K
61 CONTINUE
T(3) = CV1(1,I)
T(4) = CV1(2,I)
GO TO 65
62 CONTINUE
T(3) = CV2(1,I)
T(4) = CV2(2,I)
GO TO 65
63 CONTINUE
T(3) = CV3(1,I)
T(4) = CV3(2,I)
GO TO 65
64 CONTINUE
T(3) = CV4(1,I)
T(4) = CV4(2,I)
65 CONTINUE
T(1) = 0.0
T(2) = 0.0
IF (T(3)+68.0) 67,66,66
66 T(1) = EXP (T(3))
67 IF (T(4)+68.0) 69,68,68
68 T(2) = EXP (T(4))
69 CONTINUE
DO 80 J=1,2
GO TO (71,72,73,74),K
71 CONTINUE
T(3) = SV1(J,I)
T(4) = SV1(J,I2)
T(5) = SV1(J+2,I)
T(6) = SV1(J+2,I2)
GO TO 75
72 T(3) = SV2(J,I)
T(4) = SV2(J,I2)
T(5) = SV2(J+2,I)
T(6) = SV2(J+2,I2)
GO TO 75
73 T(3) = SV3(J,I)
T(4) = SV3(J,I2)
T(5) = SV3(J+2,I)
T(6) = SV3(J+2,I2)
GO TO 75
74 T(3) = SV4(J,I)
T(4) = SV4(J,I2)
T(5) = SV4(J+2,I)
T(6) = SV4(J+2,I2)
75 CONTINUE

```



```

C      PM(K1,J,1) = PM(K1,J,1)+T(1)*T(3)
      PM(K1,J,2) = PM(K1,J,2)+T(1)*T(4)
      PM(K1,J+2,1) = PM(K1,J+2,1)+T(2)*T(5)
      PM(K1,J+2,2) = PM(K1,J+2,2)+T(2)*T(6)
80    CONTINUE
C      SOLVE FOR C(NS) AND D(NS)
      V2=2.0*V(1)
      V21=V2-1.0
      DO 90 J=1,2
      FM(1,J)=P*PM(1,1,J)+V2*PM(1,2,J)+P*PM(1,3,J)-V2*PM(1,4,J)
90    FM(2,J)=P*PM(1,1,J)+V21*PM(1,2,J)-P*PM(1,3,J)+V21*PM(1,4,J)
      DFAC=SC(1)/((FM(1,1)*FM(2,2)-FM(2,1)*FM(1,2))*P*P)
      A(LC,NS) = 0.0
      B(LC,NS) = 0.0
      C(LC,NS) = -FM(1,2)*DFAC
      D(LC,NS) = FM(1,1)*DFAC
C      RACKSOLVE FOR THE OTHER A,B,C,D
      DO 91 K1=1,N
      A(LC,K1)=(PM(K1,1,1)*C(LC,NS)+PM(K1,1,2)*D(LC,NS))/SC(K1)
      B(LC,K1)=(PM(K1,2,1)*C(LC,NS)+PM(K1,2,2)*D(LC,NS))/SC(K1)
      C(LC,K1)=(PM(K1,3,1)*C(LC,NS)+PM(K1,3,2)*D(LC,NS))/SC(K1)
91    D(LC,K1)=(PM(K1,4,1)*C(LC,NS)+PM(K1,4,2)*D(LC,NS))/SC(K1)
      RETURN
      END
      SUBROUTINE BESSEL(NI, XI, Y)
CBESSEL *****SUBROUTINE BESSEL - 5-LAYER ELASTIC SYSTEM *****
      DIMENSION PZ(6),QZ(6),P1(6),Q1(6),D(20)
C
C
1    PZ(1)=1.0
      PZ(2) = -1.125E-4
      PZ(3) = 2.8710938E-7
      PZ(4) = -2.3449658E-9
      PZ(5) = 3.9806841E-11
      PZ(6) = -1.1536133E-12
C
      QZ(1) = -5.0E-3
      QZ(2) = 4.6875E-6
      QZ(3) = -2.3255859E-8
      QZ(4) = 2.8307087E-10
      QZ(5) = -6.3912096E-12
      QZ(6) = 2.3124704E-13
C
C
      P1(1) = 1.0
      P1(2) = 1.875E-4
      P1(3) = -3.6914063E-7
      P1(4) = 2.7713232E-9
      P1(5) = -4.5114421E-11
      P1(6) = 1.2750463E-12
C
      Q1(1) = 1.5E-2
      Q1(2) = -6.5625E-6
      Q1(3) = 2.8423828E-8

```

```

BESSL006
BESSL004
BESSL007
BESSL008
BESSL009
BESSL011
BESSL012
BESSL013
BESSL014
BESSL015
BESSL016
BESSL017
BESSL018
BESSL019
BESSL020
BESSL021
BESSL022
BESSL023
BESSL024
BESSL025
BESSL026
BESSL027
BESSL028
BESSL029
BESSL030
BESSL031
BESSL032
BESSL033
BESSL034
BESSL035

```


Q1(4) = -3.2662024E-10
Q1(5) = 7.1431166E-12
Q1(6) = -2.5327056E-13

PI = 3.1415927
PI2 = 2.0*PI

9 N = NI
X = XI
IF (X-7.0) 10,10,160

10 X2=X/2.0
FAC=-X2*X2
IF (N) 11,11,14
11 C=1.0
Y=C
DO 13 I=1,34
T=I
C=FAC*C/(T*T)
TEST=ABS (C) - 10.0**(-8)
IF (TEST) 17,17,12

12 Y=Y+C
13 CONTINUE
14 C=X2
Y=C

DO 16 I=1,34
T=I
C=FAC*C/(T*(T+1.0))
TEST=ABS (C) - 10.0**(-8)
IF (TEST) 17,17,15
15 Y=Y+C
16 CONTINUE
17 RETURN
160 IF (N) 161,161,164

161 DO 162 I=1,6
D(I) = PZ(I)
D(I+10) = QZ(I)
162 CONTINUE
GO TO 163

164 DO 165 I=1,6
D(I) = P1(I)
D(I+10) = Q1(I)
165 CONTINUE
163 CONTINUE
T1 = 25.0/X
T2=T1*T1
P = D(6)*T2+D(5)
DO 170 I=1,4
J = 5-I
P = P*T2+D(J)

BESSL036
BESSL037
BESSL038
BESSL039
BESSL040
BESSL041
BESSL042
BESSL043
BESSL044
BESSL045
BESSL046
BESSL047
BESSL048
BESSL049
BESSL050
BESSL051
BESSL052
BESSL053
BESSL054
BESSL055
BESSL056

BESSL058
BESSL059
BESSL060
BESSL061
BESSL062
BESSL063
BESSL064
BESSL065

BESSL067
BESSL068
BESSL069
BESSL070
BESSL071
BESSL072
BESSL073
BESSL074
BESSL075
BESSL076
BESSL077
BESSL078
BESSL079
BESSL080
BESSL081
BESSL082
BESSL083
BESSL084
BESSL085
BESSL086
BESSL087
BESSL088
BESSL089
BESSL090

170	CONTINUE	BESSL091
	Q = D(16)*T2+D(15)	BESSL092
	DO 171 I=1,4	BESSL093
	J = 5-I	BESSL094
	Q = Q*T2+D(J+10)	BESSL095
171	CONTINUE	BESSL096
	Q = Q*T1	BESSL097
C		BESSL098
	T4 = SQRT (X*PI)	BESSL099
	T6 = SIN (X)	BESSL100
	T7 = COS (X)	BESSL101
C		BESSL102
	IF (N) 180,180,185	BESSL103
C		BESSL104
180	T5 = ((P-Q)*T6 + (P+Q)*T7)/T4	BESSL105
	GO TO 99	BESSL106
185	T5 = ((P+Q)*T6 - (P-Q)*T7)/T4	BESSL107
99	Y = T5	BESSL108
	RETURN	BESSL109
	END	BESSL110
C	THIS SUBROUTINE CALCULATES THE MODULUS AT EACH POINT IN THE	
C	STRUCTURAL SECTION AT WHICH THE STRESSES HAVE BEEN CALCULATED AND THEN	
C	CHECKS THE RESULTING MODULI FOR COMPATIBILITY WITH THOSE ASSUMED AT THE	
C	BEGINNING OF THE CALCULATION.	
	SUBROUTINE LYDIA	
	DIMENSION RR(100),ZZ(100),E(5),V(5),HH(4),H(4),AZ(400),A(400,5),	
1	B(400,5),C(400,5),D(400,5),AJ(400),RJ1(400),RJ0(400)	
	COMMON RR,ZZ,E,V,HH,H,AZ,A,B,C,D,AJ,RJ1,RJ0	
	COMMON R,Z,AR,NS,N,L,ITN,P,RSZ,RST,RSR,RTR,ROM,RMU,SF	
	DIMENSION TITLE(12), BZ(100), X(5,4,4), SC(4), PM(4,4,4), FM(2,2),	
1	TEST(11)	
	COMMON TITLE, PSI, NLINE, NOUTP, NTEST, TEST,	
1	ITN4, LC, JT, TZZ, PR, PA, EP, T1P, T1M, T1, T2, T3, T4,	
2	T5, T6, T2P, T2M, WA, BJ1, BJ0, BZ, ZF, SZ1, SZ2, PM, SG1, SG2,	
3	PH, PH2, VK2, VKP2, VK4, VKP4, VKK8, X, SC, FM	
	COMMON EBS(6,12), VERT(6),CONST(15),DEV(20),RMOD(20),IRT,IZT,IZ	
	COMMON FRONT(4),POWER(4),UNIT(5),NZT,DEPTH(20),MARK,ITER,KARL	
	DIMENSION TEBS(4,19),EMOD(5),TVERT(4)	
C		
C		
C	IF MARK .EQ. 2 , THE ITERATION CLOSED IN THE PREVIOUS TRIAL. SET	
C	MARK .EQ. 3 AND RETURN TO THE BEGINNING OF THE NEXT PROBLEM.	
C		
	IF(MARK .EQ. 2) GO TO 60	
	GO TO 61	
60	MARK = 3	
	RETURN	
61	CONTINUE	
C		
	ITER = ITER + 1	
C		
C		
C	SET UP THE MAXIMUM NUMBER OF HORIZONTAL LAYERS FOR CALCULATION.	
	KNZT = 2 + 3 *(N - 1)	
	DO 34 NZT = 1,KNZT	

NEGATIVE DEPTH IMPLIES BOTTOM OF THE UPPER LAYER AT AN INTERFACE.
SINCE BOTH ARE TO BE CALCULATED THIS VALUE IS MADE POSITIVE.

IF (DEPTH(NZT) .LT. 0.) DEPTH(NZT) = - DEPTH(NZT)

THE VERTICAL STRESS OWING TO OVERBURDEN AT EACH DEPTH IS DETER-
MINED AND THE APPROPRIATE POISSONS RATIO SELECTED.

SIG1 = H(1) * UNIT(1)/1728.
SIG2 = SIG1 + HH(2) * UNIT(2)/1728.
SIG3 = SIG2 + HH(3) * UNIT(3)/1728.
SIG4 = SIG2 + HH(4) * UNIT(4)/1728.

IF(DEPTH(NZT) .LE. H(1)) GO TO 30
IF(DEPTH(NZT) .LE. H(2)) GO TO 31
IF(DEPTH(NZT) .LE. H(3)) GO TO 32
IF(DEPTH(NZT) .LE. H(4)) GO TO 33

30 SIG = DEPTH(NZT) * UNIT(1)/1728.
VEE = V(1)
GO TO 34

31 SIG = SIG1 + (DEPTH(NZT) - H(1)) * UNIT(2)/1728.
VEE = V(2)
GO TO 34

32 SIG = SIG2 + (DEPTH(NZT) - H(2)) * UNIT(3)/1728.
VEE = V(3)
GO TO 34

33 SIG = SIG3 + (DEPTH(NZT) - H(3)) * UNIT(4)/1728.
VEE = V(4)

THE SUM OF PRINCIPAL STRESSES OWING TO OVERBURDEN AT EACH DEPTH
IS CALCULATED.

34 CONST(NZT) = SIG + 2.0 * VEE * SIG /(1.0 - VEE)
CONST(KNZT + 1) = SIG

THE SUM OF PRINCIPAL STRESSES OWING TO THE TOTAL EFFECT OF EACH
WHEEL PLUS THE OVERBURDEN STRESS IS DETERMINED.

DO 15 NZT = 1,KNZT

TEBS(1,NZT) = EBS(2,NZT) + EBS(6,NZT)+CONST(NZT)
TEBS(2,NZT) = EBS(1,NZT) + EBS(5,NZT)+CONST(NZT)
TEBS(3,NZT) = EBS(2,NZT) + EBS(4,NZT)+CONST(NZT)
TEBS(4,NZT) = EBS(3,NZT) + EBS(3,NZT)+CONST(NZT)

DO 13 I = 1,4
IF(TEBS(I,NZT) .LT. 0.) TEBS(I,NZT) = 0.0
13 CONTINUE
15 CONTINUE

THE MODULUS CORRESPONDING TO THE SUM OF PRINCIPAL STRESSES AT

EACH POINT IS DETERMINED FROM THE APPROPRIATE EQUATION.

DO 20 NTEBS = 1,4
JKM = 1

DO 29 NZT = 1,2
IF(POWER(JKM) .LT. 0.001) GO TO 100
TEBS(NTEBS,NZT) = FRONT(JKM) * TEBS(NTEBS,NZT) ** POWER(JKM)
GO TO 29

100 TEBS(NTEBS,NZT) = FRONT(JKM)

29 CONTINUE

IF (JKM .EQ. N) GO TO 20
JKM = JKM + 1

DO 16 NZT = 3,5

IF(POWER(JKM) .LT. 0.001) GO TO 101
TEBS(NTEBS,NZT) = FRONT(JKM) * TEBS(NTEBS,NZT) ** POWER(JKM)
GO TO 16

101 TEBS(NTEBS,NZT) = FRONT(JKM)

16 CONTINUE

IF (JKM .EQ. N) GO TO 20
JKM = JKM + 1

DO 17 NZT = 6,8

IF(POWER(JKM) .LT. 0.001) GO TO 102
TEBS(NTEBS,NZT) = FRONT(JKM) * TEBS(NTEBS,NZT) ** POWER(JKM)
GO TO 17

102 TEBS(NTEBS,NZT) = FRONT(JKM)

17 CONTINUE

IF (JKM .EQ. N) GO TO 20
JKM = JKM + 1

DO 18 NZT = 9,11

IF(POWER(JKM) .LT. 0.001) GO TO 103
TEBS(NTEBS,NZT) = FRONT(JKM) * TEBS(NTEBS,NZT) ** POWER(JKM)
GO TO 18

103 TEBS(NTEBS,NZT) = FRONT(JKM)

18 CONTINUE

20 CONTINUE

THE MEAN VALUE ON EACH HORIZONTAL SECTION IS CALCULATED.

DO 21 NZT = 1,KNZT
21 TEBS(1,NZT) =(TEBS(1,NZT) + 2.0 * TEBS(2,NZT)+2.0 * TEBS(3,NZT)
1 +TEBS(4,NZT))/6.0

THE MEAN VALUE IN EACH LAYER IS DETERMINED.

EMOD(1) = (TEBS(1,1) + TEBS(1,2))/2.
EMOD(2) =(TEBS(1,3) + 2.*TEBS(1,4) + TEBS(1,5))/4.0
EMOD(3) =(TEBS(1,6) + 2.*TEBS(1,7) + TEBS(1,8))/4.0
EMOD(4) =(TEBS(1,9) + 2.*TEBS(1,10) + TEBS(1,11))/4.0


```

C
C      THE VERTICAL STRESS ON THE SUBGRADE AT EACH LOCATION ACROSS THE
C      LOADED AREA OWING TO THE TOTAL EFFECT OF EACH WHEEL LOAD PLUS THE OVER-
C      BURDEN STRESS IS CALCULATED.
C
C      FOR SUBGRADE SOIL
TVERT(1) = VERT(2) + VERT(6) + CONST(KNZT + 1)
TVERT(2) = VERT(1) + VERT(5) + CONST(KNZT + 1)
TVERT(3) = VERT(2) + VERT(4) + CONST(KNZT + 1)
TVERT(4) = VERT(3) + VERT(3) + CONST(KNZT + 1)
C
C      THE MODULUS AT EACH POINT IS INTERPOLATED FROM THE INPUT RESIL-
C      IENT MODULUS-DEVIATOR STRESS RELATIONSHIP.
C
DO 23 NVE = 1,4
DO 23 JJD = 1,18
C
IF (TVERT(NVE) .EQ. DEV(JJD)) TVERT(NVE) = RMOD(JJD)
IF (TVERT(NVE) .GT. DEV(JJD) .AND. TVERT(NVE) .LT. DEV(JJD+1)) GO TO 24
GO TO 23
24 DIFF = RMOD(JJD) - RMOD(JJD+1)
TOP = TVERT(NVE) - DEV(JJD)
BOT = DEV(JJD+1) - DEV(JJD)
TVERT(NVE) = RMOD(JJD) - DIFF * TOP/BOT
23 CONTINUE
C
C      THE MEAN SUBGRADE MODULUS IS CALCULATED.
C
EMOD(5) =(TVERT(1) + 2. * TVERT(2) + 2.*TVERT(3)+TVERT(4))/6.0
C
C      THE MODULUS USED IN THE STRESS CALCULATION AND THE MODULUS DETER-
C      MINED FROM THE CALCULATED STRESSES ARE THEN PRINTED.
C
PRINT 52,ITER
52 FORMAT(1H4/40X,*AFTER TRIAL NO. *,I4,//
1 43X *MODULUS USED* 7X *MODULUS REQUIRED* //)
PRINT 53,(I,E(I),EMOD(I),I = 1,NS)
53 FORMAT(25X,*LAYER NO.*,I4,5X,F10.0,10X,F10.0)
C
C      CHECK CORRESPONDENCE BETWEEN MODULI
C      CHI SQUARED TEST
C
IF (MARK .EQ. 2) GO TO 50
CHI = 0.0
DO 25 ICH = 2,5
25 CHI = CHI + (EMOD(ICH) - E(ICH))**2/E(ICH)
C
GO TO (201,202,203,204),KARL
201 STEVE = 0.5
GO TO 205
202 STEVE = 2.71
GO TO 205
203 STEVE = 4.61
GO TO 205

```


204 STEVE = 6.25

205 IF(CHI .GT. STEVE) GO TO 28

WHEN THIS CRITERION IS SATISFIED, ONE FINAL STRESS CALCULATION IS
OBTAINED AND THE STRESS STATE PRINTED BY THE MAIN PROGRAM.

PRINT 26,ITER

26 FORMAT(//30X,*MODULUS ITERATION CLOSES IN TRIAL NO. * ,I4//)

MARK = 2

RETURN

28 DO 27 IC = 2,5

IF THE CHI-SQUARED CRITERION IS NOT MET, A NEW ASSUMED VALUE OF
MODULUS IS COMMUNICATED BACK TO THE BEGINNING OF THE STRESS CALCULATION
AND THE PROCESS REPEATED.

27 E(IC) = (E(IC) + 2.0 * EMOD(IC))/3.0

MARK = 1

50 RETURN

FND

PART 3. PREDICTION OF FATIGUE LIFE

THE FATIGUE LIFE PREDICTION FOR A PARTICULAR PAVEMENT IS MADE ON THE BASIS OF THE DATA SUPPLIED FROM THE STRUCTURAL ANALYSIS OF THE PAVEMENT, THE EXPECTED TRAFFIC, AND THE FATIGUE BEHAVIOUR OF THE ASPHALT CONCRETE USED IN THE PAVEMENT.

PROGRAM LIST

```
DIMENSION GROUP(12),FACTOR(12,5),APPL(12),XLOAD(12),TITLE(8),
1  PROP(12),BETA(12),MONTH(12)
DIMENSION S(6),E(12,6),STIFF(12)
```

```
PRINT 70
70 FORMAT(1H1,41X,*TRAFFIC AND AXLE LOAD DATA*   ///)
```

THE TRAFFIC DATA FOR THE PAVEMENT IS FIRST LOADED AND ANALYZED.
THE WHEEL LOAD FACTORS ARE LOADED

```
DO 16 L=1,12
READ 17,GROUP(L),(FACTOR(L,N),N=1,5)
17 FORMAT(5X,A10,3X,5F10.0)
16 CONTINUE
```

GROUP(L) - THE WHEEL LOAD GROUP IDENTIFICATION
FACTOR(L,N) - THE NUMBER OF APPLICATIONS PER MONTH OF WHEEL LOAD GROUP
L, APPLIED BY TRUCKS OF CLASS, N.

SOME INFORMATION ABOUT THE PROJECT IS THEN LOADED.

```
READ 71,(TITLE(I),I=1,8)
71 FORMAT(8A10)
PRINT 72,(TITLE(I),I=1,8)
72 FORMAT(15X,8A10,///)
```

TITLE - IDENTIFICATION OF THE PAVEMENT.

```
READ 7,INDEX,ANES,ADT
7 FORMAT(I5,2F10.0)
```

INDEX - THE TYPE OF HIGHWAY FACILITY

1 = URBAN FREEWAY WITH FULL ACCESS CONTROL
2 = SUBURBAN FREEWAY WITH FULL ACCESS CONTROL
3 = RURAL FREEWAY WITH FULL ACCESS CONTROL
4 = RURAL MAJOR HIGHWAY
5 = RURAL MAJOR HIGHWAY, WITH CONSIDERABLE CROSS TRAFFIC


```

C      ANES      - THE NUMBER OF LANES IN THE PROPOSED FACILITY
C      ADT       - THE CURRENT OR ESTIMATED INITIAL AVERAGE DAILY TRAFFIC
C
C      GO TO (1,2,3,4,5),INDEX
C      1 P = 1500.
C      GO TO 6
C      2 P = 1200.
C      GO TO 6
C      3 P = 1000.
C      GO TO 6
C      4 P = 800.
C      GO TO 6
C      5 P = 600.
C
C      A ROUGH ESTIMATE OF THE CAPACITY OF THE PROPOSED FACILITY IS MADE
C      AND THIS INFORMATION PRINTED.
C
C      6 CPCTY = 6.31313 * P * ANES
C
C      PRINT 8,ADT,INDEX,ANES,CPCTY
C      8 FORMAT(29X,*PRESENT ADT* F10.0, *VEHICLES PER DAY* //
C      135X *FOR HIGHWAY TYPE* I2, * OF* F4.0, *LANES* /
C      2 35X,*THE DESIGN CAPACITY IS* F10.0,*VEHICLES PER DAY* //)
C
C      THE INITIAL (OR CURRENT) DAILY TRUCK TRAFFIC IN THE DESIGN LANE
C      IS THEN LOADED.
C
C      READ 21,AXL2,AXL3,AXL4,AXL5,AXL6,ATTR,GROW
C      21 FORMAT(7F10.0)
C
C      AXL2      - THE NUMBER OF TWO AXLE TRUCKS PER DAY
C      AXL3      - THE NUMBER OF THREE AXLE TRUCKS PER DAY
C      AXL4      - THE NUMBER OF FOUR AXLE TRUCKS PER DAY
C      AXL5      - THE NUMBER OF FIVE AXLE TRUCKS PER DAY
C      AXL6      - THE NUMBER OF SIX OR MORE AXLE TRUCKS PER DAY
C      ATTR      - AN ESTIMATE OF THE PER CENT INCREASE OWING TO TO ATTRACTED
C      TRAFFIC ON A NEW FACILITY.
C      GROW      - AN ESTIMATE OF THE ANNUAL PER CENT INCREASE IN DAILY TRUCK
C      TRAFFIC.
C
C      PRINT 73
C      73 FORMAT(29X,*PRESENT DAILY TRUCK TRAFFIC IN DESIGN LANE* //
C      1 33X,*TRUCK TYPE* 11X *VEHICLES PER DAY* //)
C      PRINT 74,AXL2
C      PRINT 75,AXL3
C      PRINT 76,AXL4
C      PRINT 77,AXL5
C      PRINT 78,AXL6
C
C      74 FORMAT(34X,*2 - AXLE*,12X,F10.0)
C      75 FORMAT(34X,*3 - AXLE*,12X,F10.0)
C      76 FORMAT(34X,*4 - AXLE*,12X,F10.0)
C      77 FORMAT(34X,*5 - AXLE*,12X,F10.0)
C      78 FORMAT(27X,*6 OR MORE AXLES* 12X,F10.0,////)
C

```


C EACH OF THE CLASSIFIED DAILY TRUCK TRAFFIC FIGURES IS MULTIPLIED
C BY THE APPROPRIATE WHEEL LOAD FACTOR TO OBTAIN A PREDICTION OF THE
C NUMBER OF APPLICATIONS PER MONTH OF EACH OF THE WHEEL LOAD GROUPS IN
C THE DESIGN LANE. ALL OF THIS INFORMATION IS PRINTED.
C

DO 22 LO = 1,12
APPL(LO) = AXL2*FACTOR(LO,1) + AXL3*FACTOR(LO,2) +
1 AXL4*FACTOR(LO,3) + AXL5*FACTOR(LO,4) + AXL6*FACTOR(LO,5)
22 CONTINUE

C PRINT 79
79 FORMAT(32X,*PRESENT NUMBERS OF AXLE LOADS PER MONTH* ///)
PRINT 80,(GROUP (I),APPL(I),I=1,12)
80 FORMAT(35X,A10,10X,F10.2)
PRINT 85,ATTR,GROW
85 FORMAT(//40X,*TRAFFIC GROWTH ESTIMATES* //
1 32X, *ATTRACTED TRAFFIC* ,F6.0, * PER CENT INCREASE* //
2 32X, *ANNUAL RATE OF GROWTH* , F6.0, * PER CENT* / 1H1)

C THE SINGLE AXLE LOAD MAGNITUDE WHICH REPRESENTS EACH AXLE LOAD
C GROUP IS LOADED.
C

READ 23, XLOAD
23 FORMAT(12F6.0)

C THE FATIGUE DATA FOR THE ASPHALT CONCRETE IS THEN LOADED.
C

READ 24,QUAY,ENN,CONF,STDER,COEFF
24 FORMAT(E10.4,4F10.0)

C QUAY - THE K OR COEFFICIENT IN THE FATIGUE LIFE - TENSILE STRAIN
C RELATIONSHIP.
C ENN - THE N OR EXPONENT IN THAT RELATIONSHIP.
C CONF - THE DESIRED LEVEL OF CONFIDENCE.
C STDER - THE STANDARD ERROR OF THE ESTIMATE OBTAINED IN THE REGRESSION
C ANALYSIS OF THE LABORATORY FATIGUE DATA.
C COEFF - THE NUMBER OF STANDARD DEVIATIONS CORRESPONDING TO THE DESIRED
C LEVEL OF CONFIDENCE.
C

C THIS DATA IS THEN PRINTED
C

PRINT 81,QUAY,ENN,STDER
81 FORMAT(45X,*FATIGUE TEST DATA* /// 31X,* NLIFE = *,E10.3,
1 13H * (1./ET1)** ,F8.3,/// 33X *STANDARD ERROR OF THE ESTIMA
2TE* , F10.4)
PRINT 82
82 FORMAT(//45X *FATIGUE PREDICTION* ///)

C FOR EACH MONTH, THE PROPORTION OF THE AVERAGE MONTHLY TRAFFIC
C APPROPRIATE TO THAT MONTH, AND THE STIFFNESS VALUE WHICH REPRESENTS THE
C MONTH ARE LOADED.
C

DO 50 M = 1,12
READ 25,MONTH(M),PROP(M),STIFF(M)

25 FORMAT(A10,2F10.0)

50 CONTINUE

THE TENSILE STRAIN - STIFFNESS RELATIONSHIP FOR EACH AXLE LOAD
MAGNITUDE TO BE CONSIDERED IS LOADED.

READ 100,S

READ 100,((E(I,J), J=1,6),I=1,12)

100 FORMAT(6F10.0)

TOTDAM = 0.0

TOTBIG = 0.0

IQUIT = 0

KAP = 0

MCOUNT = 0

ATTRF = 1.0 + ATTR/100.

FOR EACH YEAR, THE ANTICIPATED TRAFFIC VOLUME IS CALCULATED USING
THE CURRENT ADT, THE ATTRACTED TRAFFIC AND GROWTH ESTIMATES. THIS
VALUE IS CHECKED AGAINST THE CAPACITY CALCULATED EARLIER AND IF THE
EXPECTED ADT EXCEEDS THE CAPACITY, A MESSAGE IS PRINTED. SUBSEQUENT
CALCULATIONS WILL MAKE USE OF THESE CAPACITY FIGURES. THE SUMMATION OF
DAMAGE IS THEN BEGUN MONTH-BY-MONTH.

DO 51 LI = 1,50

IF(KAP - 1) 31,32,33

32 KAPLI = LI - 1

PRINT 34,KAPLI

34 FORMAT(40X *THE DESIGN TRAFFIC CAPACITY */

1 40X *IS EXCEEDED IN YEAR* I4, /

2 40X *FURTHER CALCULATIONS WILL USE*/

3 40X *THIS LEVEL OF TRAFFIC*/ 1H4)

KAP = KAP + 1

GO TO 33

31 GROWF = (1.0 + GROW/100.) ** LI

CREASE = ATTRF * GROWF

PRADT = ADT * CREASE

IF(PRADT .GT. CPCTY) KAP = KAP + 1

FOR EACH MONTH

33 DO 52 MON = 1,12

SUMDAM = 0.0

SUMBIG = 0.0

DO 49 ILOAD = 1,12

XAPPL = APPL(ILOAD) * PROP(MON) * CREASE

FOR EACH AXLE LOAD GROUP, THE STRAIN LEVEL WHICH WILL BE INDUCED
IN THE ASPHALT CONCRETE LAYER IS INTERPOLATED IN THE INPUT DATA AT THE
STIFFNESS VALUE REPRESENTING THAT MONTH.


```

DO 15 N = 1,6
  IF(STIFF(MON) .GT. S(N) .AND. STIFF(MON) .LE. S(N+1)) GO TO 116
15 CONTINUE
C
116 DIFF = E(ILOAD,N+1) - E(ILOAD,N)
  TOP = STIFF(MON) - S(N)
  BOTT = S(N+1) - S(N)
  STR = E(ILOAD,N) + (TOP/BOTT) * DIFF
C
  FTA = STR * 0.000001
C
C      THE MEAN AND SHORTEST PROBABLE LIFE AT THE DESIRED LEVEL OF CONF-
C      IDENCE ARE CALCULATED FOR THE STRAIN LEVEL FROM THE LABORATORY FATIGUE
C      RELATIONSHIP.
C
  XLOG = ALOG10(QUAY) + ENN * ALOG10(1./ETA)
  XLOGL = XLOG - COEFF * STDER
  SLIFE = 10.0 ** XLOG
  SLIFL = 10.0 ** XLOGL
C
C      THE CYCLE RATIO AT EACH LEVEL OF CONFIDENCE IS FORMED FROM THE
C      NUMBER OF APPLICATIONS PER MONTH OF THE AXLE LOAD GROUP AND THE SIMPLE
C      LOADING FATIGUE LIFE AT THE STRAIN LEVEL INDUCED IN THE PAVEMENT BY
C      THAT AXLE LOAD. THE CUMULATIVE DAMAGE PER MONTH IS SUMMED AND PRINTED.
C
  DAMM = XAPPL/SLIFE
  RIG = XAPPL/ SLIFL
  SUMDAM = SUMDAM + DAMM
  SUMBIG = SUMBIG + BIG
49 CONTINUE
  MCOUNT = MCOUNT + 1
  COUNT = MCOUNT
  YEAR = COUNT / 12.0
  TOTDAM = TOTDAM + SUMDAM
  TOTBIG = TOTBIG + SUMBIG
C
  PRINT 83, MONTH(MON),SUMDAM,SUMBIG
83 FORMAT(30X,A10,2E12.4)
C
C      THE TOTAL CUMULATIVE DAMAGE IS CHECKED AFTER EACH MONTH TO DETER-
C      MINE IF THE SUM EXCEEDS ONE (FATIGUE LIFE EXHAUSTED). IF SO THE CAL-
C      CULATION AT THAT LEVEL OF CONFIDENCE IS HALTED AND A MESSAGE PRINTED.
C      THE PREDICTION IS COMPLETE WHEN THE FATIGUE LIFE HAS BEEN PREDICTED AT
C      BOTH LEVELS OF CONFIDENCE.
  IF(TOTBIG .GE. 1.0) GO TO 30
  GO TO 52
30 IF (IQUIT .LT. 5) PRINT 87,(TITLE(I),I=1,8),CONF,YEAR
87 FORMAT(1H4/15X,8A10,/// 30X *AT A CONFIDENCE LEVEL OF *,F5.0,
1* PER CENT*/ 30X *THE SHORTEST PROBABLE FATIGUE LIFE IS* , F6.1,
2 *YEARS* //)
  IQUIT = IQUIT + 5
  IF (TOTDAM .GE. 1.0) GO TO 88
  GO TO 52
88 PRINT 89,YEAR
89 FORMAT(30X, * THE MEAN FATIGUE LIFE IS * F6.1, *YEARS*)

```


STOP

52 CONTINUE
PRINT 90
90 FORMAT(1H4)

AT THE END OF THE CALCULATIONS PERTAINING TO THE FIRST YEAR, AN ESTIMATE IS MADE OF THE SHORTEST FATIGUE LIFE WHICH WILL RESULT FROM THE DETAILED CALCULATIONS. IF THIS IS EXCESSIVE, THE CALCULATION IS STOPPED AND A MESSAGE INDICATING THAT THE PAVEMENT IS OVERDESIGNED IS PRINTED.

IF(LI .GT. 1) GO TO 51
FSHORT = 1./TOTBIG
PRINT 92,CONF,ESHORT
92 FORMAT(29X, *PRELIMINARY ESTIMATE BASED ON TRAFFIC IN FIRST YEAR*
1 //36X *AT A CONFIDENCE LEVEL OF * ,F5.0, * PER CENT*/
2 30X *THE SHORTEST PROBABLE FATIGUE LIFE IS *,G11.3,* YEARS*//)
IF(ESHORT .LT. 35.) GO TO 51
PRINT 93
93 FORMAT(35X * THE PAVEMENT IS OVERDESIGNED*)
STOP

51 CONTINUE
PRINT 91
91 FORMAT(30X, *THE FATIGUE LIFE EXCEEDS 50 YEARS*)
STOP
END

